UNITED STATES DEPARTMENT OF THE INTERIOR

GEOLOGICAL SURVEY

GEOCHEMISTRY OF THE ALTERED AREA AT GOLDFIELD, NEVADA, INCLUDING ANOMALOUS AND BACKGROUND VALUES FOR GOLD AND OTHER METALS

By

R. P. Ashley and W. J. Keith

73-12

Open-file report

1973

This report is preliminary
and has not been edited or
reviewed for conformity with
Geological Survey standards

Contents

Page

Results and discussion--rock samples--Continued

Illustrations

Page

Tables

Tables--Continued

Geochemistry of the altered area
at Goldfield, Nevada, including anomalous and background
values for gold and other metals

By R. P. Ashley and W. J. Keith

Menlo Park, California

INTRODUCTION

General

This report describes partial results of a geochemical sampling program carried out in the Goldfield mining district, Esmeralda and Nye Counties, Nev. Geochemical samples were collected from a 15-square-mile area at Goldfield which is underlain by hydrothermally altered volcanic rocks (fig. 1). This altered area contains the main productive district, which is located immediately northeast of the Goldfield townsite. It yielded almost all of the approximately $100,000,000 worth of gold, silver, and copper produced at this camp since 1903. Small areas located 2-4 miles north to northeast of the main district (fig. 1) account for production somewhere between $500,000 and $2,000,000. Two other small areas located about a mile to the east and southeast of the main district have total production probably less than $100,000. All of these areas with minor production are also within the Goldfield hydrothermally altered area.

Even though the area of hydrothermal alteration at Goldfield is much more extensive than the relatively few productive spots that have been discovered within it, the entire altered area has potential to yield new

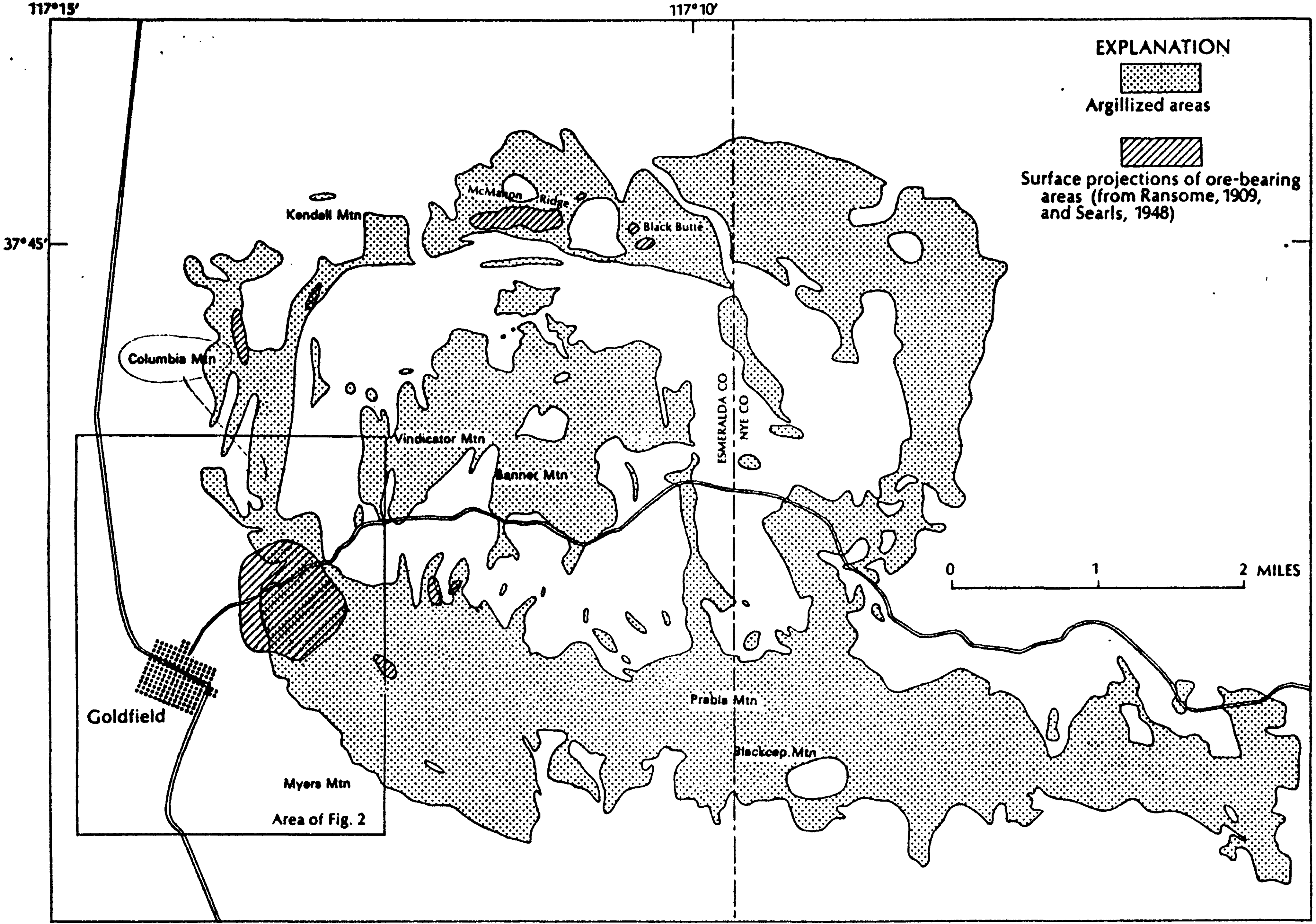

Base from U.S. Geological Survey Goldfield 1952, and Mud Lake, 1952

Alteration contacts by J. P. Albers, H. R. Cornwall, and R. P. Ashley, 1966

Figure 1.--Map of Goldfield, Nev., and vicinity, showing areas of hydrothermal alteration and ore deposits.

epithermal precious metal deposits. The known ore bodies were deposited during the later stages of hydrothermal alteration. Overall objectives of our geochemical studies at Goldfield are ~~to~~ (1) to provide information useful for designing geochemical exploration programs in the altered area, and (2) to identify parts of the area that might be favorable for further exploration. This report attempts to fulfill the first of these two objectives; it builds on a previous geochemical orientation study (Ashley and Albers, 1969, 1972). The second objective will be the subject of a subsequent report.

Geologic setting

Goldfield is the site of an early Miocene volcanic center composed of trachyandesitic, rhyodacitic, quartz latitic, and rhyolitic flows and tuffs (Ransome, 1909; Albers and Cornwall, 1968). Underlying pre-Tertiary rocks consist of Ordovician Palmetto Formation siliceous shales, argillites, and limestones extensively intruded by Mesozoic quartz monzonite. Palmetto Formation and quartz monzonite appear at the surface only in a few inliers in the western part of the area. A preliminary detailed geologic map provides the geologic information used in this report (Ashley, 1971), and forms the base for plate 1. The stratigraphic units referred to in this report are those of plate 1. Of particular interest here are the prealteration (preore) units, because they host the ore bodies, and because the prealteration volcanic units record a series of volcanic events that set the stage for hydrothermal alteration and ore deposition. Postalteration (postore) units generally occur around the periphery of the altered area. They are of interest here only for determining the history of supergene alteration in the area.

The stratigraphic units we will deal with in this report include, from oldest to youngest, the quartz monzonite, Vindicator Rhyolite, Goldfield latite, Sandstorm Rhyolite, Milltown Andesite, Goldfield dacite, and landslide deposits (see explanation, pl. 1). The quartz monzonite has fairly constant and roughly equal proportions of quartz, sodic plagioclase, and orthoclase, and 1-15 percent biotite. Much of the rock is notably leucocratic, with only 1-5 percent biotite. The Vindicator Rhyolite consists of a rhyolitic welded tuff and a rhyolite flow, the Goldfield latite consists of quartz latitic tuffs and a flow, the Sandstorm Rhyolite consists of rhyolitic air-fall tuffs and one or more flows, and the Goldfield dacite consists of relatively homogeneous porphyritic rhyodacite and minor rhyodacitic tuff breccia. The Milltown Andesite, however, contains both trachyandesite and rhyodacite flows and tuffs in abundance, and minor amounts of quartz latite and basalt. Although some flows in the Milltown Andesite approach the Goldfield dacite in composition, the average composition is probably somewhat closer to trachyandesite (see Ransome, 1909, p. 50, 52, and 56 for analyses). The unit termed "landslide deposits" is a breccia, locally very coarse, composed of debris from the Milltown Andesite and from the Goldfield dacite. Milltown Andesite debris is the more abundant. Throughout the text, the foregoing rock units will be referred to as "quartz monzonite," "Vindicator Rhyolite," "latite," "Sandstorm Rhyolite," "Milltown Andesite," "dacite," and "andesite-dacite breccia." All these units except the last one were originally named by Ransome (1909), although he called the quartz monzonite "alaskite." The units with names capitalized have been given formation status in the Lexicon of Geologic Names of the United States (Keroher and others, 1966). The other names, whether new (Ashley, 1971) or from Ransome, are informal. Several other units, including one with formation status (Espina Breccia) appear in the map explanation included with prealteration, preore units. These units are not considered here because they yielded too few samples to make useful data subsets. We will not consider any of the postalteration units in detail. A discussion of postalteration geologic events follows, centering on the history of erosion and supergene alteration.

Various pieces of geologic evidence indicate that erosion reached hydrothermally altered rocks along the south side of the altered area, at levels above the present topographic surface, between 14 and 16 million years ago, 4-7 million years after the hydrothermal alteration and ore deposition took place (Silberman and Ashley, 1970). Silicic air-fall tuffs at least partly cover this old erosion surface. Erosion removed the tuffs and continued into the altered rocks, with perhaps one or two brief interruptions, until at least 10-12 million years ago, by which time the erosion surface had reached a position close to the present topographic surface. The 10- to 12-million-year-old erosion surface was covered by basalt flows of that age. The basalt had been removed, at least from the southeastern part of the area, when the Thirsty Canyon Tuff was deposited around the periphery of the Goldfield Hills 6-7 million years ago. Rocks at and near the present erosion surface in the southeastern part of the area have been exposed to oxidation three times: first between 10 and 16 million years ago, again between 6 and 10 million years ago, and again at the present time. The south-central and southwestern parts of the area have been exposed to oxidation at least twice: between 10 and 16 million years ago and a the present time. Over the central and western parts of the area, the erosion surface present 14-16 million years ago had reached altered rocks in some places, but was probably at least 1,000 feet above the present topographic surface except along the western edge of the area. Starting 14-16 million years ago and continuing until about 10 million years ago, silicic tuffs, tuffaceous sediments, and basalt flows accumulated over the central, western, and northern parts of the area. These materials were certainly partly removed during earlier periods of erosion, but were not stripped away until the present episode of erosion which began 6-7 million years ago. Altered rocks were locally eroded before 6-7 million years ago, but probably at levels substantially above the present topographic surface. Thus, the central and western parts of the area are presently undergoing oxidation and leaching for the first time. This may also be true along the northern edge of the area, but it is also possible that altered rocks exposed at McMahon Ridge and Black Butte were oxidized once before, prior to the deposition of tuffs and flows which began 14-16 million years ago.

We recognize three types of hydrothermally altered rocks, which form concentric zones around faults and fractures: silicified rocks form adjacent to the faults and fractures and are surrounded by illite-kaolinite-bearing argillized rocks, which in turn are surrounded by montmorillonite-bearing argillized rocks. Previous work by Harvey and Vitaliano (1964) and by one of us (Ashley and Albers, 1973) has provided the criteria for distinguishing these three alteration zones in the field. In addition, we obtained X-ray diffractograms and thin sections for 254 altered rock samples taken throughout the altered area, to confirm that alteration mineralogy does not change markedly from place to place, and to make sure that we have been consistent in assigning the altered rock samples collected for chemical analysis to one of the above three categories.

In the following description of the altered rocks, we use the term "illite" to refer to a group of clay minerals having $d_{(001)}$ approximately equal to 9.9Å that do not expand when treated with ethylene glycol. We do not distinguish between 1 M_d and 2 M_1 polymorphic forms, both of which occur in these rocks. The term "kaolinite" refers to any member of the kaolinite group except halloysite (kaolinite, nacrite, dickite). We have not attempted precise identification of kaolinite-group minerals. The term "montmorillonite" refers to a group of expandable clay minerals having $d_{(001)}$ approximately equal to 14.7 to 15.5Å (samples air dried).

Low-grade altered rocks form the bulk of material found within the hydrothermally altered area. These rocks are soft and bleached, though more or less stained by limonite or jarosite as a result of oxidation. Low-grade hydrothermally altered rocks generally contain quartz, montmorillonite, kaolinite, and illite, with relict plagioclase representing various proportions of the original plagioclase. These rocks correspond to the montmorillonite subzone of the argillized zone defined by Harvey and Vitaliano (1964). They ~~commonly~~ are poorly exposed, forming residual soils except at the very edge of the altered area, where wisps of argillized material extend along fractures into otherwise massive and well-exposed unaltered volcanic rocks. Supergene jarosite seems to be restricted to these low-grade argillized rocks and gives them a distinctive pale-yellow color at many localities. Veinlets of supergene gypsum also are characteristic.

As grade of alteration increases, the montmorillonite-bearing assemblage gives way to a quartz-illite-kaolinite assemblage accompanied by little or no relict mineral material. These rocks are generally moderately hard, are often moderately well exposed, and look bleached but are usually stained to pastel reds, purples, or yellow browns by limonite. These rocks form the illite-kaolinite subzone of the argillized zone defined by Harvey and Vitaliano (1964). Variations in alteration mineralogy occur particularly in the most intensely altered part of this subzone, where adularia and opal occur locally. In the discussion of results, where we use the term "argillized " rocks, we refer to both montmorillonite and illite-kaolinite subzones.

The highest grade altered rocks are the silicified zones, composed mainly of fine-grained (0.002-0.02 mm) light- to dark-gray quartz. These zones are generally tabular because they formed along prealteration fractures that conducted the hydrothermal solution(s). They form scattered craggy outcrops throughout the altered area. In addition to quartz, alunite and kaolinite commonly occur in these rocks, usually preferentially replacing former plagioclase of alkali feldspar phenocrysts or glassy fragments. Some rocks contain alunite or pyrophyllite, or both, with or without diaspore or kaolinite. We have seen relict unoxidized altered rock only within massive parts of some silicified zones; several centimeters of oxidized material must always be broken away from the surface of the outcrop to expose such material. The depth of thorough oxidation, however, is generally at least several tens of feet throughout the altered area, and oxidation extends along fractures to depths of at least 1,000 feet. Unoxidized material within a few feet of the surface is very scarce, and none of the samples collected for this study are unoxidized. In the oxidized altered rocks limonite replaces former pyrite, otherwise unoxidized and oxidized altered rocks have the same mineral assemblages, suggesting that hypogene mineral assemblages have not been notably affected by supergene alteration. Supergene veinlets of halloysite, kaolinite, alunite, and chalcedonic quartz occur locally; we avoided these in our sampling.

Hydrothermal alteration effects are grossly similar in all the pre-alteration stratigraphic units, but differences in original lithology do produce some variations in sizes, shapes, and mineralogy of the alteration zones. Alteration zones, for instance, tend to broaden and locally follow bedding where conduit fractures cut clastic rocks such as coarse tuffs or conglomerates. Alunite, although it may be present or absent regardless of lithology, is most abundant locally in rhyolitic rocks, which are the most potassium-rich rocks in the area.

Immediately outside the Goldfield altered area many of the rock units described above show various types of diagenetic or deuteric alteration that must have existed before hydrothermal activity began in what is now the altered area. The quartz monzonite locally shows mild propylitic or sericitic alteration. All the rhyolitic units are locally opalized. The latite flow underwent strong deuteric oxidation which converted the mafic minerals to hematite and magnetite. In the tuffs included with the latite, glass was converted to nontronite. Various flows in the Milltown Andesite have been propylitized; some contain calcite and others contain zeolites. These diagenetic and deuteric alterations are recognized by being restricted to certain flows or tuff beds. Diagenitically and deuterically altered rocks are included with unaltered rocks, and in fact make up a large porportion of the samples in some of the unaltered rock data subsets. In most cases such rocks probably have not undergone drastic chemical changes relative to the original truly fresh rock.

Sampling scheme and method of collecting samples

We collected a total of 1,954 geochemical samples from the Goldfield altered area at the intersection points of a grid with 500-foot spacing. This sampling was done between July and September 1966. We assumed that metal anomalies might appear in any of the hydrothermally altered rocks regardless of intensity of alteration. The grid-sampling program was intended as a reconnaissance; it showed scattered anomalous values, but the sample spacing in most cases was too large to provide much information about the size and nature of the anomalies that gave rise to these values. Meanwhile, we received chemical analyses for a suite of samples collected from the main productive part of district (reported on by Ashley and Albers, 1969, 1973). Results of the latter sampling indicated that only the most highly altered rocks, the silicified zones forming scattered rugged exposures throughout the altered area, are likely to produce anomalous gold, silver, and lead values associated with new deposits. It became clear then that the grid sampling was not the best sampling scheme for detecting geochemical anomalies in the Goldfield altered area. The grid data is suitable, however, for delineating changes in minor element abundance which accompany increasingly strong hydrothermal alteration in various rock types. The data can also provide threshold values which separate anomalous values from background values, forming useful guides for further geochemical investigations. In the discussion that follows, we treat the grid-sampling data to evaluate changes in minor element abundances produced by hydrothermal alteration, and to determine threshold values. We subsequently renewed our attempt to identify geochemical anomalies worthy of further exploration, by selecting bedrock samples from silicified zones throughout the altered area. As previously mentioned, the results of this selective sampling will be presented in a later report.

The data to be considered in this report, if summarized in a single data matrix, would form a voluminous listing (26 elements for each of 1,674 of the 1,954 samples we collected). We have chosen to dispense with a listing and summarize the data by means of tables and diagrams, assuming that summary information is most useful to the reader.

The grid-sampling scheme was set up and the samples collected as follows. A grid on transparent plastic with lines spaced one-half inch apart was placed over the Mud Lake and Goldfield 15-minute quadrangle maps, expanded to 1:12,000 scale (1 inch = 1,000 feet). The grid was oriented north-south and east-west but was located randomly with respect to ground location of any given grid intersection point. Each grid intersection point falling within or adjacent to the altered area became a potential sample locality. This sampling scheme, although actually a systematic rather than a truly random scheme, is not biased in that each geologic unit is represented by a number of samples proportional to the size of its outcrop area (see Krumbein and Graybill, 1965, Chap. 7).

The grid intersection points were transferred by inspection to 1:16,000-scale aerial photographs, using stereoscopic images, and subsequently located in the field by inspecting the aerial photographs, again using stereoscopic images. Points in the southwestern part of the grid were also located by chain and compass traverses from mines shown on the Goldfield quadrangle map. Comparison between the two location techniques indicates that most sample localities are probably within 100 feet of the position shown on the map (pl. 1), but locally, due to combined effects of distortion in the photo images and small scale of the original quadrangle map (1:62,500), errors approach 250 feet.

Many grid-intersection localities yielded bedrock samples from surface outcrops. At those localities with soil cover, however, a hole was dug 12-18 inches deep and the material at this depth sampled. Usually such material was colluvial or alluvial soil, but in many cases bedrock appeared under colluvial soil cover only a few inches to a foot thick, and in some cases the holes yielded residual soils, which are actually very soft clay-bearing altered rocks. These altered rocks are recognized by relict textures visible in undisturbed material; in the grouping of samples presented later, they are considered altered rocks. Here an advantage of grid sampling is obvious: many bedrock samples were recovered from localities with thin cover that we would have omitted if we had collected samples only from grid intersections with exposed bedrock. Most of the unexposed soft altered rocks, furthermore, were montmorillonite-bearing argillized rocks; these rocks would be very poorly represented in our sampling if we had restricted ourselves to surface exposures. In keeping with our policy of collecting from every grid-intersection point, we obtained 178 soil samples from alluvium in washes. Although by collecting samples from washes we obtained a few bedrock samples we would otherwise have missed, these samples are very heterogeneous and yield no information useful for characterizing geochemical properties of the altered rocks; so we have deleted them from further consideration. Some rock units in certain states of alteration yielded too few samples for summary statistics, and these samples have been deleted also. We have deleted a total of 280 of the 1,954 samples collected, leaving 1,674. When we reached the edge of the altered area, traversing along any given north-south or east-west grid line, we collected samples from one or two grid-point localities beyond the altered area to provide geochemical data from fresh rocks for comparison purposes. The unsampled areas in the grid (pl. 1) are therefore somewhat smaller than the patches of unaltered rock they represent.

Analytical methods

Gold was determined by an atomic absorption method utilizing either a hot hydrobromic acid extraction from 2-gram samples (Huffman and others, 1967) or a cold hydrobromic acid extraction from 10-gram samples (Thompson and others, 1968). The former method has a sensitivity of 0.1 ppm, and the latter method a sensitivity of

0.02 ppm. Arsenic was determined by the Gutzeit colorimetric method (Ward and others, 1963, p. 38-44), and mercury was determined by an atomic absorption method (Vaughn and McCarthy, 1964; Vaughn, 1967). All other elements, including Ag, Pb, Bi, Cu, Mo, B, Ba, Be, Co, Cr, La, Mn, Nb, Ni, Sc, Sr, V, Y, Zr, Fe, Mg, Ca, and Ti were determined by 6-step semiquantitative spectrographic analysis (Grimes and Marranzino, 1968).

T. Ging, G. VanSickle, E. Martinez, T. Roemer, A. Toevs, R. Tripp, S. Rickard, J. Frisken, A. Wells, C. Huffman, J. Thomas, J. Mensik, W. Goss, G. Burrow, and G. Shipley made the gold analyses. W. R. Vaughn, W. Campbell, S. Rickard, T. Roemer, Z. Stephenson, and L. Bailey made the arsenic analyses. W. Campbell, S. Noble, E. Martinez, S. Rickard, J. Frisken, and L. Vinnola made the mercury analyses. E. Mosier, J. Motooka, J. Nishi, J. Finley, H. Neiman, G. Sears, J. Hamilton, and D. Siems made the spectrographic analyses. The analyses were performed between July 1966 and July 1969. Most were done by Field Services Branch, Branch of Exploration Research, U.S. Geological Survey, in Denver, Colo., and in mobile laboratories at Tonopah, Nev. Some were done by Analytical Laboratories Branch, U.S. Geological Survey, in Denver, Colo.

Statistical methods

Before performing statistical calculations, we converted all data values to weight percent and computed common logarithms of the values, thereby transforming all data to log percent. Use of the log transformation in geochemistry is discussed by Miesch (1967), and our reasons for using the log transformation for all our data are discussed in a previous report (Ashley and Albers, 1973). Means and standard deviations were then calculated in the usual manner using the log-transformed data: this procedure yields geometric means and geometric deviations. For most of the elements in most of the data subsets some data is censored, that is, one or more samples contain amounts less than a lower detection limit, or in some cases, greater than an upper detection limit. The geometric means and deviations were adjusted by Cohen's method to account for this censored data in all cases where less than 50 percent of the data falls either below a lower detection limit or above an upper detection limit (Cohen, 1959, 1961). Where more than 50 percent of the data for an element fall below a lower detection limit, the average amount of this element must be smaller than the detection limit, so we did not calculate a geometric mean and deviation. None of our data sets have more than 50 percent of data above an upper detection limit. Miesch (1967) fully explains the use of Cohen's method in calculations for geochemical data.

To determine correlations we used Spearman's rank correlation coefficient (Siegel, 1956; Flanagan, 1957; Lovering, 1963). We accept correlation coefficients statistically significant at the 95-percent-confidence level as indicating an association that might be geologically meaningful. Although correlations are not emphasized in this report, we obtained correlation coefficients for all pairs of elements in all data subsets larger than 20 samples, wherever enough data existed above the detection threshold of each element to permit computation.

In addition to the calculations described above, histograms and frequency tables were computed for each element in each data subset. All these computations were done by computer, using the U.S. Geological Survey

STATPAC system. Using the frequency tables, log-probability plots were prepared for some elements in selected data subsets. Calculations for the analysis of variance described in the section following this one were also done by computer.

At many points in the discussion we refer to differences between the geometric means for two data subsets. Where we claim that a significant difference exists between two geometric means, the data have met statistical tests for differences between variances (F-test) and means (_t_-test). If a difference between two means is significant at the 95-percent-confidence level, we then consider whether the difference is geologically significant. Testing for a statistical difference at the 95-percent-confidence level rather than at a higher or lower confidence level (such as 90 or 99 percent) is arbitrary, but 95 percent is commonly used. Where differences are not statistically significant at the 95-percent-confidence level, we feel that it is potentially misleading to consider geological explanations for such differences, because chances are large enough that no real difference exists. Calculations for the F and _t_ tests were performed by hand (Moroney, 1956).

Sampling and analytical errors--analysis of variance

It is important to know whether sources of variation in the data due to sampling and analytical errors are larger or smaller than sources of variation which depend on geological factors. If such errors are indeed the larger source of variation, it is potentially misleading at best, and probably futile to attempt any geologic interpretation of the data. Although we have not included contour maps of the grid data here, it is also interesting to know whether the variance arising from differences within the 500-foot grid cells is greater or less than variance arising from differences between the 500-foot grid cells. If the variance within cells were greater, it would mean that the 500-foot sample spacing was too large, and that more closely spaced sampling probably would show geochemical features not shown by the 500-foot grid sampling. If the variance between cells were greater, then the 500-foot sample spacing would be adequate to show statistically significant (and probably geologically significant) geochemical variations, and a smaller sample spacing would be unnecessary.

To determine the sources of variance in our grid data, we designed a three-level random nested sampling scheme (see Krumbein and Graybill, 1965, Chap. 9). We decided to collect about 500 samples for this phase of the project, so we selected 36 500-foot grid cells from approximately the southwestern third of the area by taking X and Y coordinates from a random number table. The coordinates of these cells are listed in table 1. We subdivided each of the 36 cells into 50-foot grid cells and selected eight of these cells within each 500-foot cell, again obtaining X~~,~~ and Y coordinates from a random number table. The center of each of these 50-foot cells became a sample locality, to give a total of 288 localities. At each locality we collected two samples side by side on the outcrop or in the hole dug if outcrop was lacking. In table 2, level 1 refers to the 36 500-foot cells, level 2 to the 288 localities distributed within the 500-foot cells (eight to a cell), and level 3 refers to the 576 samples collected from the 288 localities (two samples per locality). The variance associated with replication (level 3) gives an idea of the amount of combined sampling and analytical error. Comparing this variance with the variance

Table 1.--Grid cells selected at random for analysis of variance study

Cell Number	x 1/	y 1/		Cell Number	x	Y		
1	25	6		28	21	35		
2	15	9		29	8	36		
3	32	10		30	6	37		
4	36	10		31	29	38		
5	51	11		32	5	39		
6	34	13		33	11	40		
7	41	13		34	29	41		
8	43	13		35	31	41		
9	27	14		36	5	43		
10	29	14						
11	15	15						
12	25	15						
13	27	15						
14	35	15						
15	15	17						
16	39	17						
17	24	20						
18	11	22						
19	14	24						
20	17	24						
21	7	26						
22	30	26						
23	8	29						
24	23	29						
25	19	30						
26	30	30						
27	34	31						

1/ Origin at lower left of grid (pl. 1).

Table 2.--Analysis of variance results for selected elements

Element	% of data outside detection limit	Values substituted for data outside detection limit (ppm)	Level	Degrees of freedom	Sum of squares	Mean square	F ratio	$F_{(0.05)}$	Variance of higher level > variance of lower level at 95% confidence level
Pb	5.9	5 (N)[1] 7 (L)	1 [2]	37	35.52	0.96	5.90	1.49	Yes
			2	251	40.85	0.16	3.11	1.24	Yes
			3	287	15.04	0.052			
Mg	12.7	0.008(L) 5 (G)	1	37	43.54	1.18	6.19	1.49	Yes
			2	251	47.74	0.19	2.33	1.24	Yes
			3	287	23.42	0.082			
As	47.2	1(L)	1	37	49.51	1.34	2.64	1.49	Yes
			2	251	127.3	0.51	2.41	1.24	Yes
			3	287	60.28	0.21			
Cu	1.0	1 (N) 1.5 (L)	1	37	16.73	0.45	4.44	1.49	Yes
			2	251	25.53	0.10	2.54	1.24	Yes
			3	287	11.47	0.040			
Ba	0.5	3(L)	1	37	29.82	0.81	8.73	1.49	Yes
			2	251	23.16	0.092	2.62	1.24	Yes
			3	287	10.09	0.035			
Mn	2.6	5 (N) 7 (L)	1	37	91.53	2.47	6.52	1.49	Yes
			2	251	95.20	0.38	11.38	1.24	Yes
			3	287	9.56	0.033			

[1] N = readings given as "not detected," L = "less than," G = "greater than." For lead, N's were replaced with 5 ppm, and L's with 7 ppm.

[2] 576 samples (level 3) from 288 localities located randomly on 50-foot grids (level 2) within 36 randomly located 500-foot cells (level 1).

associated with the 288 different localities (level 2) shows whether sampling and analytical variations are subordinate to those presumably due to geologic differences between localities. Comparing variance associated with the localities (level 2) with that associated with the 500-foot grid cells (level 1) shows whether we should have sampled at a closer interval (specifically, a 50-foot interval) to detect significant geochemical changes. We collected the samples for this phase of the study between June and August 1967.

The analysis of variance method we used is that of Anderson and Bancroft (1952), applying the F-test for tests of significance (Snedecor, 1956). We carried out the analysis of variance for nine elements: gold, silver, lead, mercury, arsenic, copper, molybdenum, barium, and manganese. This group includes all the ore-related elements considered in this report except bismuth, which occurs above its 10-ppm detection threshold in only a few samples. We performed the analysis of variance for all nine elements, but we have omitted gold, silver, and molybdenum from table 1 because all three have more than 50 percent of data below their respective detection thresholds, so results are of questionable value. We included barium because its behavior is representative of many minor elements (not ore related) in Goldfield altered rocks, but it is more abundant than any other, minimizing data lost below the detection threshold. Manganese, though a minor element, shows behavior somewhat different from barium, and in fact much like the behavior shown by the important major elements magnesium and calcium.

The analysis of variance method used cannot accommodate censored data, so we replaced the qualified data values with the arbitrary values shown in the second column of table 2 (see tables 14-38, following text, for detection limits). The remainder of table 2 summarizes the results.

For Pb, Hg, As, Cu, Ba, and Mn, sampling and analytical error combined are definitely subordinate to variations found between localities, and variations between localities, within 500-foot grid cells, in turn are subordinate to the variations between grid cells. The last three columns of table 2 show that the F-ratios for level 2/level 3 and level 1/level 2 are in every case greater than the F-ratios determined for the appropriate degrees of freedom at the 95-percent-confidence level. In fact, the computed F-ratio (third from the last column, table 1) substantially exceeds the F value for the 99.99-percent-confidence level in every case. Thus, our 500-foot sampling interval is sufficiently small to detect important geochemical variations, and we are confident that geological differences, rather than sampling and analytical errors are the cause of the differences.

Data subsets

The geochemical data are subdivided along two independent lines. The first subdivision is by formation or stratigraphic unit. In most cases this serves to group the samples by original rock type, since most of the stratigraphic units each include only one compositional type (see p. 3). The second subdivision of the data is by degree of hypogene hydrothermal alteration.

Both subdivisions of the data, by original rock type and degree of alteration, are based on features generally recognizable in the field. Original rock type is obscure for some silicified and illite-kaolinite rocks; here field classification is difficult. The geologic base of plate 1 (Ashley, 1971) should be adequate, however, for most geochemical work near Goldfield. We did not attempt to group samples by stratigraphic unit at the time we collected them; ~~we made this~~ subdivision of the data was made in 1970-71, after the geologic mapping was completed. We did attempt to recognize the various types of altered rock in the field, using the work of Harvey and Vitaliano (1964) as a guide. After we obtained X-ray diffractograms and thin sections for samples from the altered area, we re-examined all the rock samples and residual soil samples visually to refine our alteration designations. The 254 altered rock samples examined include 88 samples taken from every other grid intersection throughout the grid (but omitting colluvial and alluvial soil samples).

The data are summarized in a series of figures (figs. 2-27) and tables 3-12). The results of statistical calculations used for the figures and tables are summarized in tables 14-38, following the text. Each figure shows the changes that occur in a single element with increased intensity of alteration, for the various stratigraphic units. Some alteration subsets are missing due to insufficient data; a subset was omitted if it contained less than 10 samples. Threshold values for recognizing anomalies are derived for several ore-related elements, including gold, silver, lead, bismuth, mercury, arsenic, copper, and molybdenum, in silicified rock (table 13). Threshold values may be computed for any other data subsets using the information tabulated in tables 14-38.

RESULTS AND DISCUSSION--ROCK SAMPLES

Major elements

Iron

Progressively more strongly altered rocks in all but two of the stratigraphic units show no significant change in iron content (fig. 2). Milltown Andesite and dacite show statistically significant decreases from unaltered to silicified rocks, but these changes are quantitatively small. This relationship is typical of unoxidized altered rocks at Goldfield because during alteration most of the iron, residing mainly in mafic minerals, was converted to pyrite rather than being removed by the hydrothermal solution. It is rather surprising, however, to see this relationship in the oxidized altered rocks under discussion here, because during oxidation iron tends to be leached from altered rocks, and especially strongly leached from silicified rocks (Ashley and Albers, 197). We have two possible explanations for the fact that amounts of iron in the oxidized rocks collected for this study change little with progressive alteration. First, the area around the Combination and January mines, where we carried out our earlier study (Ashley and Albers, 1973), may not be representative of the entire altered area with respect to distribution of iron. There silicified rocks are strongly fractured relative to surrounding argillized rocks, a condition that probably promoted strong leaching of iron from the silicified rocks during oxidation. This condition may not be well enough developed elsewhere in the altered area to be particularly important. The second possible explanation is sampling bias in the case of silicified rocks collected at grid-intersection points. When occupying a given

Figure 2

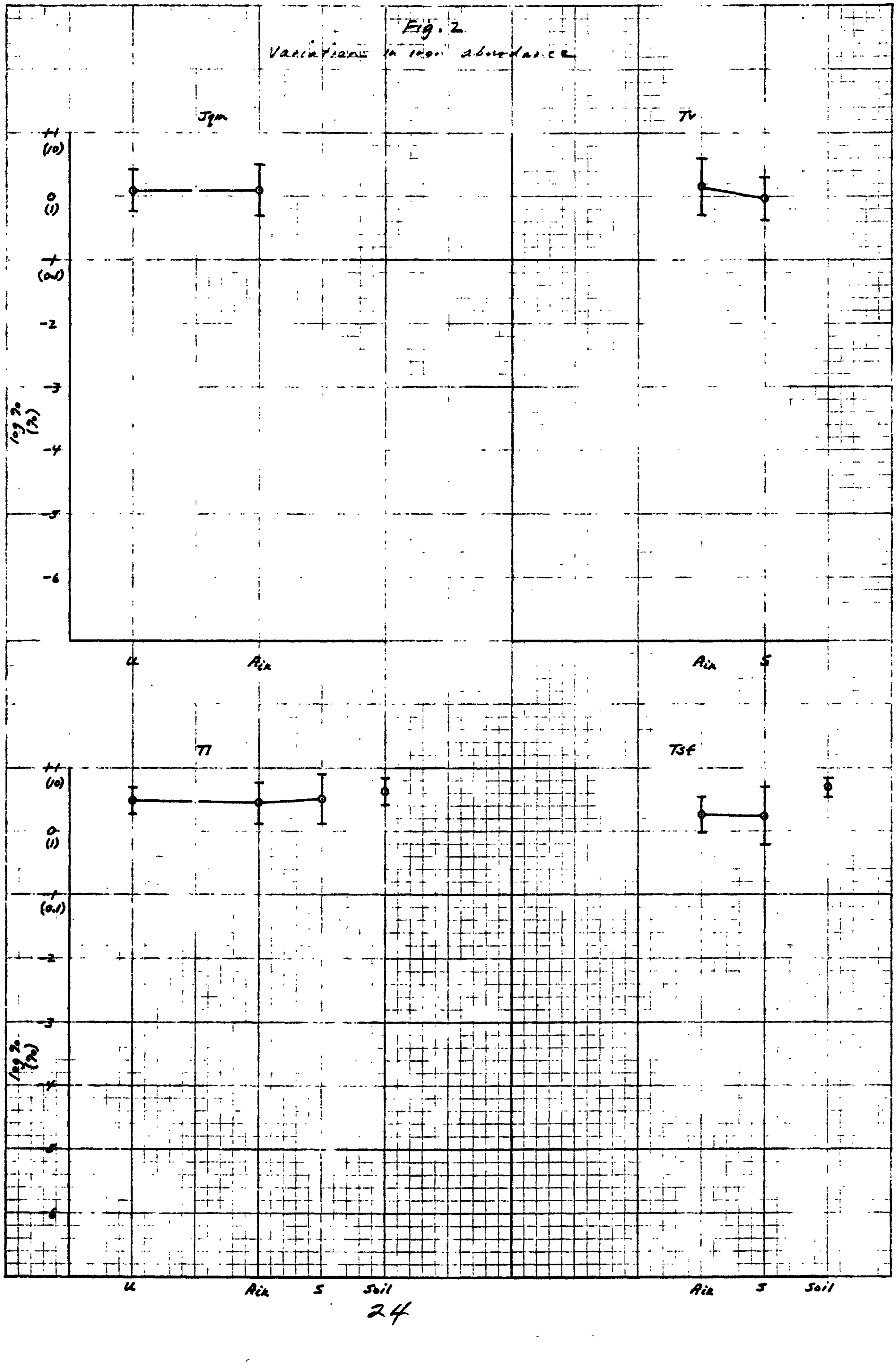
Fig. 2
Variations in iron abundance
Jgm
Tv
Tl
Tsf
+1 (10)
0 (1)
-1 (0.1)
-2
-3
-4
-5
-6
log % (%)
U
Air
S
Soil

Figure 2--Continued

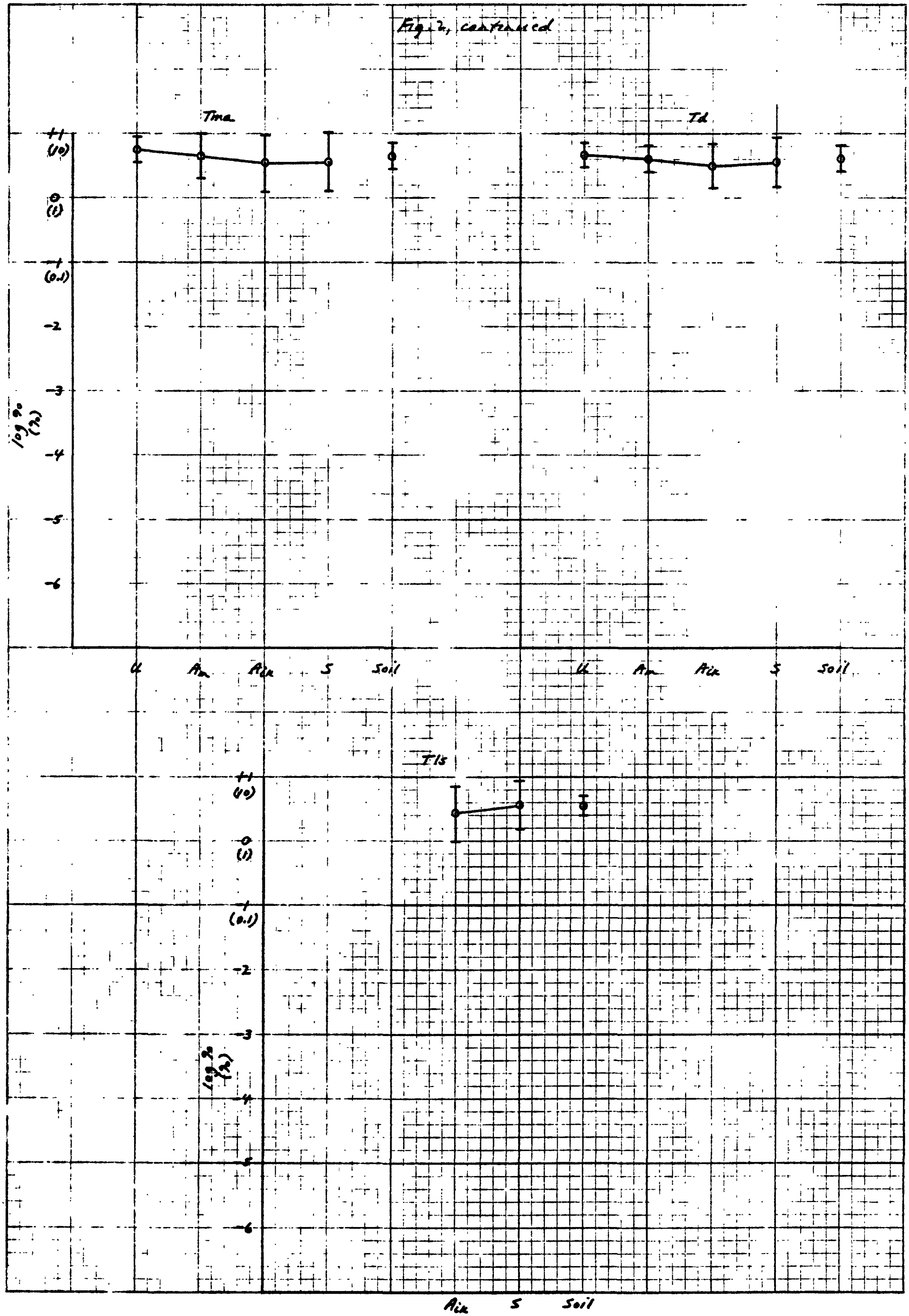

P. 25 follows

Figure 2.--Explanation (applies to figs. 2-27).

Stratigraphic units:

Jqm = quartz monzonite

Tv = Vindicator Rhyolite

Tl = latite

Tsf = Sandstorm Rhyolite

Tma = Milltown Andesite

Td = dacite

Tls = andesite-dacite breccia

Alteration zones, rock samples

U = unaltered rocks

Am = montmorillonite-bearing argillized rocks

Aik = illite-kaolinite-bearing argillized rocks

S = silicified rocks

Soil = soil samples

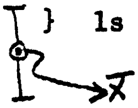

} 1s or 1 $\hat{\sigma}$ (one geometric deviation)

$\bar{X}$ or $\hat{\mu}$ (geometric mean) sample locality with exposed silicified rock, we commonly collected the most easily removed material available within a radius of about 10 feet. Blocks easily removed from the outcrop are often bounded by limonite-coated fracture surfaces. Thus, many of the silicified rocks we collected were relatively rich in limonite minerals (hematite and goethite), whereas we took pains to avoid this bias in our previous study.

The relative amounts of iron in the various stratigraphic units are not surprising, considering major-element compositions of the units (see table 3). The quartz monzonite, which has a very low color index in most places, has the least iron. Original iron contents of the Vindicator Rhyolite and Sandstorm Rhyolite cannot be directly determined because so much of each unit is altered that data from unaltered rocks is too scanty to calculate element abundances. The iron contents of Vindicator Rhyolite and Sandstorm Rhyolite before hydrothermal alteration were probably nearly as small as that of the quartz monzonite. The latite, actually a quartz latite, is more mafic than the preceding units, and probably has more iron than either of the two rhyolitic units did. The Milltown Andesite (mainly trachyandesites and rhyodacites) and the dacite (actually a rhyodacite) are more mafic than any of the above units, and have the most iron. Before hydrothermal alteration the andesite-dacite breccia must have had about the same iron content as the Milltown Andesite and dacite. Argillized (illite-kaolinite) and silicified andesite-dacite breccia now have essentially the same amounts of iron as comparably altered Milltown Andesite and dacite (the figures 3 and 4 percent are not significantly different).

(p. 25a follows)

Table 3.--Iron abundances

[Geometric mean, given in log percent and antilog of mean, in parentheses, given in percent]

	Unaltered	Argillized montmorillonite-bearing	Argillized illite-kaolinite	Silicified
Jqm	0.1(1)	—	0.1(1)	—
TV	—	—	0.2(1.5)	0(1)
Tl	0.5(3)	—	0.5(3)	0.5(3)
Tsf	—	—	0.3(2)	0.2(1.5)
Tma	0.8(6)	0.6(4)	0.5(3)	0.6(4)
Td	0.7(5)	0.6(4)	0.5(3)	0.6(4)
Tls	—	—	0.4(3)	0.6(4)
Range (%)	1-6	4	1-3	1-4

P. 26 follows

Magnesium and calcium

Of the four major elements considered, magnesium and calcium provide reliable geochemical criteria for determining, at least approximately, the intensity of hydrothermal alteration. Magnesium and calcium generally decrease markedly with increasing intensity of hydrothermal alteration (figs. 3 and 4). Comparison with unoxidized altered rocks indicates that supergene activity subsequent to hypogene alteration may reduce the absolute amounts of magnesium and calcium even further, but abundance relationships between various data subsets are probably not notably changed. Depletion of these two elements mainly reflects the progressive removal of metal cations and associated mineralogic changes that accompany progressively stronger hydrothermal alteration. When fresh rocks are converted to montmorillonite-bearing rocks, mafic minerals are usually completely destroyed, releasing magnesium and calcium. Some of this magnesium and calcium, however, is retained in the montmorillonite, which partly replaces the mafic minerals, and, in volcanic rocks, partly replaces the groundmass also. Some calcium is also retained in relict plagioclase, which is only partly destroyed at this stage of alteration. Illite, which replaces biotite along with leucoxene and pyrite, contains important amounts of magnesium and small amounts of calcium (Grim, 1968, p. 580). Kaolinite contains small amounts of magnesium and calcium (Grim, 1968, p. 576).

With more intense hydrothermal alteration, montmorillonite gives way to kaolinite and any remaining plagioclase alters to illite and kaolinite. As montmorillonite breaks down, more magnesium and calcium are released, but some of each remain in the new illite and kaolinite that take its place. If the rocks contain accessory sphene, it will persist into the illite-kaolinite subzone, accounting for some of the calcium.

Figure 3

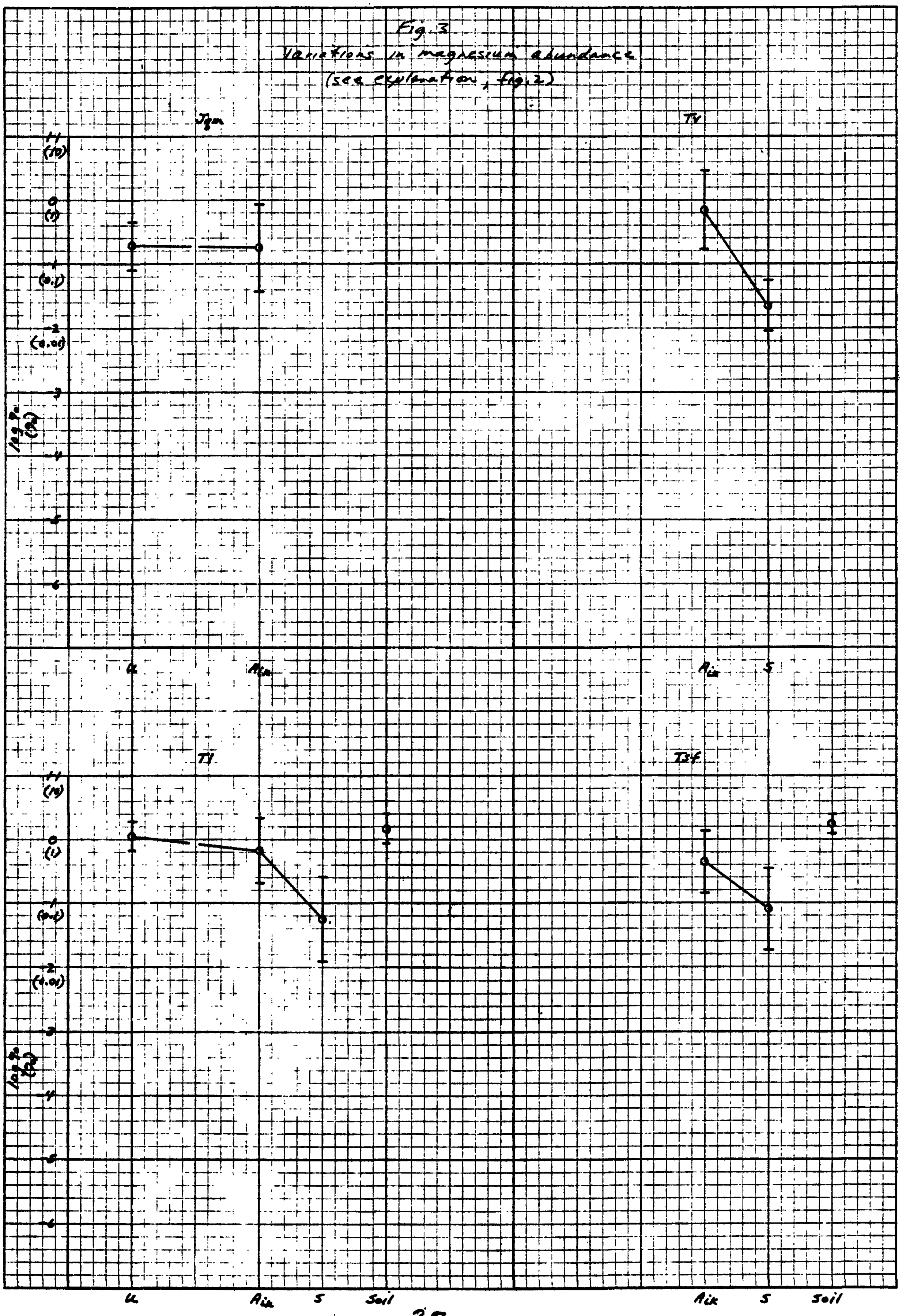

Fig. 3

Variations in magnesium abundance

(see explanation, fig. 2)

Figure 3--Continued

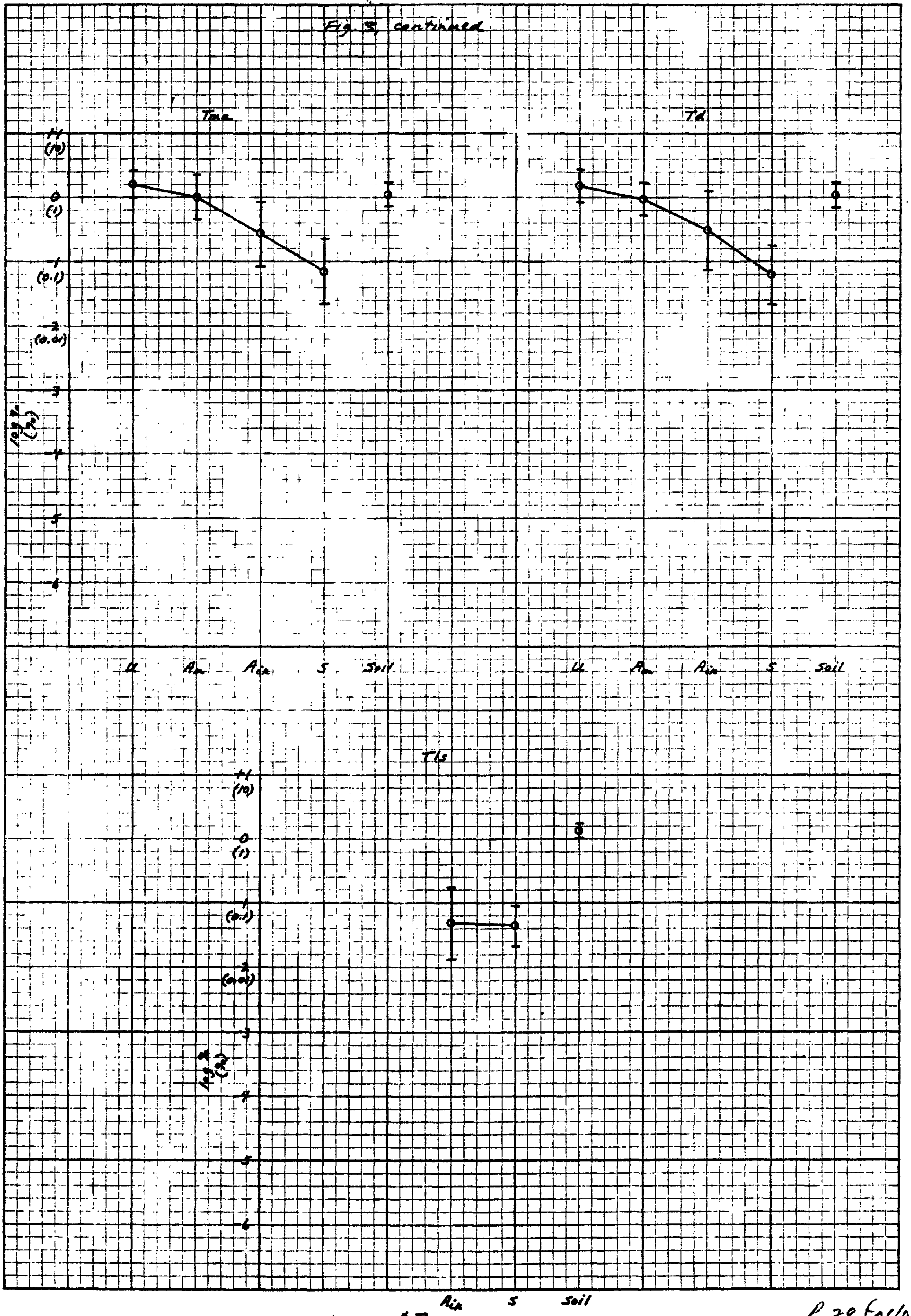

P. 28 follows

Figure 4

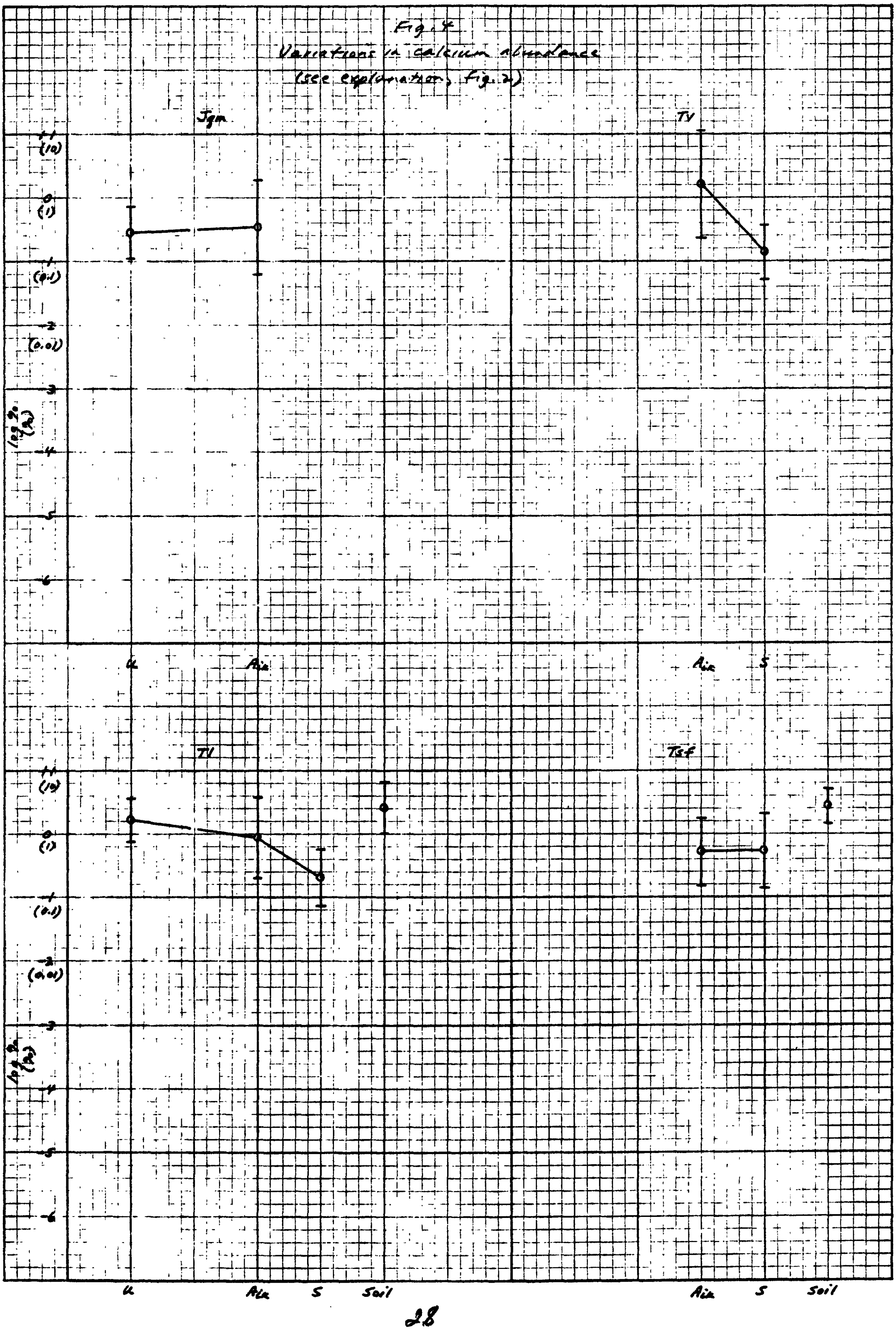

Fig. 4
Variations in calcium abundance
(see explanation, Fig. 2)

Figure 4--Continued

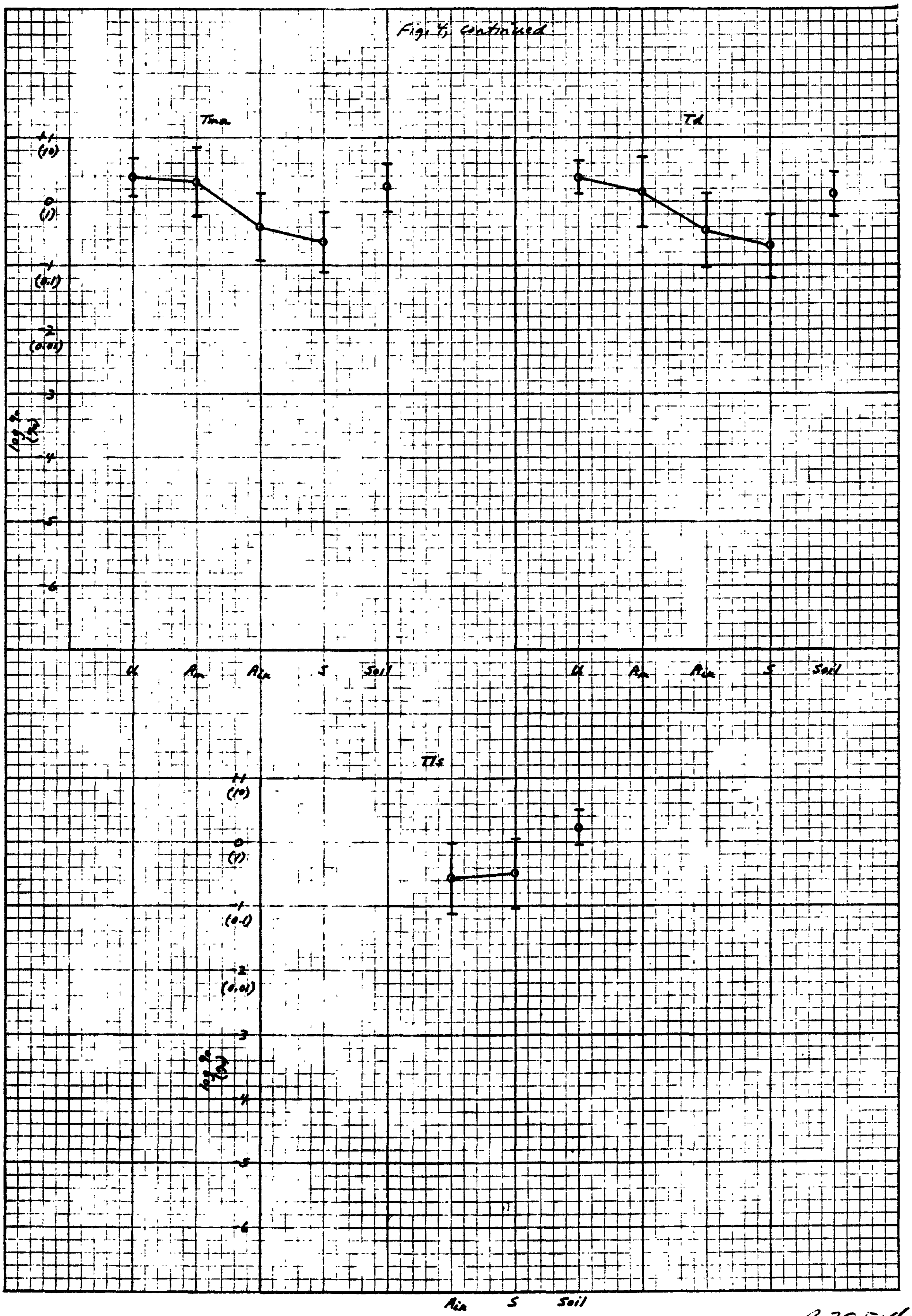

P. 29 follows

Further alteration yields silicified rocks. Silicification involves recrystallization of quartz to a tightly interlocking aggregate, accompanied by loss of all illite, loss of some or all kaolinite, loss of any sphene, and formation of alunite and (or) pyrophyllite with or without diaspore. Loss of all illite and some proportion of the kaolinite releases even more magnesium and calcium, leaving amounts of magnesium generally between 0.01 and 0.1 percent, and amounts of calcium generally a little over 0.1 percent. Amounts drop even lower in scarce silicified rocks composed almost entirely of quartz and pyrite; these rocks represent the most intensely altered materials in the area. Relict magmatic quartz remains unchanged even in these rocks, and pyrite, once formed, is retained regardless of intensity of alteration. During oxidation, pyrite is destroyed and limonite produced, but otherwise none of the alteration mineral assemblages appear to be modified greatly.

The quartz monzonite and the andesite-dacite breccia show no change in magnesium or calcium contents, suggesting that in both cases the two available subsets are both composed of similar rocks or similar proportions of differently altered rocks. The latter is probably the case for the unaltered and illite kaolinite-bearing quartz monzonite data subsets, because bleaching of biotite and clouding of plagioclase were our main field criteria for recognizing argillized rock. ~~but~~ However biotite is often scarce and plagioclase in fresh rock is ~~often~~ frequently clouded with deuteric sericite. The abundant relict quartz that persists in the quartz monzonite makes it difficult to evaluate the properties of residual soils that form over it; consequently some montmorillonite-bearing rocks may be included with the illite-kaolinite subset because we did not detect the swelling properties of minor montmorillonite present in quartz-rich residual soil. The andesite-dacite breccia presents a different problem, because the two data subsets involved supposedly represent moderately and highly altered rocks. Rocks that appeared to have substantial clay contents we classified as illite-kaolinite rocks in the field. We found subsequently that at least some of these rocks contain alunite rather than illite, so that their mineral assemblages are similar to those of silicified rocks even though their quartz contents are lower[1]. Possibly the entire unit is more strongly altered than we suspected when we sampled it in the field, and all or nearly all the samples should be considered silicified.

Magnesium and calcium abundances in unaltered rocks are not unusual for the rock types involved. The quartz monzonite contains the least magnesium and calcium, the latite contains somewhat more, and Milltown Andesite and dacite contain the most (tables 4 and 5). Many illite-kaolinite and silicified rock subsets for Vindicator Rhyolite, latite, and Sandstorm Rhyolite have more magnesium and calcium than do similarly altered Milltown Andesite, dacite, and andesite-dacite breccia. Before alteration the reverse must have been true. The only explanation we can offer is that supergene leaching has removed significant amounts of material particularly from the latter three units. These units have probably been subjected to oxidizing conditions for a longer period of time than have the older four units (see introduction, above, and section on copper and molybdenum, below).

---

[1] We found some similar rocks in ~~our study of~~ the area around the Combination and January mines (Ashley and Albers, 1973).

Table 4.--Magnesium abundances

[Geometric mean, given in log percent, and antilog of mean, in parentheses, given in percent]

	Unaltered	Argillized montmorillonite-bearing	Argillized illite-kaolinite	Silicified
Tqm	-0.7(0.2)	—	-0.7(0.2)	—
Tv	—	—	-1.5(0.7)	-1.6(0.02)
Tl	0.1(1)	—	-0.2(0.7)	-1.2(0.06)
Tsf	—	—	-0.4(0.4)	-1.1(0.08)
Tma	0.2 (1.5)	0 (1)	-0.6(0.3)	-1.1(0.07)
Td	0.2 (1.5)	0 (1)	-0.5(0.3)	-1.2(0.06)
Tls	—	—	-1.3 (0.05)	-1.4(0.05)
Range (%)	0.2- 1.5	1	0.05- 0.7	0.02-0.08

Table 5.--Calcium abundances

[Geometric mean, given in log percent, and antilog of mean, in parentheses, given in percent]

	Unaltered	Argillized montmorillonite-bearing	Argillized illite-kaolinite	Silicified
Tqm	-0.5 (0.3)	—	-0.5 (0.3)	—
Tv	—	—	0.2 (1.5)	-0.9 (0.15)
Tl	0.2 (1.5)	—	-0.1 (0.9)	-0.7 (0.2)
Tsf	—	—	-0.3 (0.5)	-0.3 (0.6)
Tma	0.4 (3)	0.3 (2)	-0.4 (0.4)	-0.6 (0.2)
Td	0.4 (2)	0.2 (1.5)	-0.4 (0.4)	-0.7 (0.2)
Tls	—	—	-0.6 (0.3)	-0.5 (0.3)
Range (%)	0.3 - 3	1.5 - 2	0.3 - 1.5	0.15 - 0.6

Titanium

Amounts of titanium decrease significantly with stronger hydrothermal alteration in Vindicator Rhyolite, latite, Milltown Andesite, and dacite, but changes are small compared to those seen in magnesium and calcium (fig. 5). When mafic minerals break down in the early stages of alteration, most of the original titanium is retained as leucoxene (cloudy, very fine grained anatase) which persists into silicified rocks, suffering only small losses with additional recrystallization and mineralogic changes. Sphene, which persists until silicification begins, yields leucoxene also, apparently with only minor loss of titanium. In very strongly altered rocks, which have lost almost all metal cations, leaving quartz with minor pyrite, rutile takes the place of leucoxene.

Since titanium abundance generally changes little with alteration, differences in original titanium content of the various units are the largest source of the variation shown in table 6. Relative titanium abundances inferred for the various stratigraphic units prior to hydrothermal alteration are as follows: quartz monzonite contains the smallest amount; Vindicator Rhyolite and Sandstorm Rhyolite contain similar amounts which are larger than that in the quartz monzonite; the latite contains still more; and Milltown Andesite, dacite, and andesite-dacite breccia contain the most, all three having about the same amounts.

Figure 5

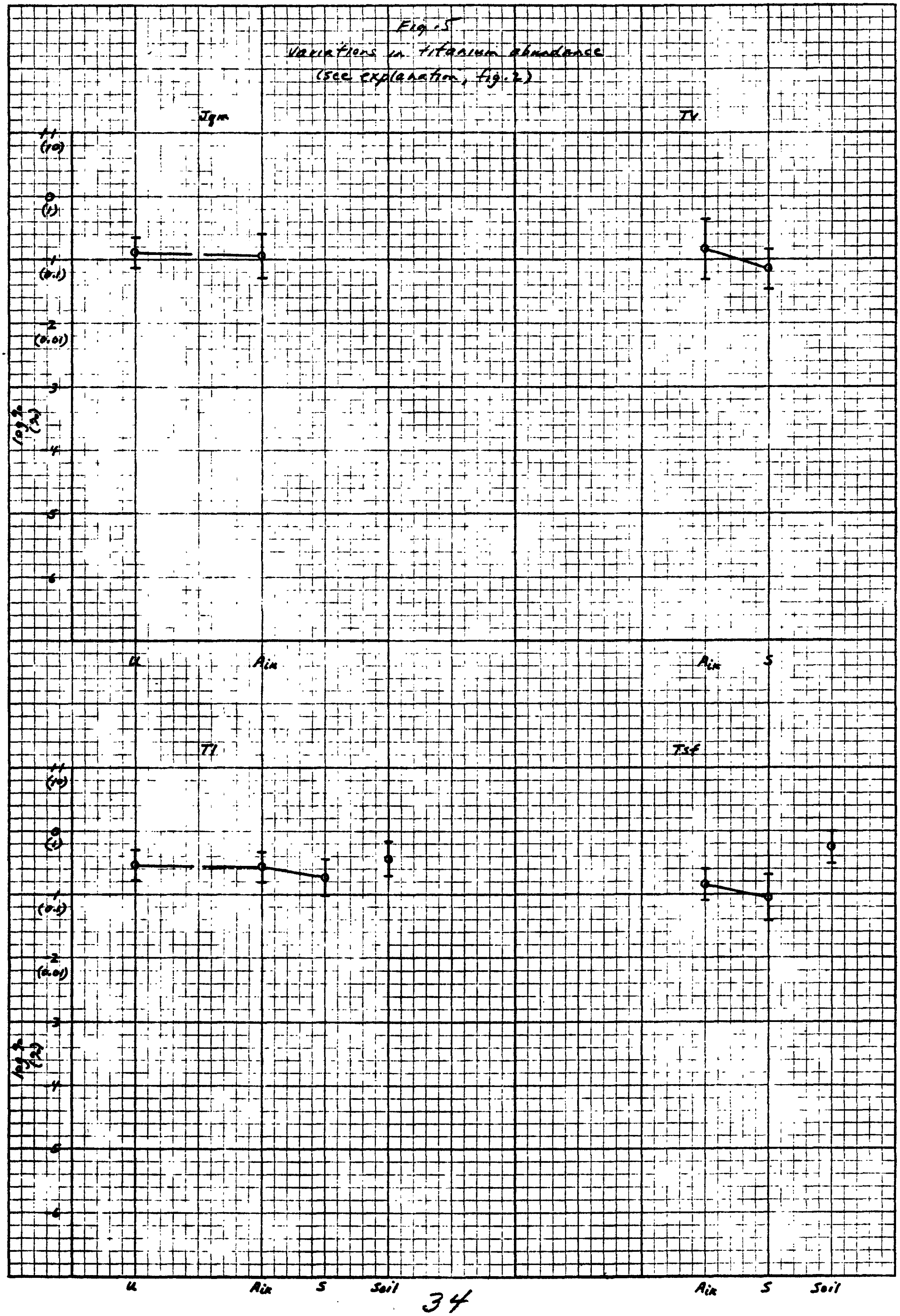
Fig. 5
Variations in titanium abundance
(see explanation, fig. 2)
Jgm
Tv
+1
(10)
0
(1)
-1
(0.1)
-2
(0.01)
-3
-4
-5
-6
log %
(%)
U
Air
Air
S
Tl
Tsf
U
Air
S
Soil
Air
S
Soil

Figure 5--Continued

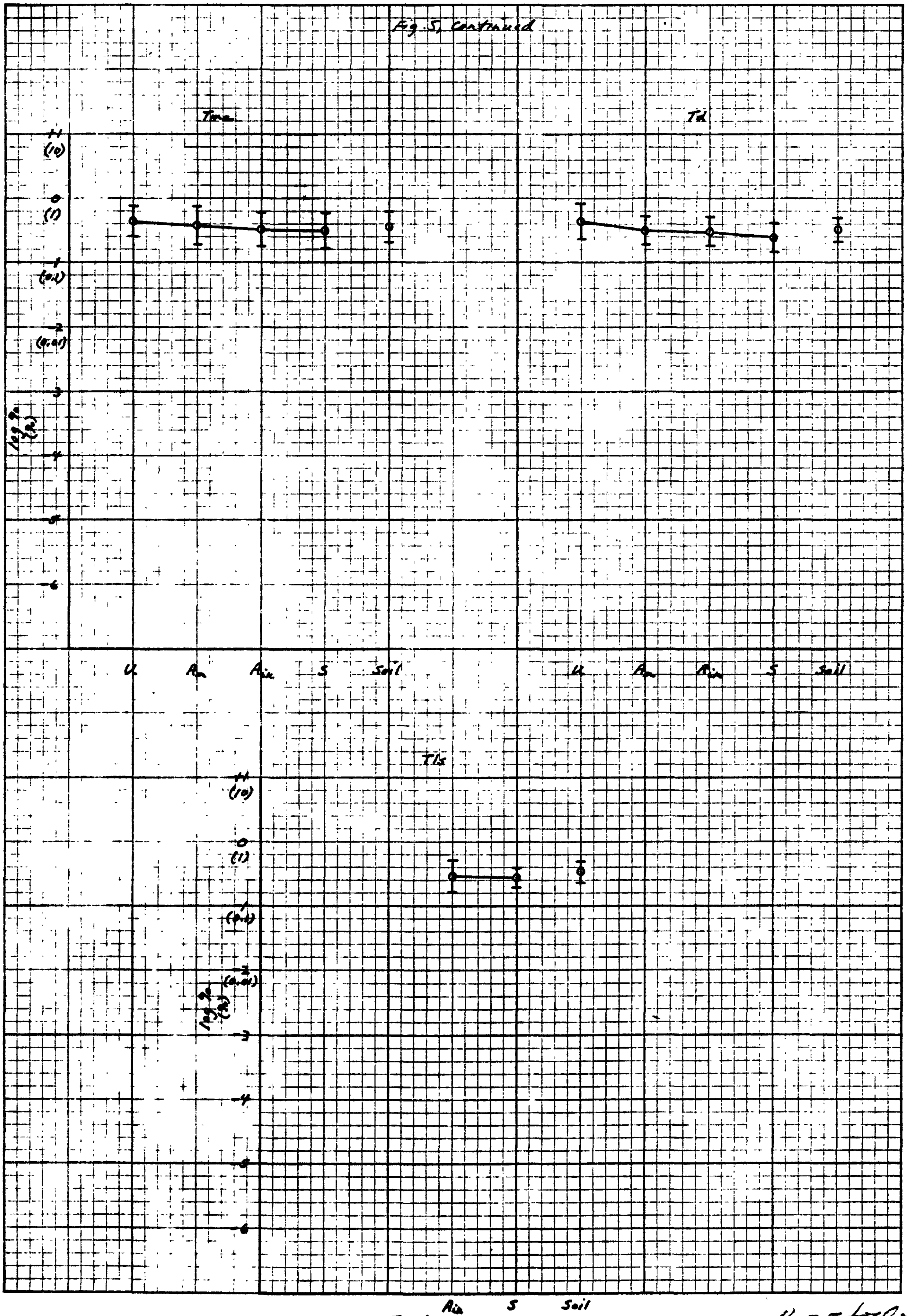

p. 35 follow

Table 6.--Titanium abundances

[Geometric mean, given in log percent, and antilog of mean, in parentheses, given in percent]

	Unaltered	Argillized montmorillonite-bearing	Argillized illite-kaolinite	Silicified
Jqm	-0.9(0.15)	—	-0.9(0.1)	—
Tv	—	—	-0.8(0.15)	-1.2(0.07)
Tl	-0.5(0.3)	—	-0.6(0.3)	-0.7(0.2)
Tsf	—	—	-0.8(0.15)	-1.1(0.09)
Tma	-0.4(0.5)	-0.4(0.4)	-0.5(0.3)	-0.5(0.3)
Td	-0.4(0.4)	-0.5(0.3)	-0.5(0.3)	-0.6(0.2)
Tls	—	—	-0.5(0.3)	-0.6(0.3)
Range (%	0.15-0.5	0.3-0.4	0.1-0.3	0.07-0.3

Ore-related elements: gold, silver, bismuth, lead, mercury, arsenic, copper, molybdenum

General

The elements Au, Ag, Bi, Pb, Hg, As, Cu, and Mo are eight of the 12 or more elements that typify the ore association at Goldfield. Of these elements, gold, silver, and lead are likely to be particularly useful for geochemical prospecting (Ashley and Albers, 1969, 1973). The other five elements will be treated here but are likely to be of limited use as geochemical indicators for various reasons. Specifically, bismuth has an unfavorably high detection threshold by the spectrographic method commonly used in exploration geochemistry, mercury anomalies tend to show low anomaly contrast, and arsenic, copper, and molybdenum are more or less concentrated with limonite, which shows erratic distribution because it represents residual iron left from supergene leaching.

The results are consistent with previous findings (Ashley and Albers, 1973) that gold, silver, lead, bismuth, mercury, and arsenic are enriched in the silicified zones that contained ore bodies, and are resistant enough to supergene leaching so that after oxidation, silicified zones still have larger quantities of these elements than do surrounding argillized rocks. On the other hand, supergene leaching strongly affects the abundance and distribution of copper, and probably of molybdenum also. The data for oxidized rocks obtained for this report show that as strength of hydrothermal alteration increases lead definitely increases; mercury definitely increases but changes are small; arsenic and molybdenum generally increase, but in some cases differences between argillized rocks and silicified rocks are small; and copper is generally unchanged, but may increase in some cases.

Gold, silver, and bismuth

Gold and silver values remain below their respective detection thresholds (0.02 or 0.1 ppm for gold and 0.5 or 1.0 ppm for silver) for all unaltered and altered rocks except for silicified rocks of the Sandstorm Rhyolite (figs. 6 and 7). These silicified rocks average 0.07 ppm gold and 0.5 ppm silver[2/] (see table 22). All the data subsets have less than 10 ppm bismuth (fig. 8). With the poor data available little can be said about these three elements, but percentages of data below the detection threshold are generally smallest for silicified rock data subsets (table 7), suggesting that amounts may increase with increasingly intense alteration.

Lead

In the latite and dacite, which yielded sufficient data for unaltered, argillized, and silicified rock subsets, lead increases with increasing intensity of alteration (fig. 9 and table 8). The geometric mean for silicified Milltown Andesite samples is not significantly larger than the geometric means for the other Milltown Andesite data subsets, but the geometric deviation is significantly larger, reflecting the fact that some silicified Milltown Andesite samples have substantially more lead than any samples in the other Milltown Andesite data subsets. The Vindicator

---

[2/] The antilog of the geometric mean for silver in this data subset is 3 ppm, but adjustment of this mean by Cohen's method yields a value the same as the detection threshold (0.5 ppm) because half the data fall below the detection threshold and the data above the detection threshold shows a large range of values.

Figure 6

Fig. 6
Variations in gold abundance
(see explanation, fig. 2)

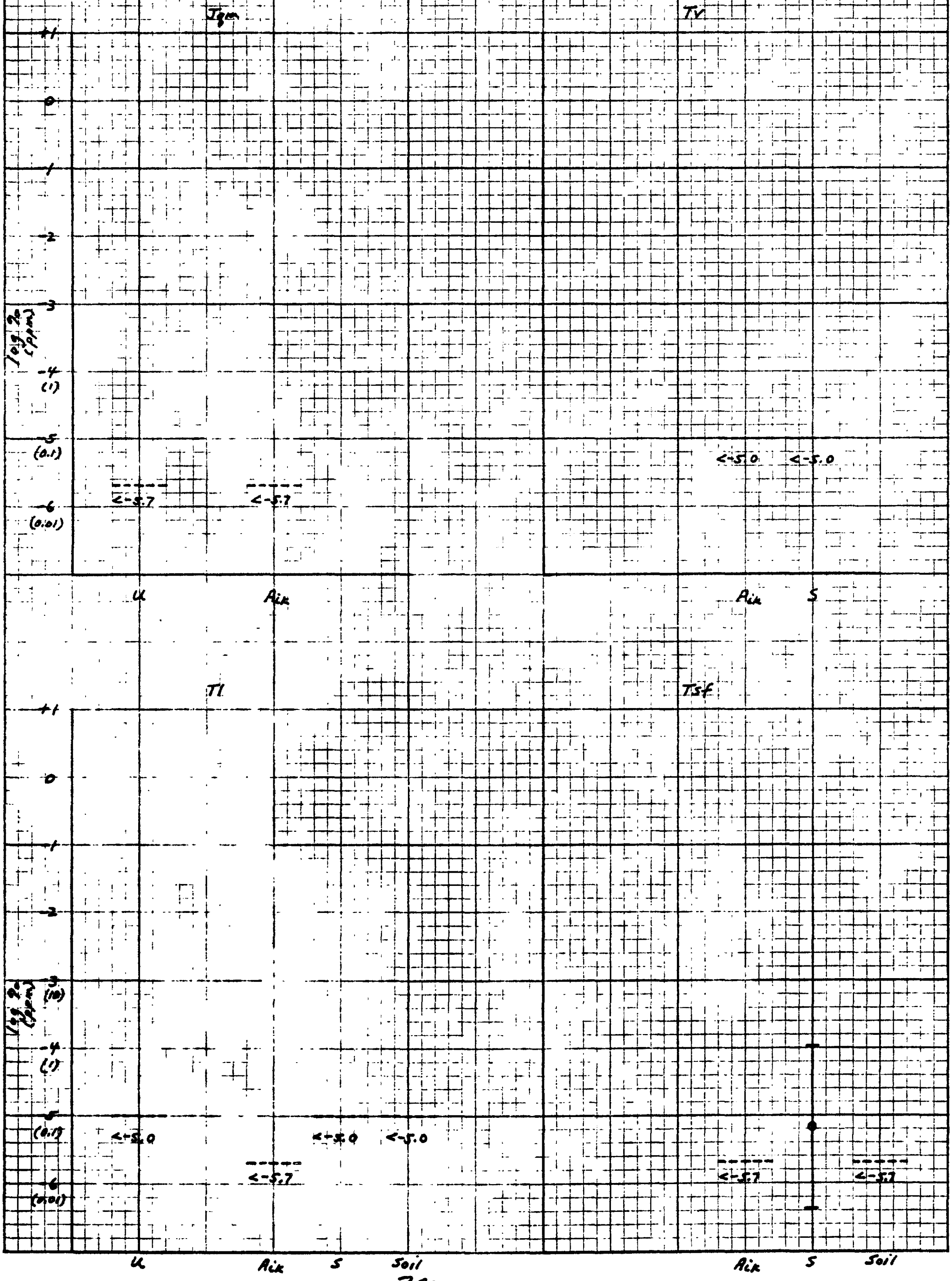

Figure 6--Continued

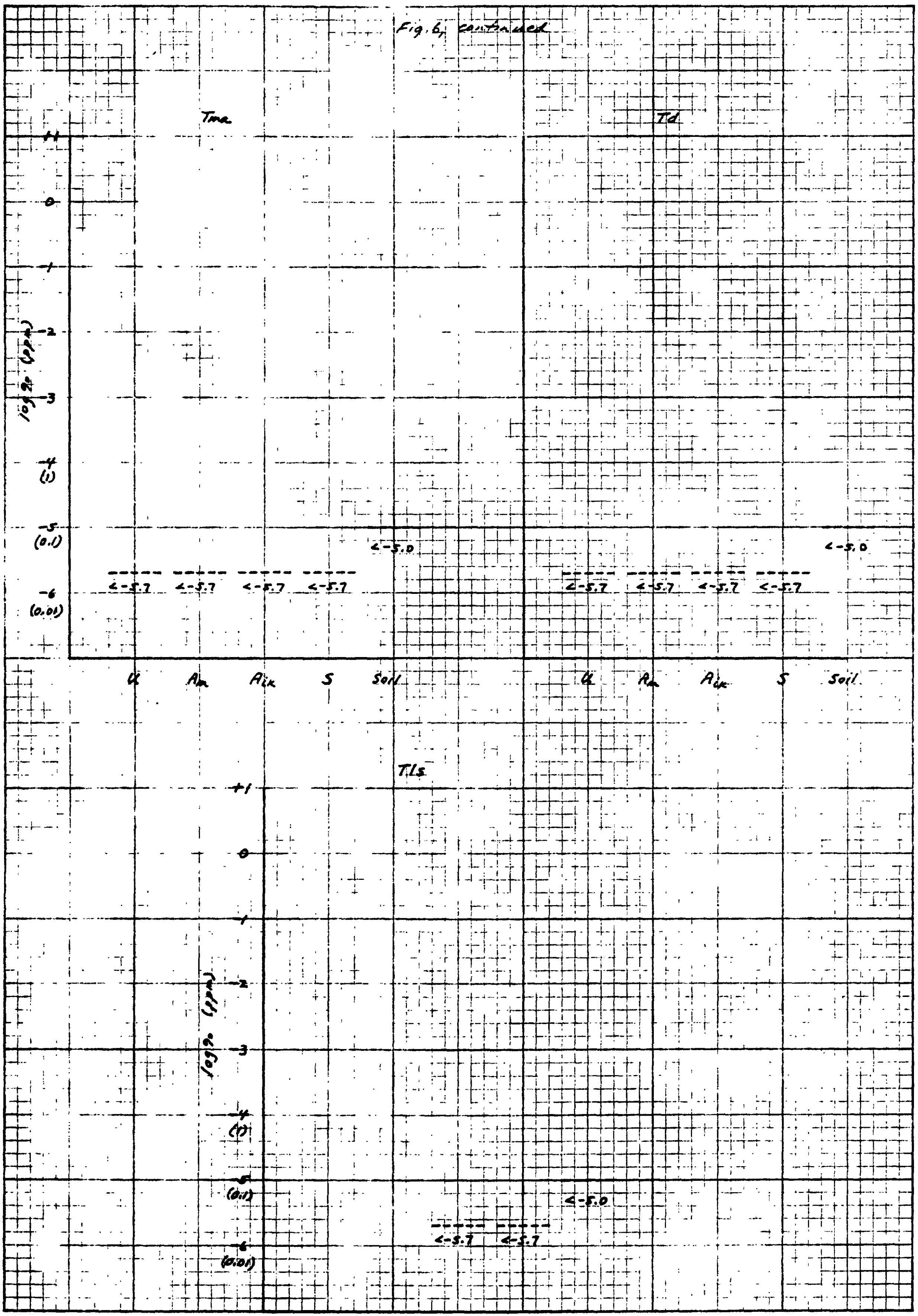

P. 39 follows

Figure 7

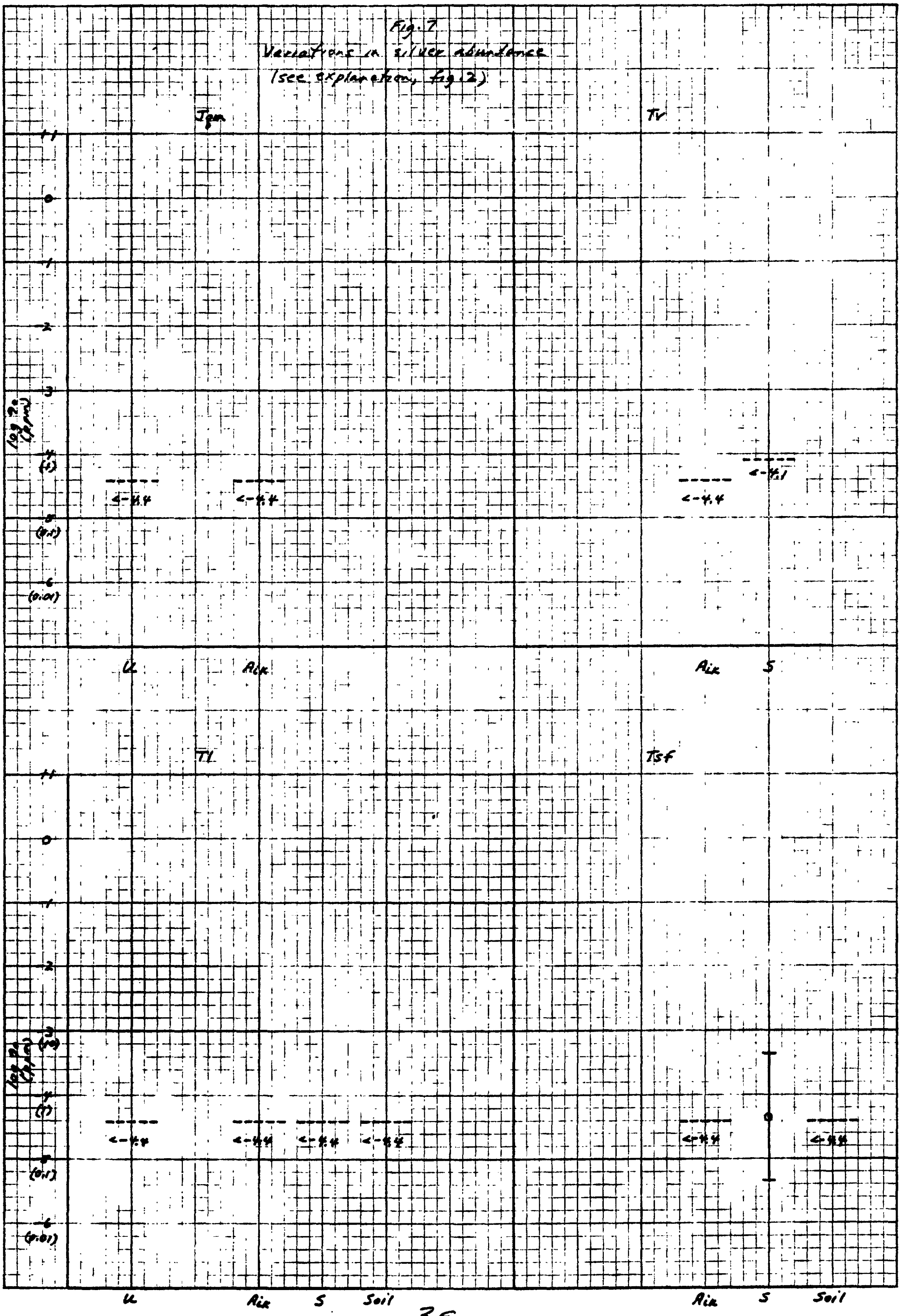

Fig. 7
Variations in silver abundance
(see explanation, fig. 2)

Figure 7--Continued

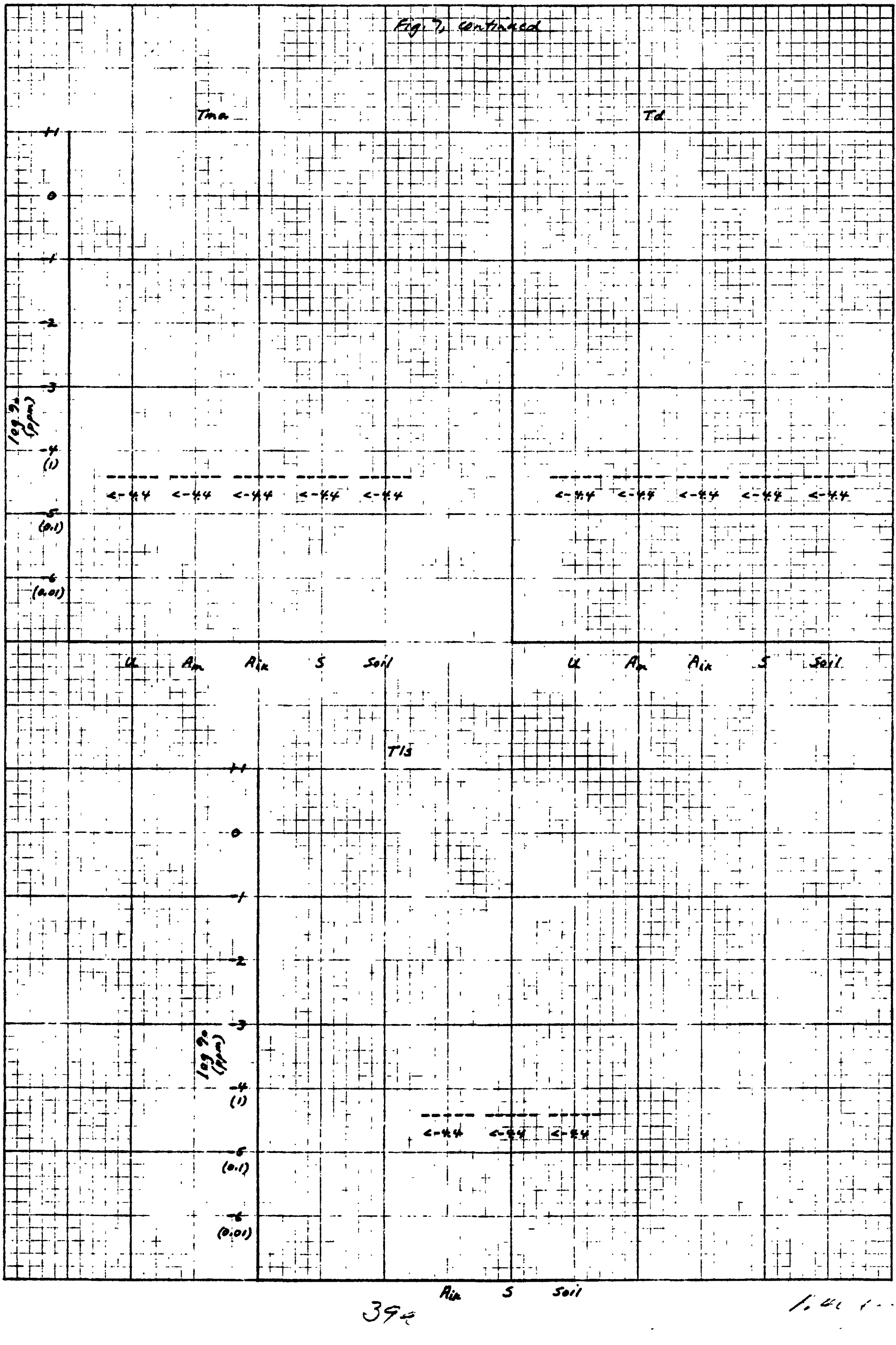

39a

Figure 8

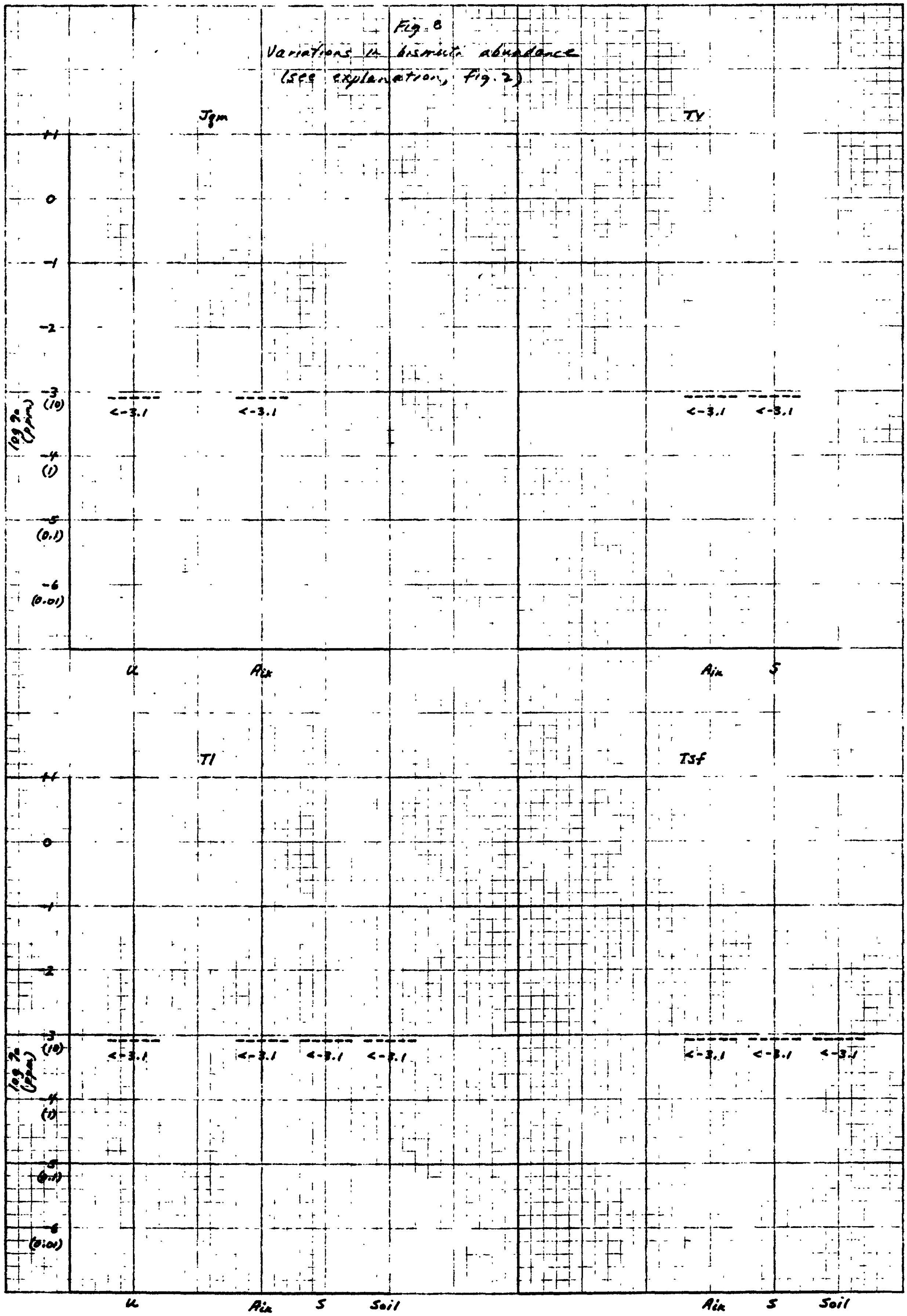

Fig. 8
Variations in bismuth abundance
(see explanation, fig. 2)

Figure 8--Continued

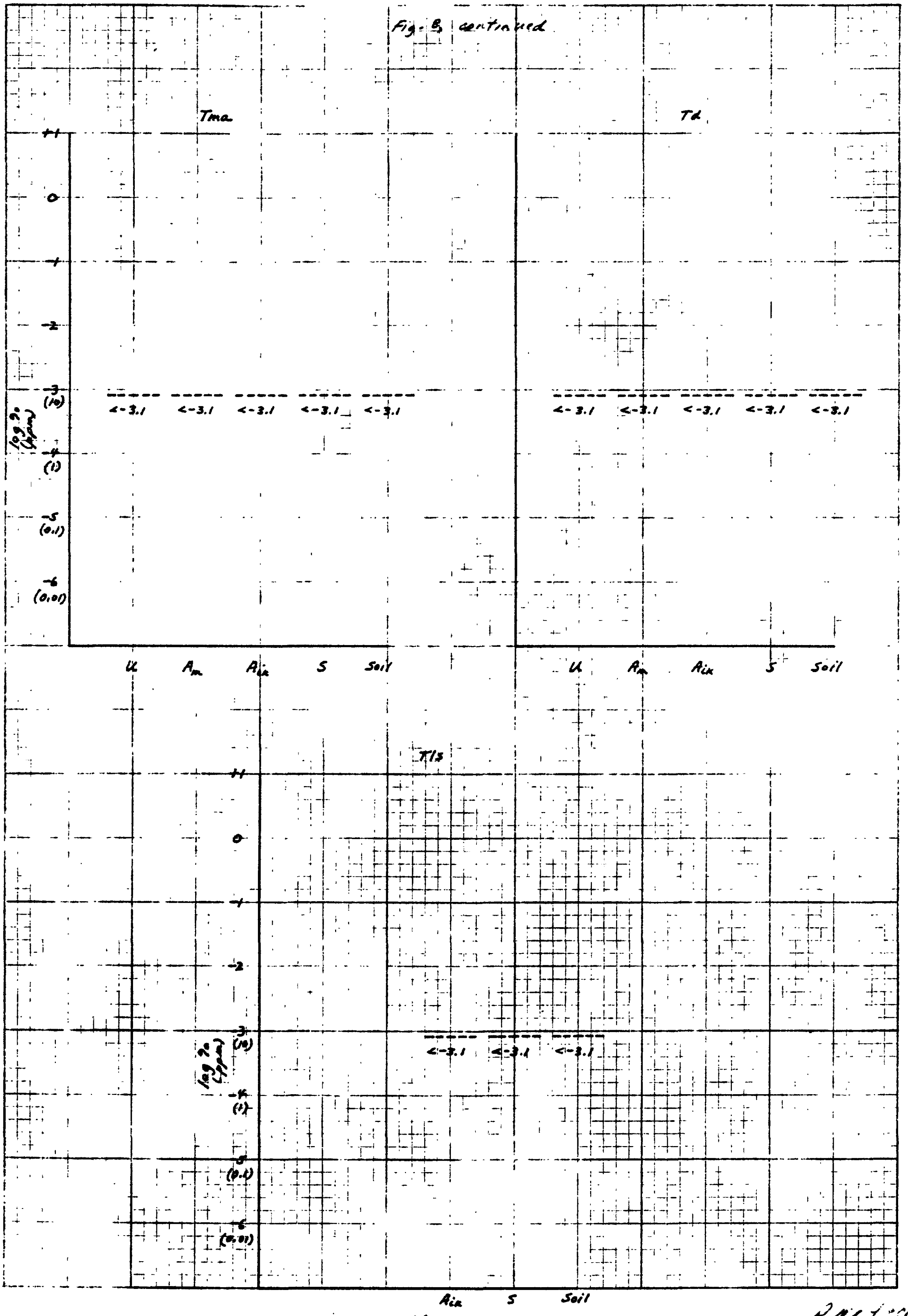

40a

P.41 follows

Table 7.--Percentage of data below detection threshold for gold, silver, and bismuth

	Unaltered	Argillized mont-bearing	Argillized	Silicified
Au, Tgm	100 (13)[1]	—	100 (13)	—
Au, TV	—	—	100 (16)	92 (13)
Au, Tl	100 (33)	—	96 (47)	94 (33)
Au, Tsf	—	—	92 (13)	38 (16)
Au, Tma	98 (82)	96 (85)	90 (124)	78 (139)
Au, Td	89 (65)	86 (51)	85 (82)	82 (88)
Au, Tls	—	—	88 (16)	86 (21)
Ag, Tgm	92 (13)	—	92 (13)	—
Ag, Tv	—	—	94 (16)	85 (13)
Ag, Tl	100 (33)	—	98 (47)	97 (33)
Ag, Tsf	—	—	92 (13)	50 (16)
Ag, Tma	99 (82)	95 (85)	98 (124)	82 (139)
Ag, Td	100 (65)	94 (51)	98 (82)	83 (88)
Ag, Tls	—	—	100 (16)	100 (21)
Bi, Tgm	92 (13)	—	85 (13)	—
Bi, TV.	—	—	100 (16)	100 (13)
Bi, Tl	100 (33)	—	98 (47)	88 (33)
Bi, Tsf	—	—	100 (13)	100 (16)
Bi, Tma	100 (82)	100 (85)	100 (124)	97 (139)
Bi, Td	100 (65)	100 (51)	100 (82)	95 (88)
Bi, Tls	—	—	100 (16)	95 (21)

[1] Number of samples in parentheses.

Figure 9

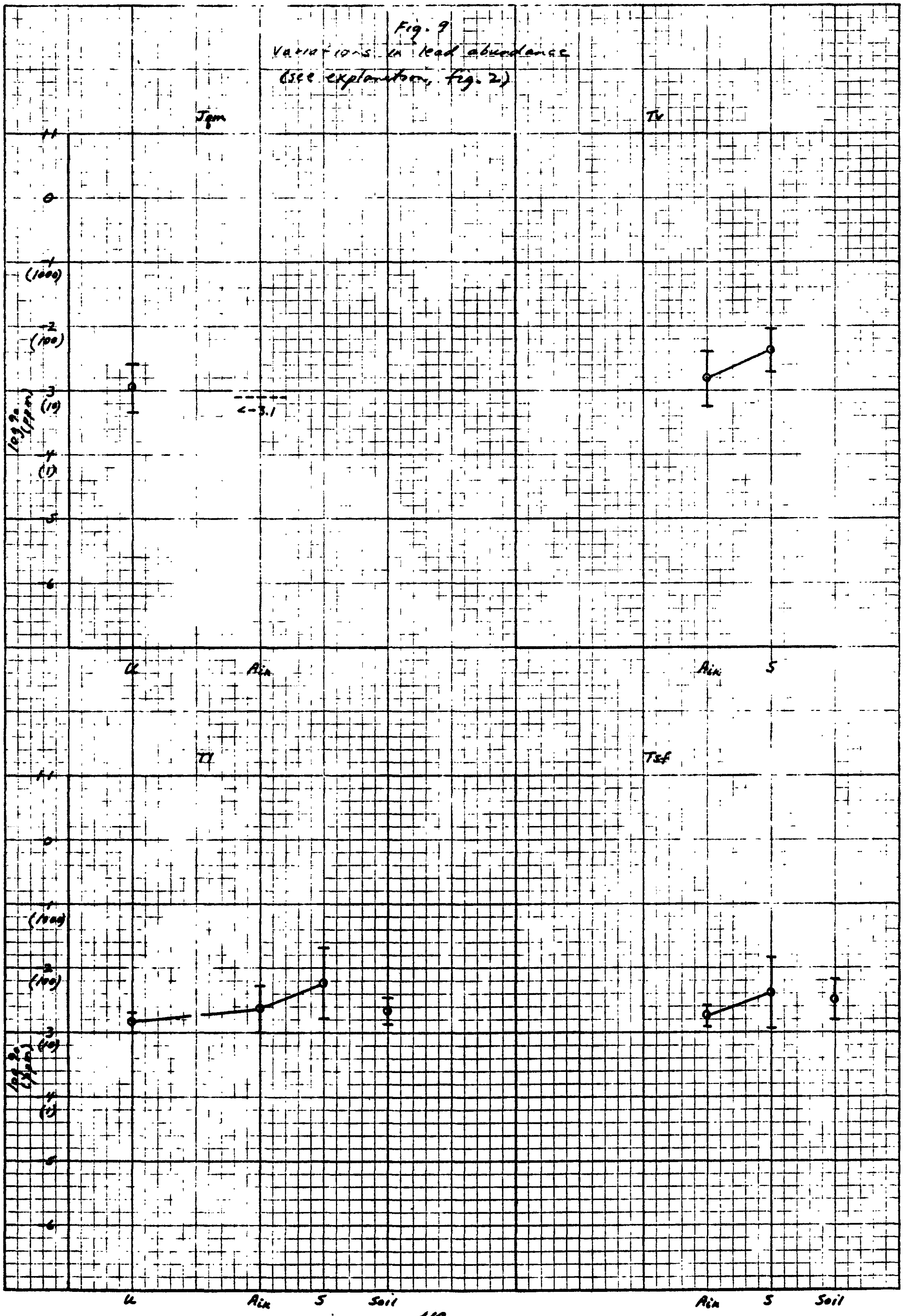
Fig. 9
Variations in lead abundance
(see explanation, fig. 2)
Jgm
Tv
1
0
-1 (1000)
-2 (100)
-3 (10)
-4 (1)
-5
-6
log ppm
<-3.1
U
Air
S
Tl
Tsf
Soil

Figure 9.--Continued

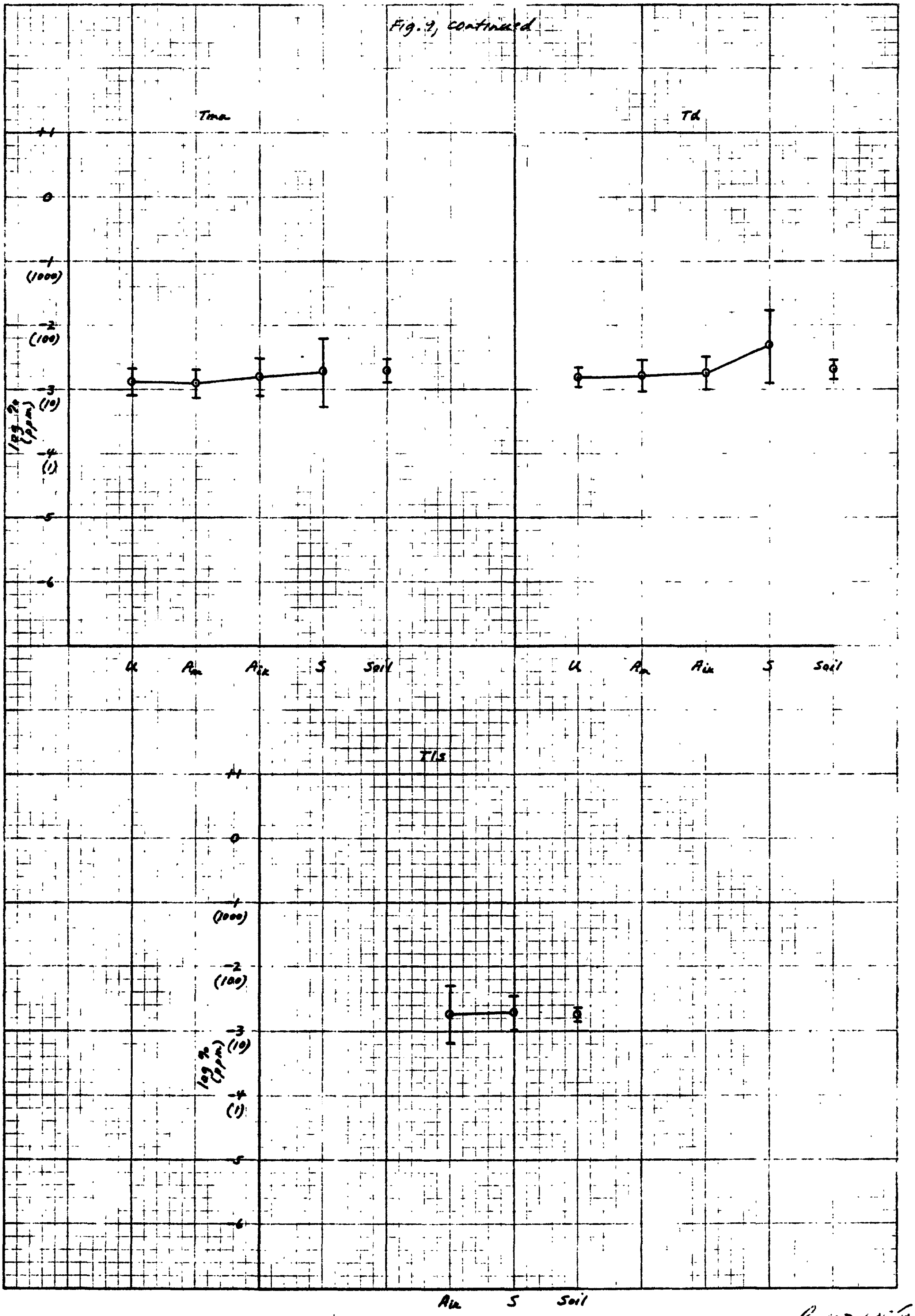

P. 43 follows

Table 8.--Lead abundances

[Geometric mean, given in log percent, and antilog of mean, in parentheses, given in ppm]

	Unaltered	Argillized, montmorillonite-bearing	Argillized illite-kaolinite	Silicified
Jgm	-3.0 (10)	—	<-3.1 (10)	—
Tv	—	—	-2.8 (15)	-2.4 (40)
Tl	-2.8 (15)	—	-2.7 (20)	-2.2 (60)
Tsf	—	—	-2.7 (20)	-2.4 (40)
Tma	-2.9 (15)	-2.9 (15)	-2.8 (15)	-2.8 (15)
Td	-2.8 (15)	-2.8 (15)	-2.7 (20)	-2.3 (50)
Tls	—	—	-2.7 (20)	-2.7 (20)
Range (ppm)	10-15[1]	15	<10-20	15-60

[1] 15 for the three Tertiary volcanic units tested.

[2] 15-20 exclusive of Jgm

Rhyolite shows more lead in silicified than in argillized rocks. The geometric means for argillized and silicified Sandstorm Rhyolite are not significantly different, but the geometric deviations are significantly different. In the andesite-dacite breccia data subsets the amounts of lead are about the same. In the case of the quartz monzonite, illite-kaolinite rocks may contain less lead than unaltered rocks, but whether or not a significant difference exists cannot be tested.

It seems unlikely that original rock composition plays an important role in determining the behavior of lead during hydrothermal alteration. The lead value for illite-kaolinite-bearing quartz monzonite is likely only slightly less than 10 ppm, so all the geometric means for lead in unaltered rocks and argillized rocks are not much different regardless of stratigraphic unit, even though the data suggest small increases with increasing intensity of alteration. In Vindicator Rhyolite, latite, and dacite, lead shows similar behavior: it increases markedly in silicified rocks; these three units had different original compositions. Some silicified Sandstorm Rhyolite samples contain notably more lead than illite-kaolinite samples from this stratigraphic unit, but not enough silicified samples are enriched in lead to produce a significant difference in the geometric means for these two Sandstorm Rhyolite data subsets. The same is true for Milltown Andesite silicified rock and illite-kaolinite rock data subsets, although Sandstorm Rhyolite and Milltown Andesite had different original compositions. The Milltown Andesite, dacite, and andesite-dacite breccia are similar in composition, but lead shows different behavior in each of these units.

Possibly the differing lead values in the various silicified rock data subsets reflect the percentages of samples that came from anomalous or ore-bearing silicified rocks. Additional sampling (data not included in this report) indeed showed that anomalous values characterize well-exposed silicified zones (veins) that produced ore, and also characterize groups of silicified zones, only some of which contained ore. The vein systems at the Sandstorm and Kendall mines (northwestern part of map, pl. 1) and McMahon Ridge (vicinity of Daisy mine, northern part of map, pl. 1) are good examples. Five of the 16 silicified Sandstorm Rhyolite samples are from the Sandstorm Kendall vein or its near vicinity, and one is from the vein system mined at the Conqueror mine, 0.6 mile northeast of the Sandstorm. These six samples (37.5 percent of the data subset) include three of the four highest values in the data subset, ranging from 150 to 500 ppm. These samples from known productive areas thus contribute most of the values that give the silicified Sandstorm Rhyolite data subset a considerably higher geometric deviation for lead than the illite-kaolinite-bearing Sandstorm Rhyolite data set. For the other units whose silicified rock subsets show relatively high averages for lead, however, samples from productive areas do not adequately explain the high geometric means. Only one of 33 silicified latite samples (3 percent), four of 88 silicified dacite samples (4.5 percent), and none of the 13 Vindicator Rhyolite samples are from productive areas. On the other hand, six of the 139 silicified Milltown Andesite samples (4.3 percent) are from known productive areas, including the McMahon Ridge vein system; although the silicified Milltown Andesite subset has a relatively large geometric deviation, silicified Milltown Andesite shows a low average lead value compared to silicified dacite, which has a similar percentage of samples from productive areas. We hope that new geochemical anomalies are at least partly responsible for the high lead values in the Vindicator Rhyolite, latite, and dacite. A new lead anomaly in the vicinity of Preble Mountain, to be described in a subsequent report, is probably partly responsible for the relatively high average lead value in silicified dacite.

Mercury

Mercury remains the same or shows slight increases with increasing intensity of alteration (fig. 10). The geometric means for mercury in rocks showing the same degree of hydrothermal alteration are rather similar regardless of stratigraphic unit, although the maximum and minimum values for each column of table 9 except montmorillonite-bearing rocks are significantly different statistically. Units such as the latite and dacite have relatively small amounts of mercury in every alteration category, suggesting that original rock type had some influence on the behavior of mercury during alteration. The silicified Sandstorm Rhyolite data subset shows the largest mercury content. The six samples in this data set that came from the productive areas mentioned in the section above account for several but not all of the high values in this data subset. Differences between mercury content of silicified rocks from the other stratigraphic units do not follow the pattern shown by lead, and do not suggest any consistent geographic variations.

Figure 10

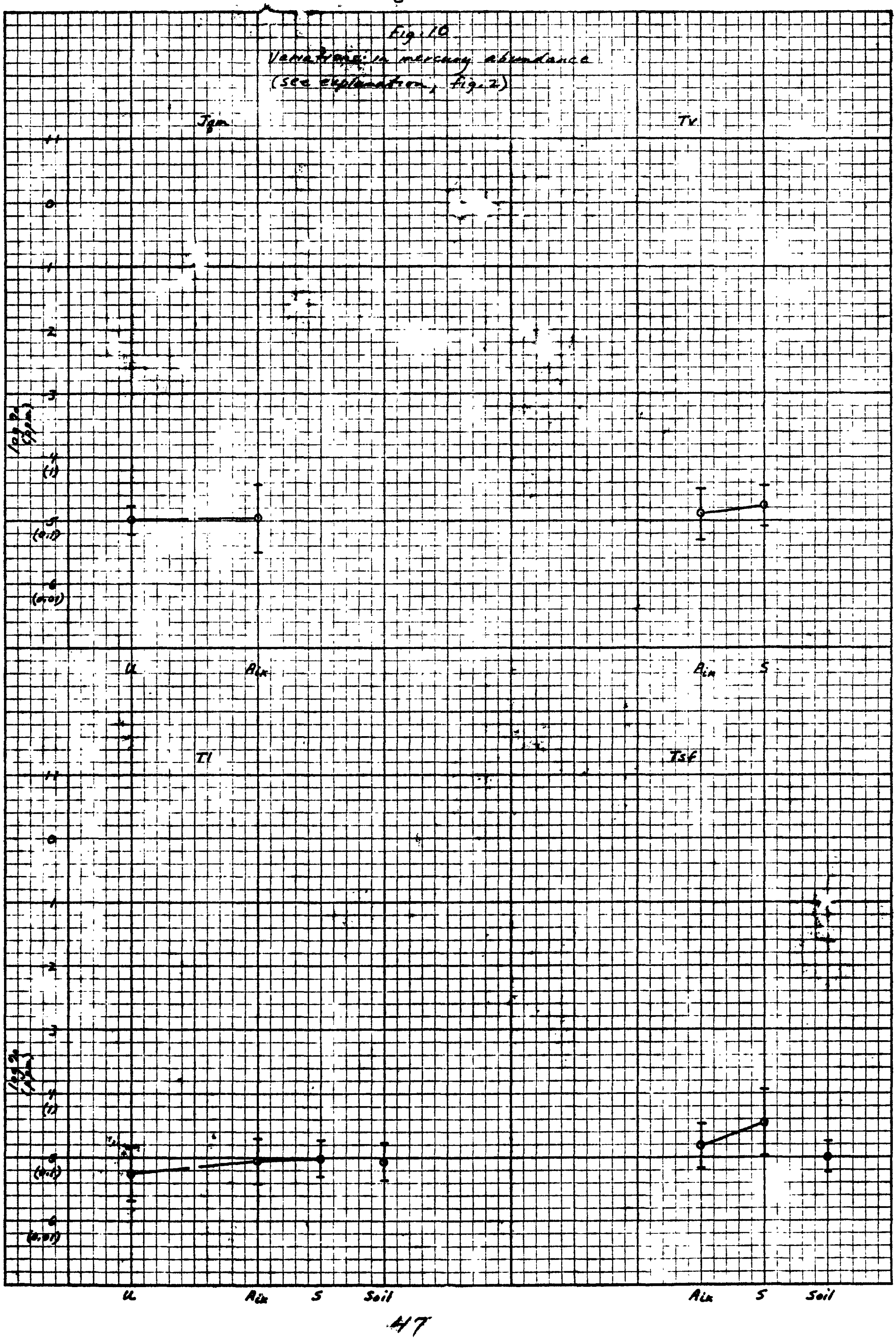
Fig. 10
Variations in mercury abundance
(see explanation, fig. 2)
Tgm
Tv
log Hg (ppm)
+1
0
1
2
3
4 (1)
5 (0.1)
6 (0.01)
U
Alx
Ain
S
Tl
Tsf
log Hg (ppm)
+1
0
1
2
3
4 (1)
5 (0.1)
6 (0.01)
U
Alx
S
Soil
Alx
S
Soil

Figure 10--Continued

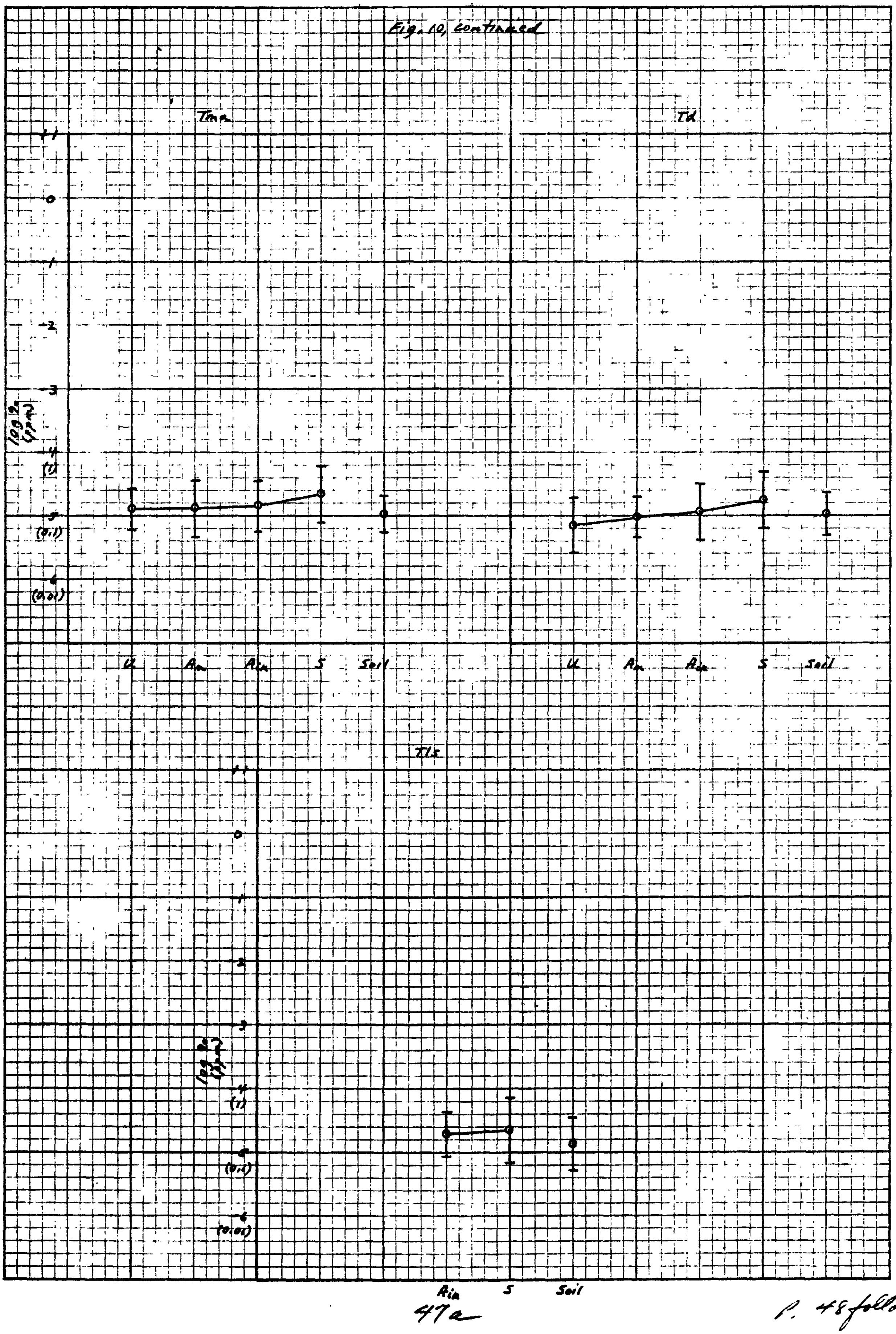

P. 48 follow

Table 9.--Mercury abundances

[Geometric mean, given in log percent, and antilog of mean, in parentheses, given in ppm]

	Unaltered	Argillized montmorillonite-bearing	Argillized illite-kaolinite	Silicified
Tgm	-5.0(0.1)	—	-5.0(0.1)	—
Tv	—	—	-4.9(0.15)	-4.8(0.15)
Tl	-5.3(0.06)	—	-5.1(0.09)	-5.0(0.1)
Tsf	—	—	-4.8(0.15)	-4.4(0.4)
Tma	-4.9(0.15)	-4.9(0.15)	-4.8(0.15)	-4.7(0.2)
Td	-5.2(0.07)	-5.0(0.1)	-4.9(0.1)	-4.8(0.2)
Tls	—	—	-4.7(0.2)	-4.7(0.2)
Range (ppm)	0.06-0.15	0.1-0.15	0.09-0.2	0.1-0.4

Arsenic

Arsenic probably generally increases in abundance with progressive alteration, but in the Sandstorm Rhyolite, Milltown Andesite, and andesite-dacite breccia, the amounts in illite-kaolinite and silicified rocks are not significantly different (fig. 11, table 10). The majority of samples in many data subsets contain less than 10 ppm arsenic, so we cannot verify rigorously that enrichment exists or determine the degree of enrichment in silicified rocks relative to unaltered rocks.

Comparisons made for arsenic between stratigraphic units yield essentially the same results as the comparisons made above for mercury, even though data for unaltered and montmorillonite-bearing rocks are not as good as for mercury, and absolute amounts of arsenic are generally about 100 times larger than coexisting amounts of mercury. The only notable exception is that silicified Vindicator Rhyolite and silicified Sandstorm Rhyolite contain essentially the same amounts of arsenic.

Copper and molybdenum

In all stratigraphic units except the latite, amounts of copper in silicified rocks are not significantly different from amounts in illite-kaolinite rocks (fig. 12, table 11); in the latite, silicified rocks contain significantly more copper than illite-kaolinite rocks. The dacite is the only unit in which significantly more molybdenum definitely occurs in silicified rocks than in illite-kaolinite rocks (fig. 13, table 12; amounts of molybdenum exceed the 2 ppm detection threshold in only six subsets). On the other hand, we have no good indication that silicified rocks contain less molybdenum than argillized rocks in any unit.

Figure 11

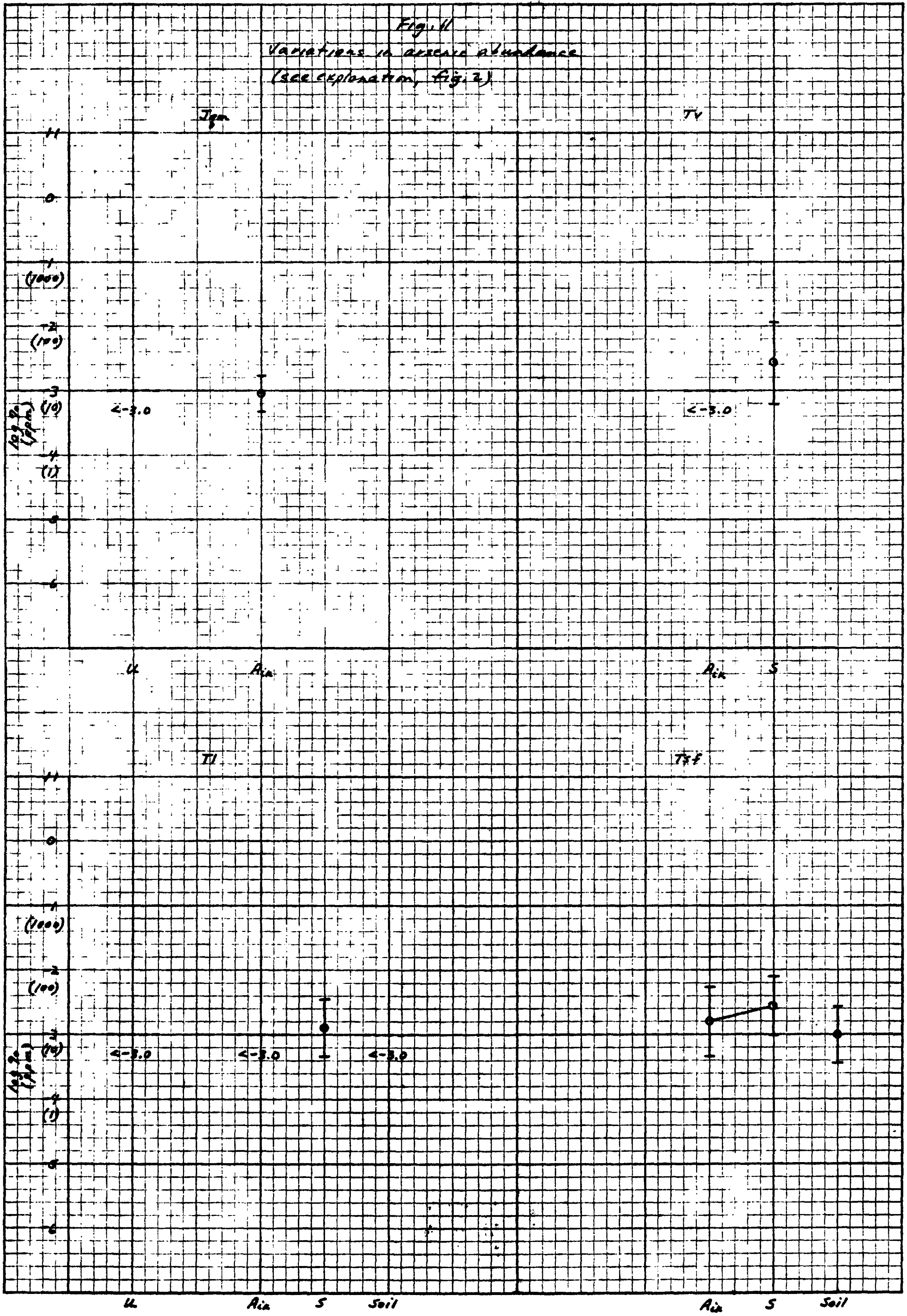
Fig. 11
Variations in arsenic abundance
(see explanation, fig. 2)
Jgm
Tv
+1
0
-1
(1000)
-2
(100)
-3
(10)
-4
(1)
-5
-6
log %
(ppm)
<-3.0
<-3.0
U
Air
Air
S
Tl
Tsf
<-3.0
<-3.0
<-3.0
U
Air
S
Soil
Air
S
Soil

Figure 11--Continued

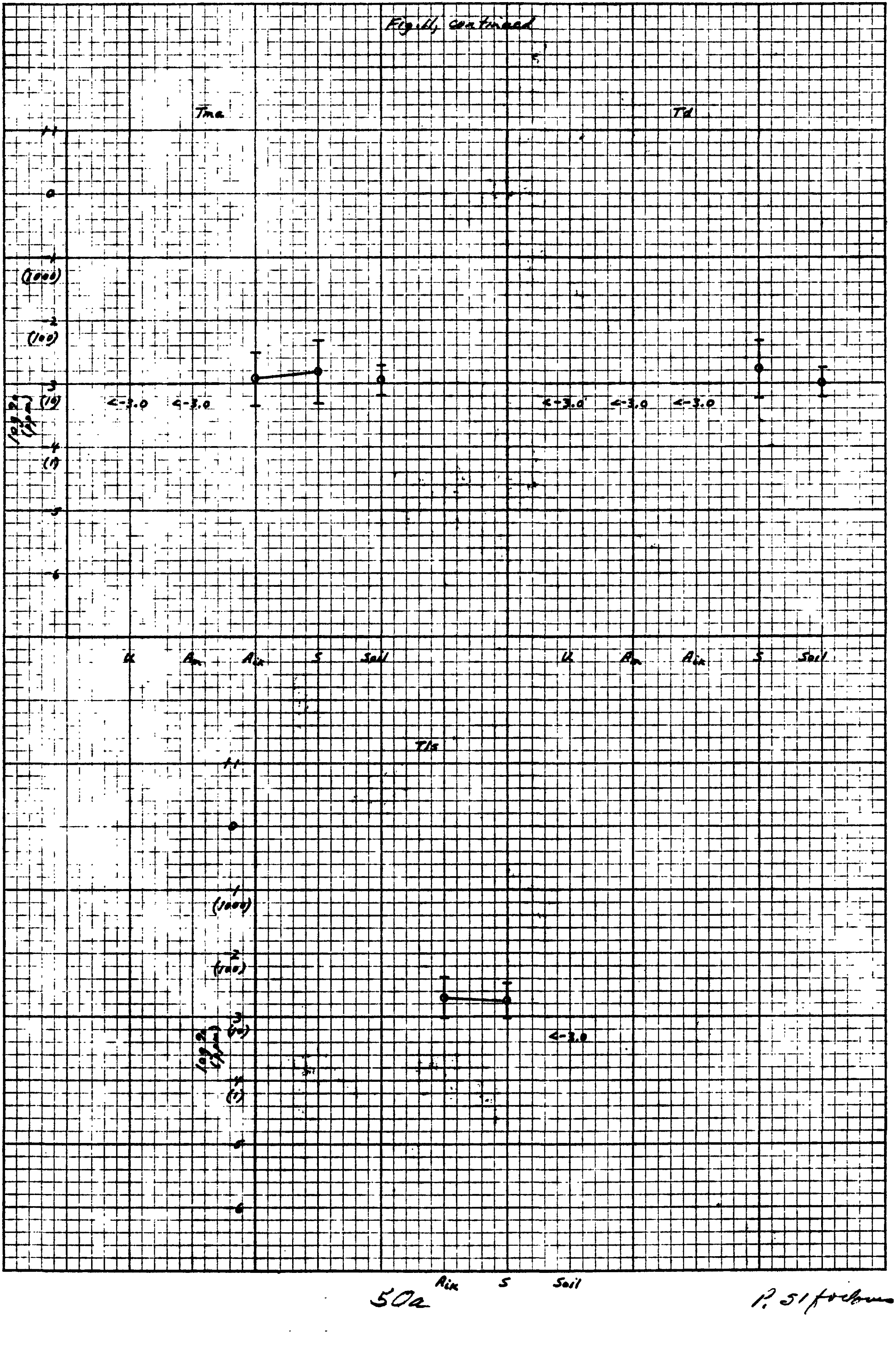

P. 51 follows

Table 10.--Arsenic abundances

[Geometric mean, given in log percent, and antilog of mean, in parentheses, given in ppm]

	Unaltered	Argillized montmorillonite-bearing	Argillized illite-kaolinite	Silicified
Jgm	<-3.0 (10)	—	-3.0 (9)	—
Tv	—	—	<-3.0 (10)	-2.6 (30)
Tl	<-3.0 (10)	—	<-3.0 (10)	-2.9 (15)
Tsf	—	—	-2.8 (15)	-2.6 (30)
Tma	<-3.0 (10)	<-3.0 (10)	-2.9 (10)	-2.8 (15)
Td	<-3.0 (10)	<-3.0 (10)	<-3.0 (10)	-2.8 (15)
Tls	—	—	-2.7 (20)	-2.8 (20)
Range (ppm)	All <10	All <10	<10-20	15-30

Figure 12

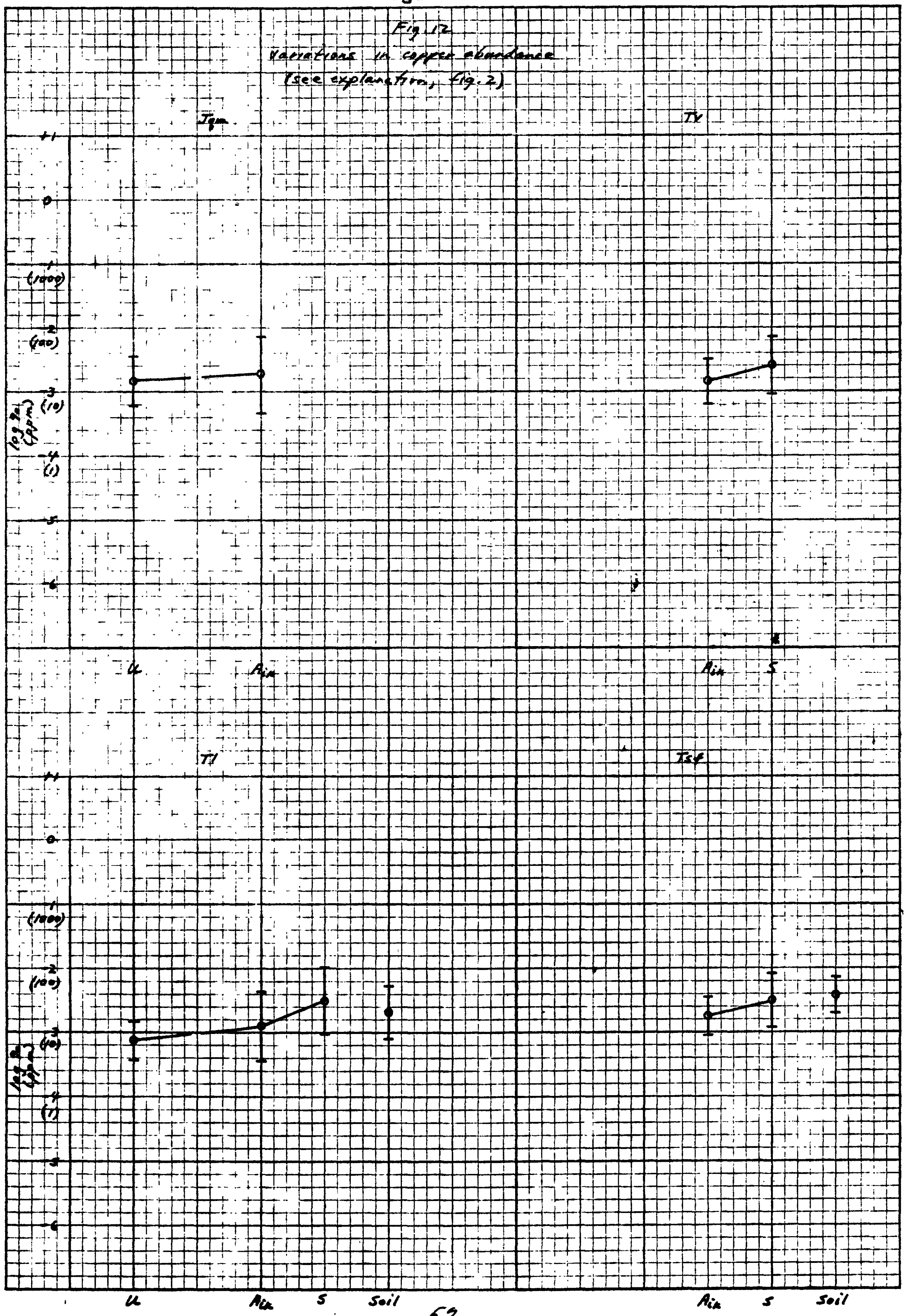
Fig. 12
Variations in copper abundance
(see explanation, fig. 2)

Figure 12--Continued

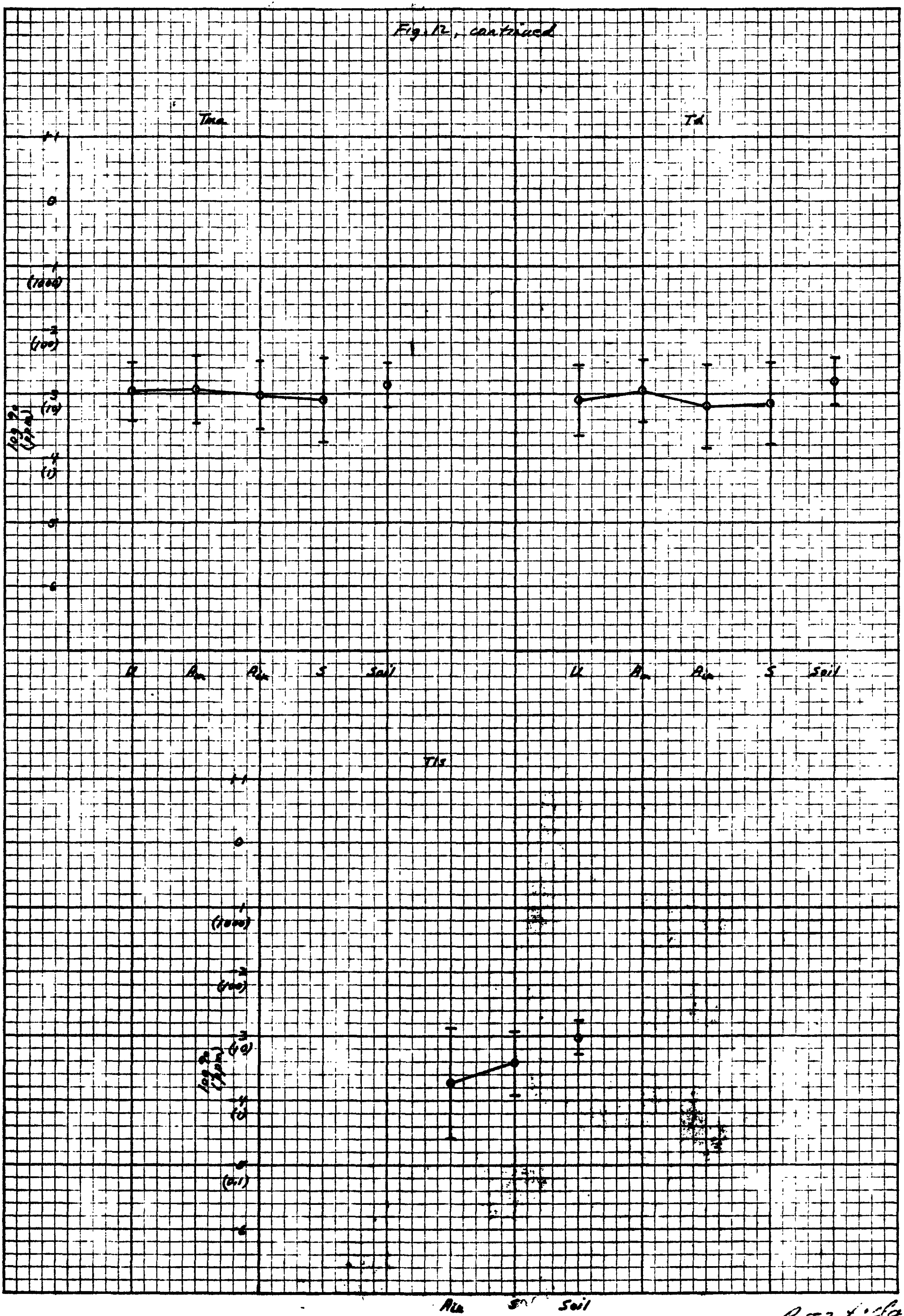

P.53 f [illegible]

Table 11.--Copper abundances

[Geometric mean, given in log percent, and antilog of mean, in parentheses, given in ppm]

	Unaltered	Argillized montmorillonite-bearing	Argillized illite-kaolinite	Silicified
Tgm	-2.8 (15)	—	-2.7 (20)	—
Tv	—	—	-2.9 (15)	-2.6 (30)
Tl	-3.1 (8)	—	-2.9 (10)	-2.5 (30)
Tsf	—	—	-2.8 (15)	-2.5 (30)
Tma	-3.0 (10)	-2.9 (10)	-3.0 (10)	-3.1 (8)
Td	-3.1 (8)	-3.0 (10)	-3.2 (7)	-3.2 (7)
Tls	—	—	-3.7 (2)	-3.4 (4)
Range (ppm)	8-15	10	2-20	4-30

Figure 13

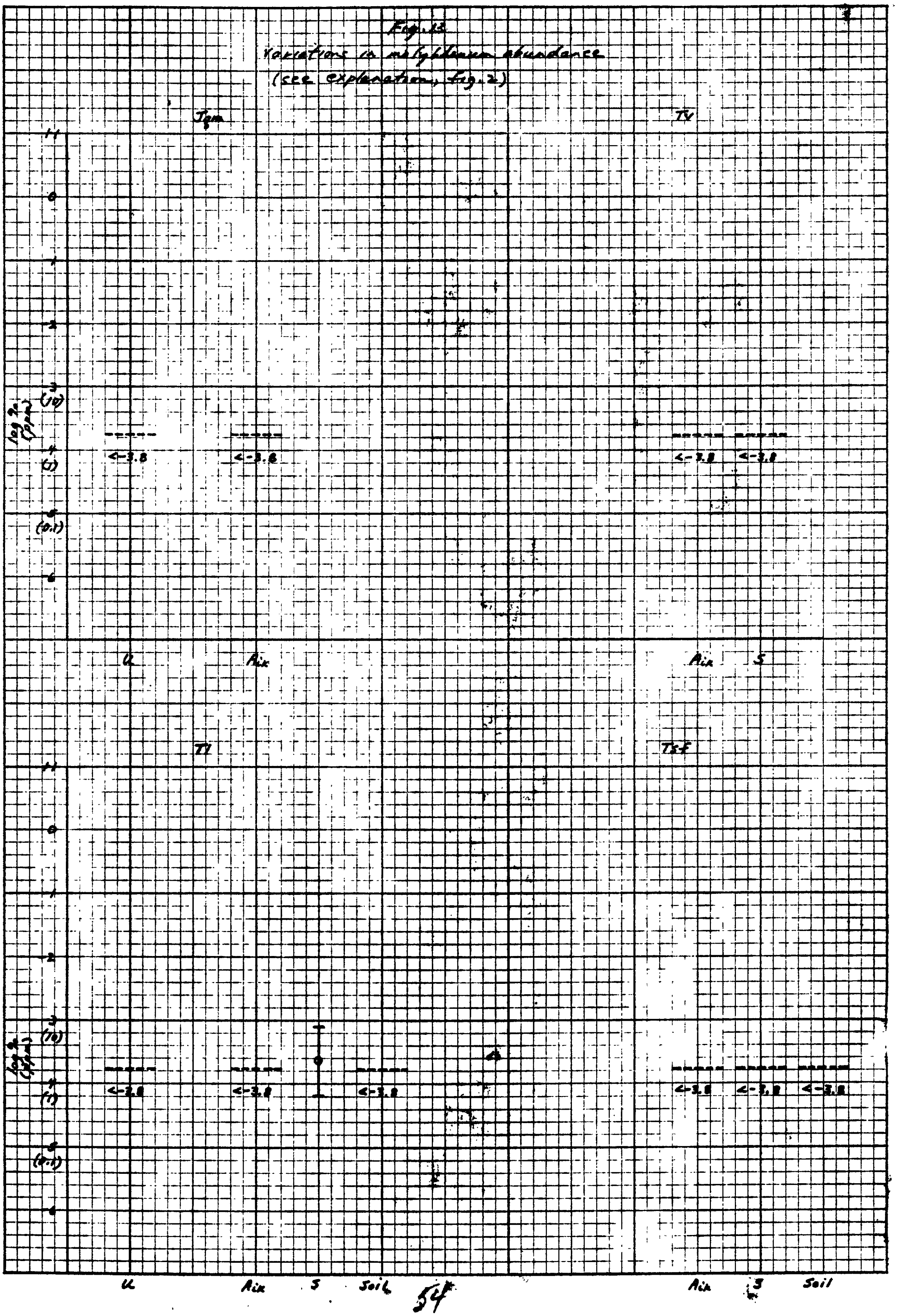

Fig. 13
Variations in molybdenum abundance
(see explanation, Fig. 2)

Figure 13--Continued

Table 12.--Molybdenum abundances

[Geometric mean, given in log percent, and antilog of mean, in parentheses, given in ppm]

	Unaltered	Argillized montmorillonite-bearing	Argillized illite-kaolinite	Silicified
Jgm	<-3.8 (2)	—	<-3.8(2)	—
Tv	—	—	<-3.8 (2)	≤-3.8(2)
Tl	≤-3.8 (2)	—	≤-3.8(2)	-3.7 (2)
Tsf	—	—	<-3.8(2)	<-3.8 (2)
Tma	≤-3.8 (2)	<-3.8(2)	-3.7 (2)	-3.6 (3)
Td	≤-3.8 (2)	<-3.8(2)	-3.7(2)	-3.5 (3)
Tls	—	—	≤-3.8(2)	-3.5 (3)
Range (ppm)	All <2	All<2	<2 - 2	<2 - 3

In our earlier study (Ashley and Albers, 1973) we found that copper and molybdenum, although certainly more abundant in ore-bearing silicified rocks than in adjacent illite-kaolinite rocks before oxidation, were leached so strongly during oxidation that the oxidized silicified and argillized rocks now contain nearly equal amounts of copper, and the silicified rocks contain less molybdenum than the argillized rocks.

Where copper and molybdenum occur in larger amounts in silicified rocks than they do in illite-kaolinite rocks, the unexpectedly high values are probably due to the sampling bias described in the section on iron (see above), because copper and molybdenum are particularly strongly associated with limonite (Ashley and Albers, 1973). Furthermore, correlation coefficients determined for copper, molybdenum, arsenic, and iron in silicified latite, Milltown Andesite, dacite, andesite-dacite breccia, and all silicified rocks show that copper and iron are strongly correlated in four of these five data subsets, and molybdenum and iron are strongly correlated in three (including "all silicified rocks" in both cases). Arsenic may also be associated with limonite. It is likely, however, that in the three units where arsenic is probably most abundant in silicified rocks, hypogene enrichment of arsenic is more important than supergene coprecipitation with limonite, because arsenic and iron are correlated in only one of the five data subsets mentiond above. (See also, discussion of behavior in Ashley and Albers, 1973.)

Illite-kaolinite rocks and silicified rocks show distinctly different copper concentrations in different stratigraphic units (table 11). The quartz monzonite, Vindicator Rhyolite, latite, and Sandstorm Rhyolite show similar values, with 10-20 ppm in illite-kaolinite rocks and 30 ppm in silicified rocks. The Milltown Andesite and dacite show similar and distinctly lower values, with 10 and 7 ppm in illite-kaolinite rocks and 8 and 7 ppm in silicified rocks. The altered andesite-dacite breccia contains less copper than any of the other units, with 2 and 4 ppm in the two available subsets. In spite of possible sampling bias in the case of silicified rocks, the fact that illite-kaolinite rocks and silicified rocks show similar relationships indicates that these differences are real, even if the values for the silicified rocks are somewhat higher than they should be. Differences in original rock type cannot be responsible, because Milltown Andesite and andesite-dacite breccia are lithologically similar. Also, unaltered latite and unaltered dacite are not much different in major element composition, and they contain about the same amounts of copper, but altered latite contains considerably more copper than similarly altered dacite. The only explanation we can offer is that many of the Milltown andesite and dacite samples and all of the andesite-dacite breccia samples have been exposed to supergene conditions longer, and are therefore more strongly leached than samples from the other units (see introduction).

The quartz monzonite, Vindicator Rhyolite, latite, and Sandstorm Rhyolite all occur mainly in the central and western parts of the area, which are presently being subjected to supergene alteration for the first time. The majority of Milltown Andesite and dacite samples are from the southwestern and south-central parts of the area, which have been subjected to supergene alteration twice, and some are from the northern part of the area, which has been subjected to supergene alteration once or twice. The andesite-dacite breccia is restricted to the southeastern part of the area, which has been subjected to supergene alteration three times. Thus, rocks that have been exposed to supergene conditions only once, and presumably for the shortest period of time, have the largest amounts of copper, whereas rocks that have been exposed to supergene conditions on three occasions, and presumably for the longest period of time, have the smallest amounts of copper. Even the units that have been subjected to supergene leaching for the shortest periods of time have probably already lost most of the copper they received during hydrothermal alteration, because downward-percolating waters during the first period of oxidation should have low pH's and high Eh's due to breakdown of pyrite. Copper sulfides are highly soluble under such conditions (Garrels and Christ, 1965, p. 240; Hansuld, 1966). Copper was probably less mobile during subsequent periods of oxidation, which involved little or no destruction of pyrite, but copper still shows significant solubility at pH's near 7 and the moderate Eh's typical of common weathering environments. It is reasonable to expect, therefore, that copper leaching would proceed rapidly while pyrite was being oxidized but would continue at a reduced rate after all the available pyrite had been consumed.

Considering molybdenum variations between stratigraphic units, only the Milltown Andesite and dacite yielded enough data above the detection threshold (2 ppm) to calculate geometric means for illite-kaolinite rocks; the two values are not significantly different (table 12). Four units yielded geometric means for silicified rocks, but again these values are not significantly different. Geometric means cannot be calculated for any other data subsets. Although in our previous study (Ashley and Albers, 1973) we found a number of similarities in the behavior of copper and molybdenum, there are no obvious similarities between table 11 and table 12.

Background and anomalous values for the ore-related elements

General

The purpose of this section is to provide guidelines for evaluating geochemical data from the Goldfield altered area. From previous work (Ashley and Albers, 1973), we feel that collecting bedrock samples from silicified zones is the approach most likely to yield positive results, so we will discuss only geochemical data for silicified rocks. Regarding Au, Ag, Pb, Bi, Hg, As, Cu, and Mo, we believe that gold, silver, and lead are indispensable for geochemical prospecting at Goldfield. Bismuth and mercury may provide interesting additional data. Copper and molybdenum are of dubious value because they are leached and redistributed during oxidation. Arsenic apparently shows some behavior similar to that of the first five elements, but it also is capable of considerable supergene mobility. We prefer to group it with copper and molybdenum.

Definition of background and anomalous values

A number of methods have been used for distinguishing anomalous values from geochemical background[3]. Several methods are summarized by Hawkes and Webb (1962, p. 22-31). Determination of a threshold value is most clear cut where an element shows a bimodal frequency distribution, in which the lower mode clearly represents values found in unmineralized rocks, and the upper mode clearly represents values from mineralized rocks. In this case the minimum frequency point between the two modes provides the threshold value separating anomalous values from background values. The course of action is also clear where the frequency distribution shows positive skewness (a long tail toward higher values), especially if the data have been log transformed: here the threshold value is the point at which the abnormally long upper tail of the distribution departs from a normal distribution fit to the main mass of

---

[3] Because we are interested merely in classifying data values as anomalous or otherwise, for simplicity we refer to all values below the threshold value as "background." This differs somewhat from Lepeltier's (1969) usage, in which "background" for an element is the median value. Hawkes and Webb (1962) refer to the "background range" in talking about all values that are not anomalous; they use "background" to refer to a mean or median value. For those who prefer this strict definition of the term "background," table 13 includes the appropriate information. Our usage of "background" and "threshold" accords with definitions given by Andrews-Jones (1968).

the data. Lepeltier (1969) and Wedow and Ericksen (1971) have recently described use of log-probability graphs to determine threshold values in such cases. Histograms and log-probability plots for almost all the elements in the silicified rock subsets considered here, however, show essentially unimodal distributions without breaks that could be significant in terms of metallization[4/]. Faced with this situation, we decided to define threshold values for each element in each silicified rock subset by methods modified from Hawkes and Webb (1962, p. 30-31), as follows. For subsets in which 50 percent or more of the data for a given

---

[4/] Log-probability plots were made for all eight ore-related elements for silicified latite, Milltown Andesite, dacite, and all silicified rocks. We constructed 95-percent-confidence level envelopes around visually best-fit lines to detect significant breaks in slope, using the graphical method described by Lepeltier (1969). For silicified Vindicator Rhyolite, Sandstorm Rhyolite, and andesite-dacite breccia, we did not prepare log-probability plots for more than a few elements, because too few samples exist to plot confidence limits; with few samples, confidence envelopes are very wide. Only two log-probability plots show a significant excess of high values: those for mercury in dacite and mercury in all silicified rocks. These plots yield threshold values of -4.1 log percent (0.8 ppm) and -3.9 log percent (1.4 ppm) respectively, compared with -3.9 and -3.8 log percent by the method described below, which yield the 1.4 and 1.5 ppm figures shown for dacite and all silicified rocks in table 13. The plot for gold in all silicified rocks shows an excess of high values above the 97.7 percentile. This break occurs at such a high percentile that we cannot tell whether it is significant, using Lepeltier's (1969) method for constructing the confidence envelope.

element is above the lower detection limit, values greater than or equal to two geometric deviations above the geometric mean (2.3 percent of the values in a lognormal distribution) are considered anomalous. All values less than one geometric deviation above the geometric mean (84 percent of the values in a lognormal distribution) are considered background, with no qualifications. Values between one and two geometric deviations above the geometric mean are, strictly speaking, background values, but because all the silicified zones are anomalous features in many respects, it may prove useful to identify samples in this range of values. Values three geometric deviations above the mean, considered important by Hawkes and Webb (1962) are not considered here; they represent only 0.13 percent of the data from a lognormal distribution, so such values would be too scarce to reveal the dimensions of anomalies unless one took vast numbers of samples. For subsets in which more than 50 percent of the data for a given element is below the lower detection limit, we consider the top 2.3 percent of the data (all data greater than or equal to the 97.7 percentile) anomalous. Here we have also separated values greater than or equal to the 84 percentile and less than the 97.7 percentile. The 84 percentile and the 97.7 percentile are equivalent to one geometric deviation and two geometric deviations above the mean (50 percentile) for a lognormal distribution. We used log-probability plots to determine the values at the 84 and 97.7 percentiles for each element with more than 50 percent censored data (see Lepeltier, 1969).

Threshold values

Table 13 summarizes means for each of the eight elements in each of the six stratigraphic units with adequate data for silicified rocks, in every case where a mean could be calculated. In some cases the figure given is simply a geometric mean (designated $\bar{x}$), but in most cases it is a geometric mean adjusted by Cohen's method (designated $\hat{\mu}$). Also given, wherever available, are the values resulting from adding one geometric deviation to the mean and adding two geometric deviations to the mean. For any element shown, values equal to or greater than the two-geometric-deviations figure are considered anomalous. Values less than that are considered background, but we suspect it might be worthwhile to note samples in the range between one and two geometric deviations. Where data above the detection threshold are not sufficient for calculating a geometric mean and deviation, figures for the top 16 percent and top 2.3 percent of the data are given in lieu of one-* and two-geometric-deviation figures. If less than 16 percent of the samples in a data subset have amounts of an element greater than the detection threshold, the detection threshold itself is given instead of the value at the 84 percentile, and the percentage figure shown is the percentage of samples in the data subset above the detection threshold. The percentage figure given for molybdenum in silicified Vindicator Rhyolite is greater than 16 percent because the cumulative frequency for the next higher reporting interval is 85 percent. We chose the 23 percent point, which happens to be the detection threshold, rather than the 15 percent point, so that the entire top 16 percent is included. For some elements in the small data sets, data is insufficient

STATISTICAL WORK SHEET
GEOLOGICAL SURVEY

Table 13.--Background and anomalous values for various silicified-rock data subsets

Element	Silicified Tv N=13		Silicified Tl N=33		Silicified Tsf N=16		Silicified Tma N=139		Silicified Td N=88		Silicified Tls N=21		All silicified rocks N=323 1/		Background values		Anomalous values
Au	—	—	—	—	$\hat{\mu}$	0.07	—	—	—	—	—	—	—	—	≤0.02	0.04-0.40	≥0.45
	Top 7.6%	0.1 2/	Top 6.1%	0.020	$\hat{\mu}+1\hat{\sigma}$	1.0	Top 16%	0.03	Top 16%	0.02	Top 14.3%	0.020 3/	Top 16 %	0.030			
	Top 2.3%	—	Top 2.3%	0.08	$\hat{\mu}+2\hat{\sigma}$	16	Top 2.3%	0.3	Top 2.3%	0.15	Top - 3%	—	Top 2.3%	0.45			
Ag	—	—	—	—	$\hat{\mu}$	0.5	—	—	—	—	— 6/	—	—	—	<0.5	0.5-2	≥3
	Top 15.4%	1.0 4/	Top 3%	0.5 5/	$\hat{\mu}+1\hat{\sigma}$	5	Top 16%	0.5	Top 16%	0.5	—	—	Top 16.4%	0.5			
	Top 2.3%	—	Top 2.3%	—	$\hat{\mu}+2\hat{\sigma}$	50	Top 2.3%	2	Top 2.3%	1.0	—	—	Top 2.3%	2			
Pb	$\bar{x}$	40	$\hat{\mu}$	60	$\hat{\mu}$	40	$\hat{\mu}$	15	$\hat{\mu}$	50	$\hat{\mu}$	20	$\hat{\mu}$	30	≤100	150-300	≥500
	$\bar{x}+1s$	90	$\hat{\mu}+1\hat{\sigma}$	200	$\hat{\mu}+1\hat{\sigma}$	150	$\hat{\mu}+1\hat{\sigma}$	60	$\hat{\mu}+1\hat{\sigma}$	150	$\hat{\mu}+1\hat{\sigma}$	40	$\hat{\mu}+1\hat{\sigma}$	100			
	$\bar{x}+2s$	200	$\hat{\mu}+2\hat{\sigma}$	800	$\hat{\mu}+2\hat{\sigma}$	600	$\hat{\mu}+2\hat{\sigma}$	200	$\hat{\mu}+2\hat{\sigma}$	600	$\hat{\mu}+2\hat{\sigma}$	700	$\hat{\mu}+2\hat{\sigma}$	500			
Bi	— 7/	—	—	—	— 7/	—	—	—	—	—	—	—	—	—	<10	10-15	≥20
	—	—	Top 12.1%	10	—	—	Top 2.9%	10	Top 4.6%	10	Top 4.8%	10 8/	Top 5.6%	10			
	—	—	Top 2.3%	15	—	—	Top 2.3%	10	Top 2.3%	20	Top 2.3%	—	Top 2.3%	20			
Hg	$\bar{x}$	0.17	$\bar{x}$	0.10	$\bar{x}$	0.37	$\hat{\mu}$	0.22	$\hat{\mu}$	0.18	$\bar{x}$	0.23	$\hat{\mu}$	0.19	≤0.54	0.55-1.50	≥1.60
	$\bar{x}+1s$	0.35	$\bar{x}+1s$	0.19	$\bar{x}+1s$	1.2	$\hat{\mu}+1\hat{\sigma}$	0.61	$\hat{\mu}+1\hat{\sigma}$	0.50	$\bar{x}+1s$	0.74	$\hat{\mu}+1\hat{\sigma}$	0.54			
	$\bar{x}+2s$	0.72	$\bar{x}+2s$	0.38	$\bar{x}+2s$	4.1	$\hat{\mu}+2\hat{\sigma}$	1.7	$\hat{\mu}+2\hat{\sigma}$	1.4	$\bar{x}+2s$	2.4	$\hat{\mu}+2\hat{\sigma}$	1.5			
As	$\hat{\mu}$	30	$\hat{\mu}$	10	$\hat{\mu}$	30	$\hat{\mu}$	20	$\hat{\mu}$	20	$\hat{\mu}$	20	$\hat{\mu}$	20	≤40	60-140	≥160
	$\hat{\mu}+1\hat{\sigma}$	100	$\hat{\mu}+1\hat{\sigma}$	40	$\hat{\mu}+1\hat{\sigma}$	80	$\hat{\mu}+1\hat{\sigma}$	50	$\hat{\mu}+1\hat{\sigma}$	50	$\hat{\mu}+1\hat{\sigma}$	30	$\hat{\mu}+1\hat{\sigma}$	50			
	$\hat{\mu}+2\hat{\sigma}$	500	$\hat{\mu}+2\hat{\sigma}$	100	$\hat{\mu}+2\hat{\sigma}$	250	$\hat{\mu}+2\hat{\sigma}$	150	$\hat{\mu}+2\hat{\sigma}$	150	$\hat{\mu}+2\hat{\sigma}$	70	$\hat{\mu}+2\hat{\sigma}$	150			
Cu	$\bar{x}$	30	$\bar{x}$	30	$\bar{x}$	30	$\hat{\mu}$	8	$\hat{\mu}$	7	$\hat{\mu}$	4	$\hat{\mu}$	10	≤30	50-200	≥300
	$\bar{x}+1s$	80	$\bar{x}+1s$	100	$\bar{x}+1s$	90	$\hat{\mu}+1\hat{\sigma}$	40	$\hat{\mu}+1\hat{\sigma}$	30	$\hat{\mu}+1\hat{\sigma}$	10	$\hat{\mu}+1\hat{\sigma}$	50			
	$\bar{x}+2s$	200	$\bar{x}+2s$	300	$\bar{x}+2s$	200	$\hat{\mu}+2\hat{\sigma}$	200	$\hat{\mu}+2\hat{\sigma}$	150	$\hat{\mu}+2\hat{\sigma}$	40	$\hat{\mu}+2\hat{\sigma}$	200			
Mo	—	—	$\hat{\mu}$	2	—	—	$\hat{\mu}$	3	$\hat{\mu}$	3	$\hat{\mu}$	3	$\hat{\mu}$	3	≤10	15-30	≥50
	Top 23.1%	2 9/	$\hat{\mu}+1\hat{\sigma}$	8	Top 16%	3	$\hat{\mu}+1\hat{\sigma}$	10	$\hat{\mu}+1\hat{\sigma}$	10	$\hat{\mu}+1\hat{\sigma}$	10	$\hat{\mu}+1\hat{\sigma}$	10			
	Top 2.3%	—	$\hat{\mu}+2\hat{\sigma}$	30	Top 2.3%	8	$\hat{\mu}+2\hat{\sigma}$	50	$\hat{\mu}+2\hat{\sigma}$	40	$\hat{\mu}+2\hat{\sigma}$	30	$\hat{\mu}+2\hat{\sigma}$	40			

Explanation
$\bar{x}$ = geometric mean
s = geometric deviation
$\hat{\mu}$ = geometric mean adjusted by Cohen's method
$\hat{\sigma}$ = geometric deviation adjusted by Cohen's method

1/ Includes ② pulled out samples of silicified Palmetto Formation, ⑧ pulled out samples of silicified quartz monzonite, and 3 samples of silicified (?) Espina Breccia.
2/ Only one value above detection threshold of 0.1 ppm.
3/ Only 3 values, all 0.020 ppm, above detection threshold of 0.020 ppm.
4/ Only 2 values above detection threshold of 1 ppm.
5/ Only one value above detection threshold of 0.5 ppm.
6/ All data < 0.5 ppm.
7/ All data < 10 ppm.
8/ Only one value, 10 ppm, above detection threshold of 10 ppm.
9/ Only three values above detection threshold of 3 ppm.

to yield a meaningful "top 2.3 percent" figure. Situations such as this are unavoidable with relatively small data subsets.

Table 13 brings out the fact that for all the elements notable differences, whatever their causes, do exist between the various stratigraphic units. For a detailed geochemical survey covering just one part of the altered area, the threshold value or values should be those determined for the prevailing stratigraphic unit or units. Gold, silver, and possibly mercury in silicified Sandstorm Rhyolite may be exceptions: several samples from productive veins have contributed to the unusually high mean values for these three elements in Sandstorm silicified rocks. To state the problem another way, the number of samples taken from silicified Sandstorm Rhyolite is small enough so that an unusually large percentage of the samples may by chance be unusually rich in gold and silver. Although it is also possible that the figures are quite representative, additional sampling within the Sandstorm Rhyolite should precede any detailed sampling program there, to make sure whether lower figures than those given in table 13 should be used.

In succeeding work we selectively sampled silicified zones throughout the Goldfield altered area. Rather than use the individual threshold values for each stratigraphic unit, we adopted the easier method of using threshold values derived from geometric means and deviations calculated for all the silicified rock samples. Using this method simplified data processing, but we sacrificed the ability to screen out some sources of variation not related to metallization. If applying threshold values for individual units is tedious or questionable for any reason, the threshold values based on the averages for all silicified rocks should give adequate, easily used guidelines for evaluating the geochemical data. The geometric means and deviations for all silicified rocks form the last four columns of table 13. The figures in the last three columns are taken from the preceding column (all silicified rocks); in some cases the values have been adjusted to coincide with analytical reporting intervals used by U.S. Geological Survey laboratories.

The geometric means for all silicified rocks should be rather good estimates for overall element abundances, because the percentage of samples from a given stratigraphic unit is approximately the same as the percentage of the total silicified rock outcrop area that falls within that stratigraphic unit. Assuming that outcrop areas are approximately proportional to the relative volumes of the various units, each unit is weighted properly in the "all silicified rocks" data subset. Maintaining this assumption, the grid sampling scheme provides proper weighting for any other areal inhomogeneities whether we have recognized them or not.

The threshold values for gold and silver shown in the last column of table 13 are within the ranges of values that we derived from detailed work in a small part of the main productive area (Ashley and Albers, 1973). We decided there that more than 0.3 ppm gold would probably be anomalous, whereas more than 3 ppm would almost certainly be anomalous, compared with 0.45 ppm from table 13. Analogous values for silver are 1 and 10 ppm, compared with 3 ppm from table 13. The values for lead, 70 and 200 ppm, are lower than the 500 ppm derived here. To obtain the 200 ppm value, however, we subjectively subdivided a broad negatively skewed frequency distribution for lead in the silicified rocks we studied. One deviation above the geometric mean for that distribution falls within the 500 ppm reporting interval.

Other elements

Elements routinely determined by semiquantitative spectrographic analysis in Field Services Section laboratories of the U.S. Geological Survey include Fe, Mg, Ca, Ti, Ag, As, Au, B, Ba, Be, Bi, Cd, Co, Cr, Cu, La, Mn, Mo, Nb, Ni, Pb, Sb, Sc, Sn, Sr, V, W, Y, Zn, and Zr. The data for Fe, Mg, Ca, and Ti, and Ag, Bi, Cu, Mo, and Pb have been discussed in earlier sections of this report. Lower detection limits for As, Au, Cd, Sb, Sn, W, and Zn are too high to provide useful data. For this study As and Au, and Hg as well, have been determined by other methods (see section on analytical methods). The remaining elements, including B, Ba, Be, Co, Cr, La, Mn, Nb, Ni, Sc, Sr, V, Y, and Zr, are discussed in this section. Figures 14 through 27 present the data graphically; the elements are arranged in alphabetical order.

Lack of change in magnesium and calcium with increasing intensity of hydrothermal alteration in unaltered and illite-kaolinite-bearing quartz monzonite data subsets raised the suspicion that these two subsets are actually composed of similar rocks or similar mixtures of different rocks. The same is true of data subsets for illite-kaolinite-bearing and silicified andesite-dacite breccia. Data for the 14 minor elements considered here lend weight to this suspicion, because between the two quartz monzonite data subsets, five of the 14 elements show no significant difference, and between the andesite-dacite breccia data subsets, eight of the 14 show no significant difference. Unexpected, however, is the fact that seven elements show no significant difference between illite-kaolinite-bearing and silicified Sandstorm Rhyolite. Although calcium is not depleted in

Figure 14

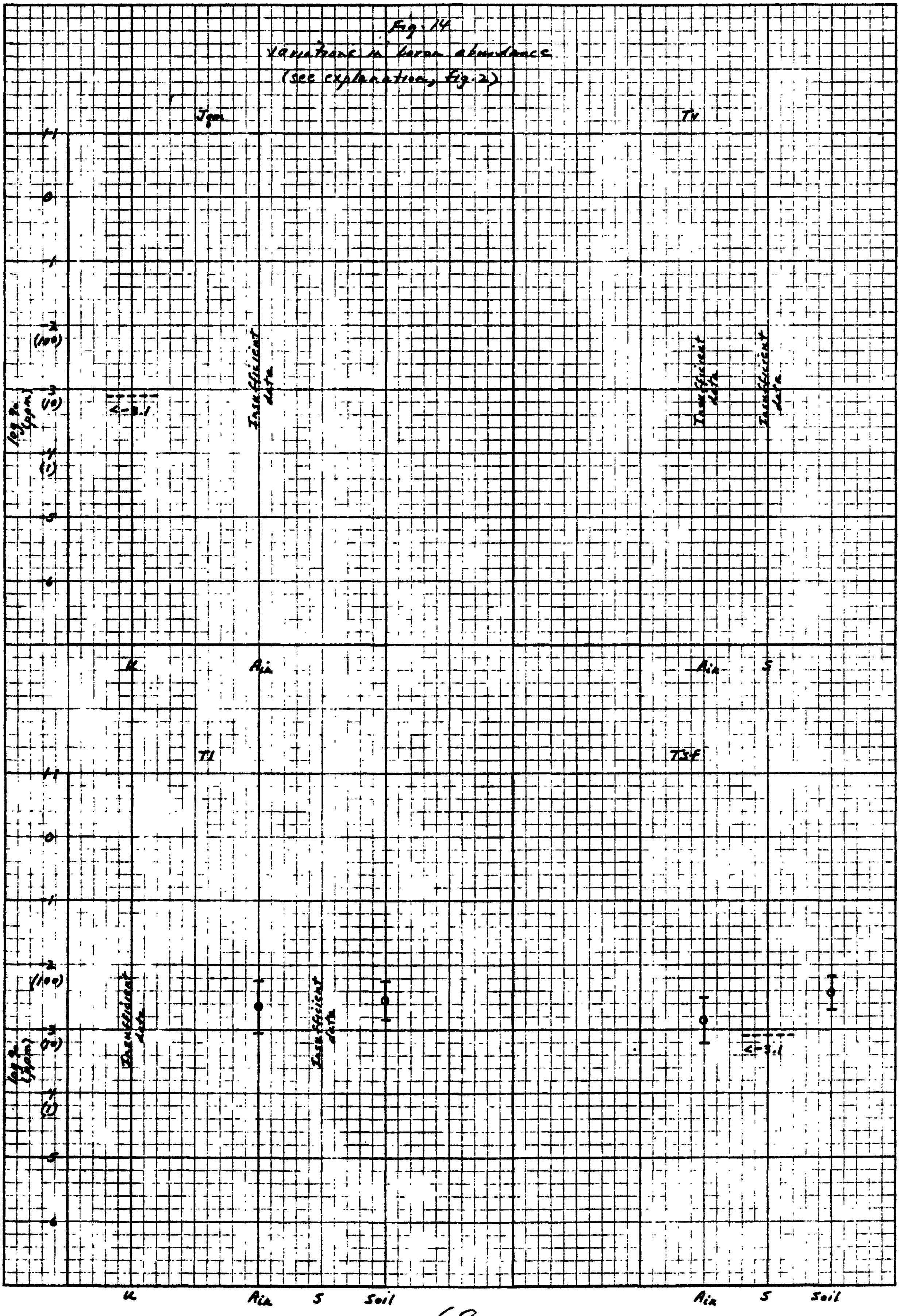

Fig. 14
Variations in boron abundance
(see explanation, fig. 2)

Figure 14.--Continued

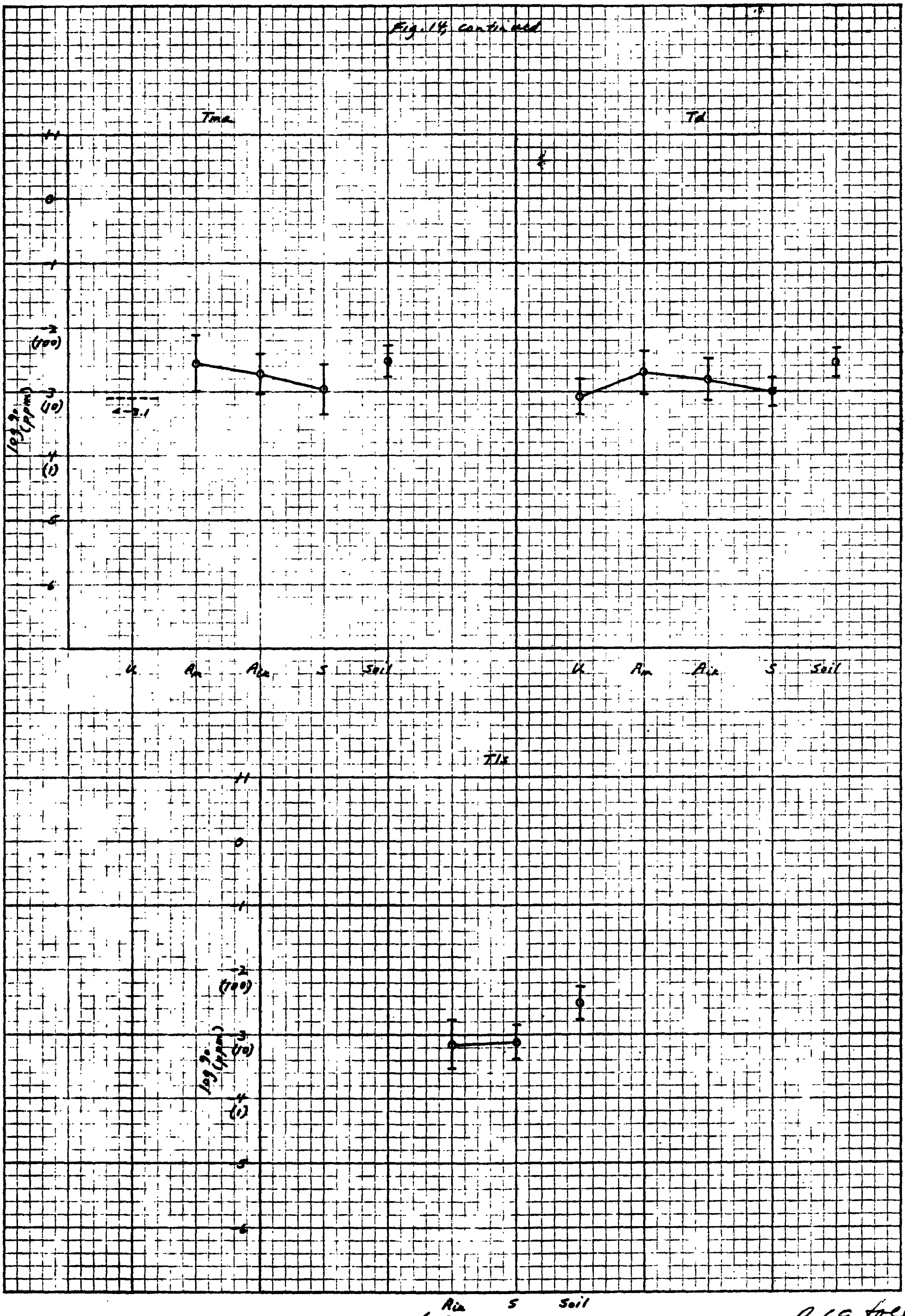

P. 69 follow

Figure 15

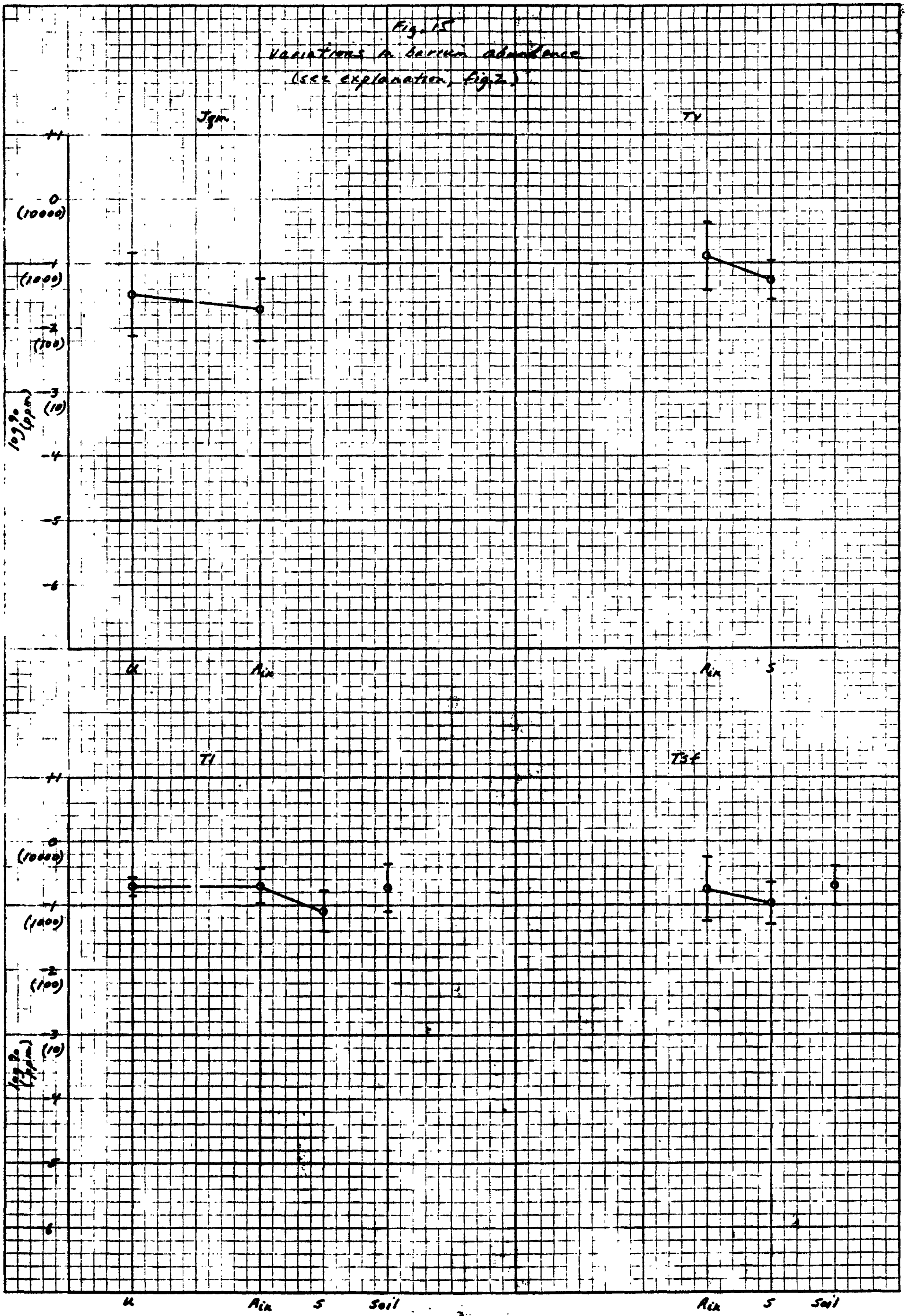

Fig. 15
Variations in barium abundance
(see explanation, fig. 2)
Jgm
Ty
Tl
Tsf
log %
(ppm)
+1
0
(10000)
-1
(1000)
-2
(100)
-3
(10)
-4
-5
-6
U
Air
S
Soil

Figure 15--Continued

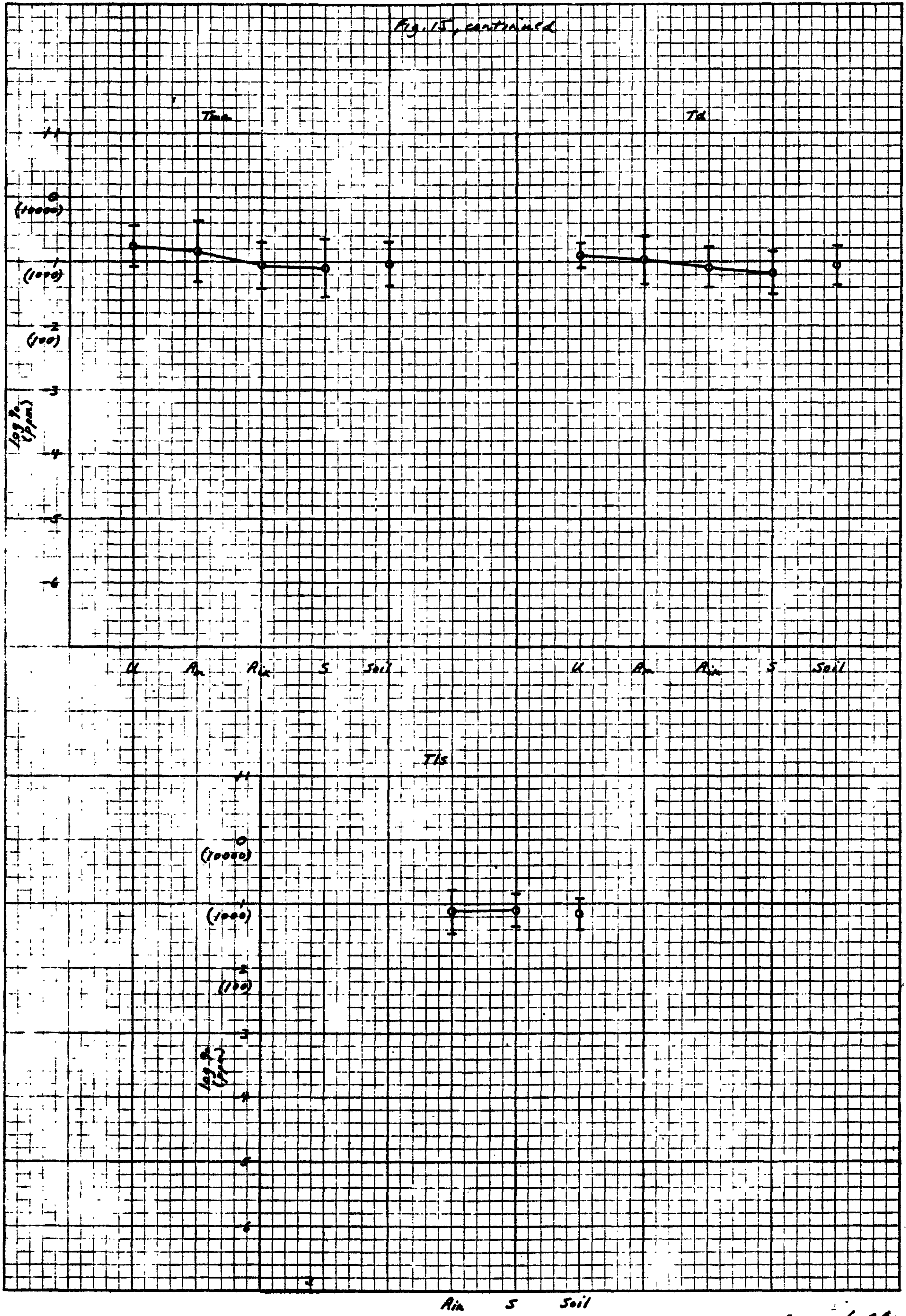

P. 70 following

Figure 16

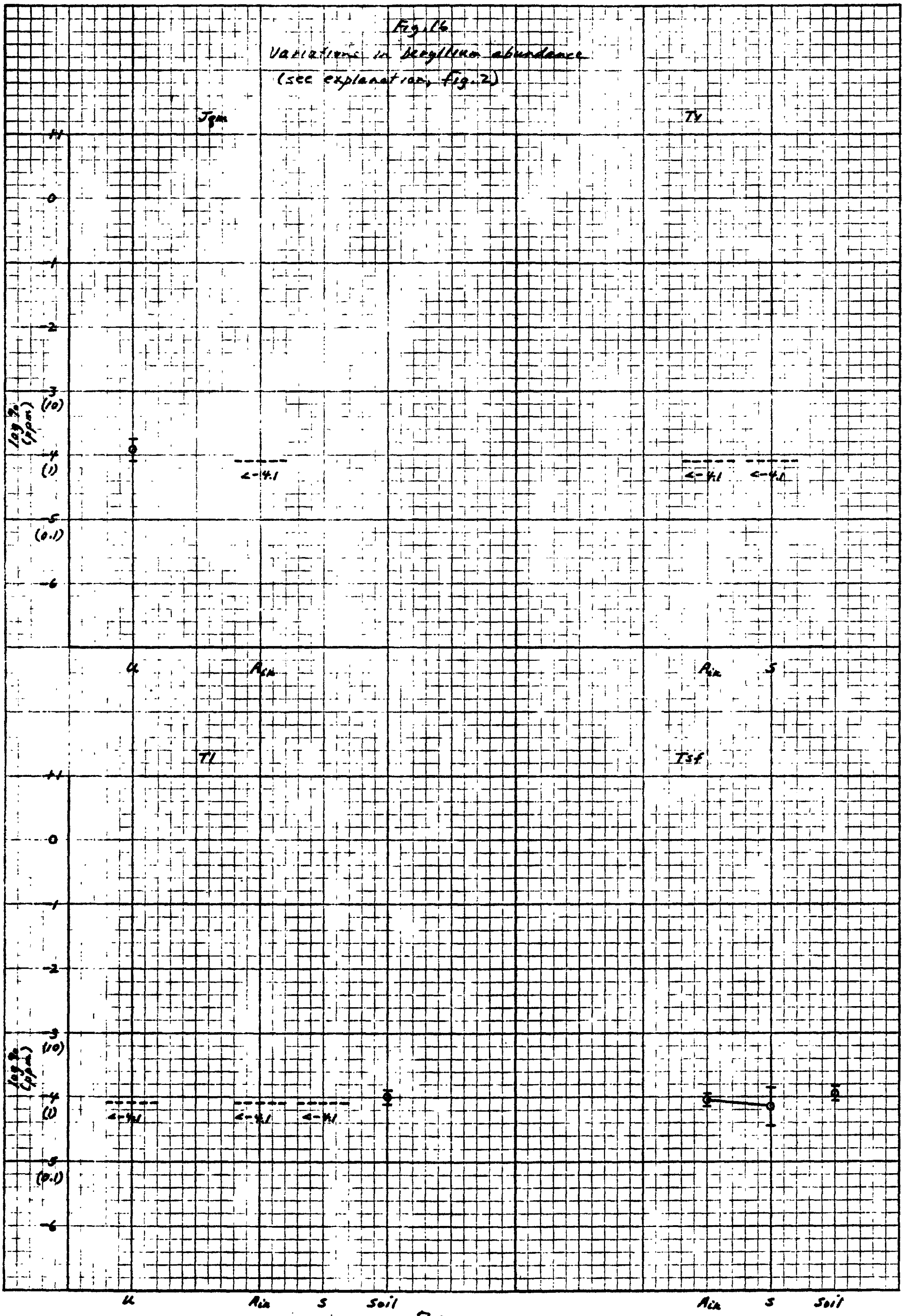
Fig. 16
Variations in beryllium abundance
(see explanation, Fig. 2)
Jgm
Ty
Tl
Tsf
+1
0
-1
-2
-3 (10)
-4 (1)
-5 (0.1)
-6
log % (ppm)
<-4.1
U
Ain
S
Soil

Figure 16--Continued

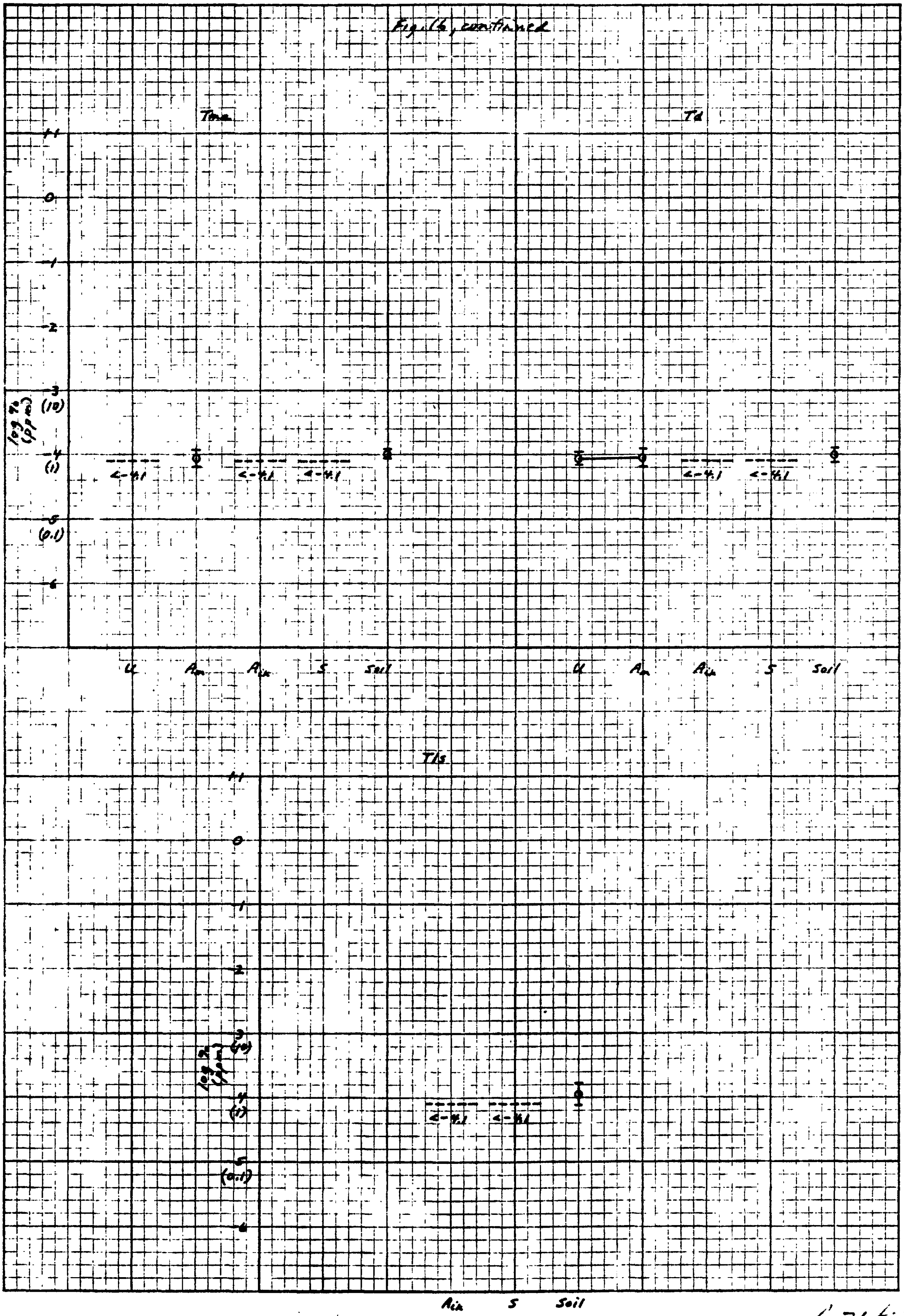

704

1.71f

Figure 17

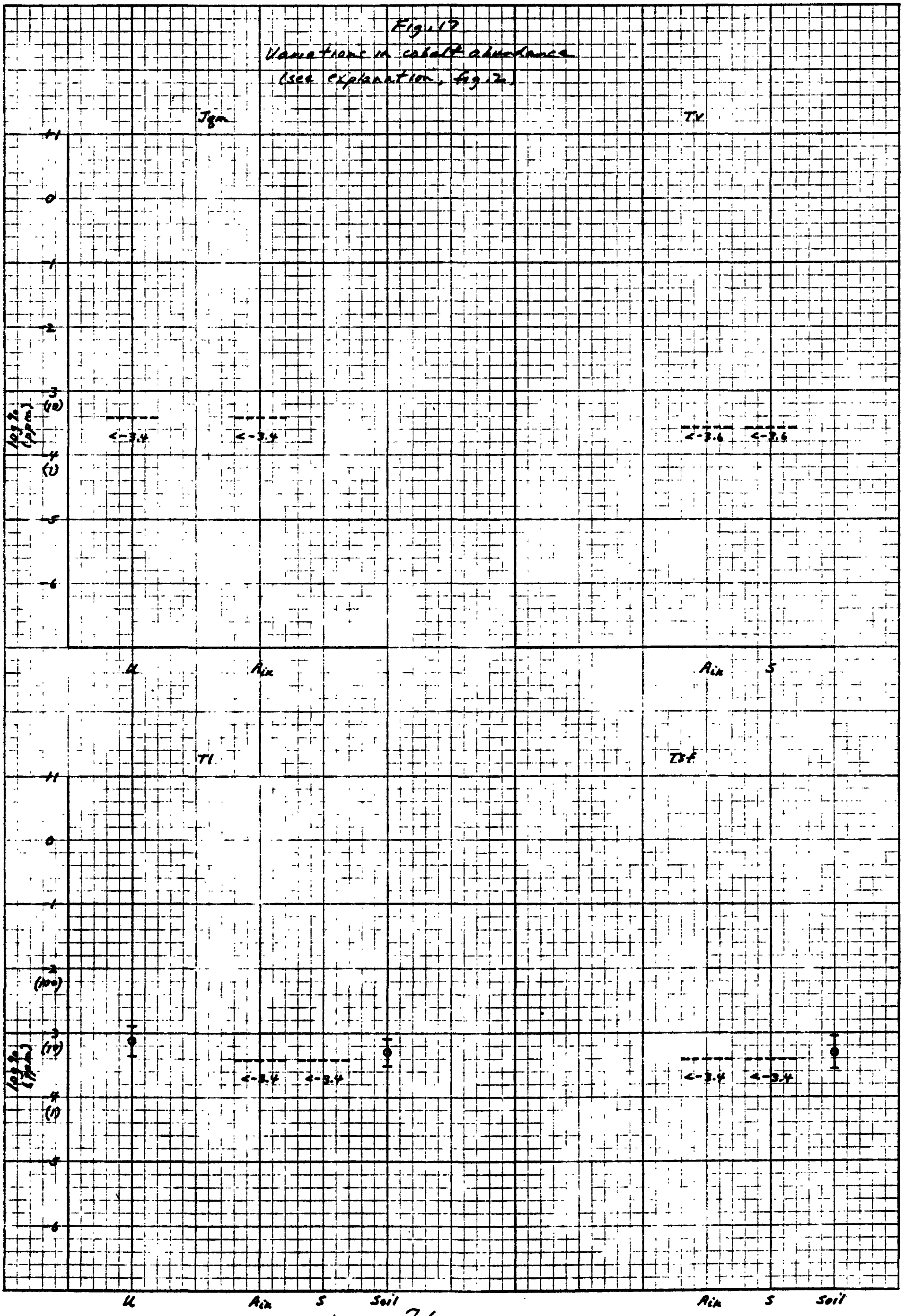
Fig. 17
Variations in cobalt abundance
(see explanation, fig 2)
Jgm
Tv
+1
0
-1
-2
-3 (10)
-4 (1)
-5
-6
log 2 (ppm)
<-3.4
<-3.4
<-3.6
<-3.6
U
Air
Air
S
Tl
Tsf
+1
0
-1
-2 (100)
-3 (10)
-4 (1)
-5
-6
log 2 (ppm)
<-3.4
<-3.4
<-3.4
<-3.4
U
Air
S
Soil
Air
S
Soil

Figure 17--Continued

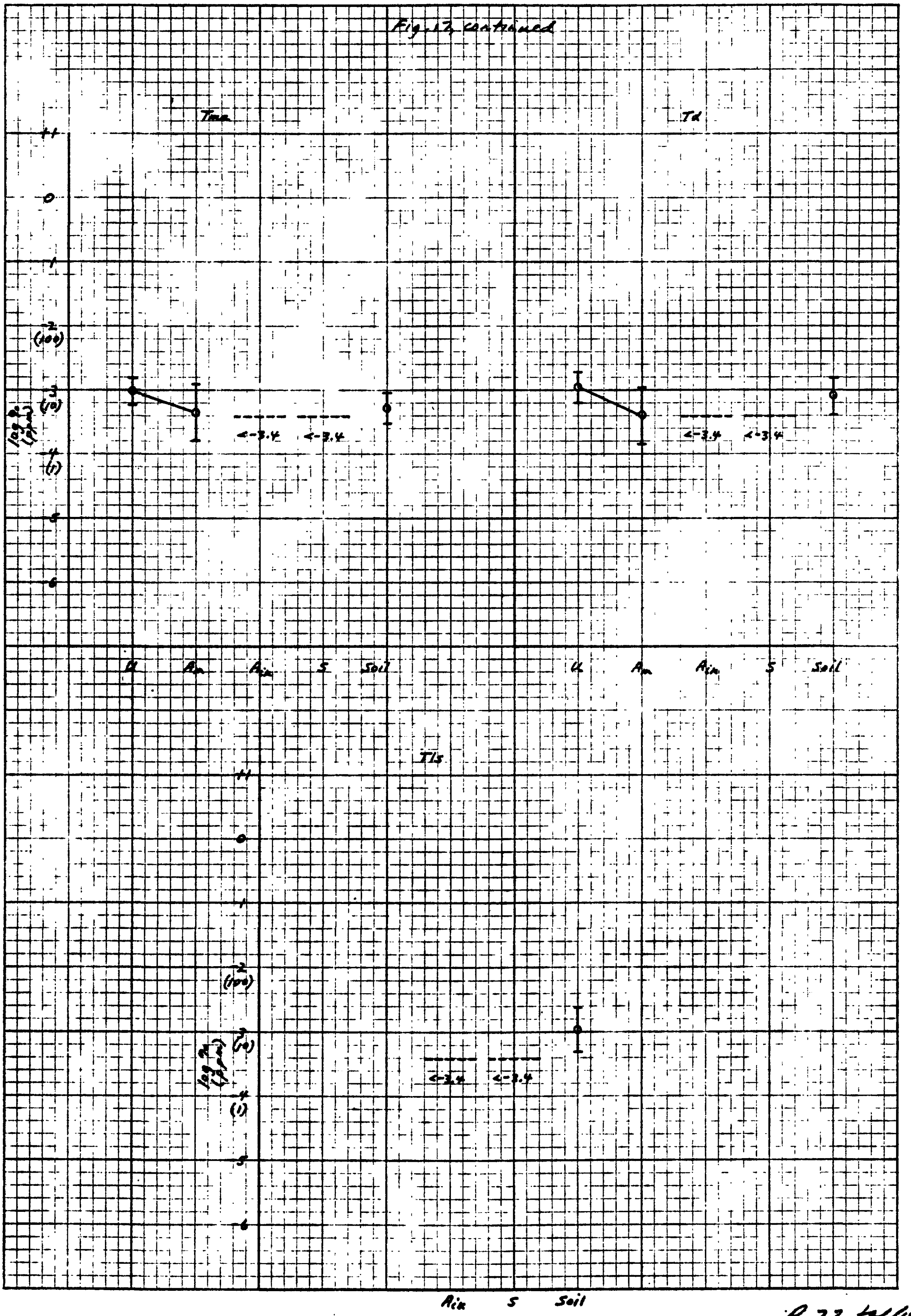

71a

P. 72 follows

Figure 18

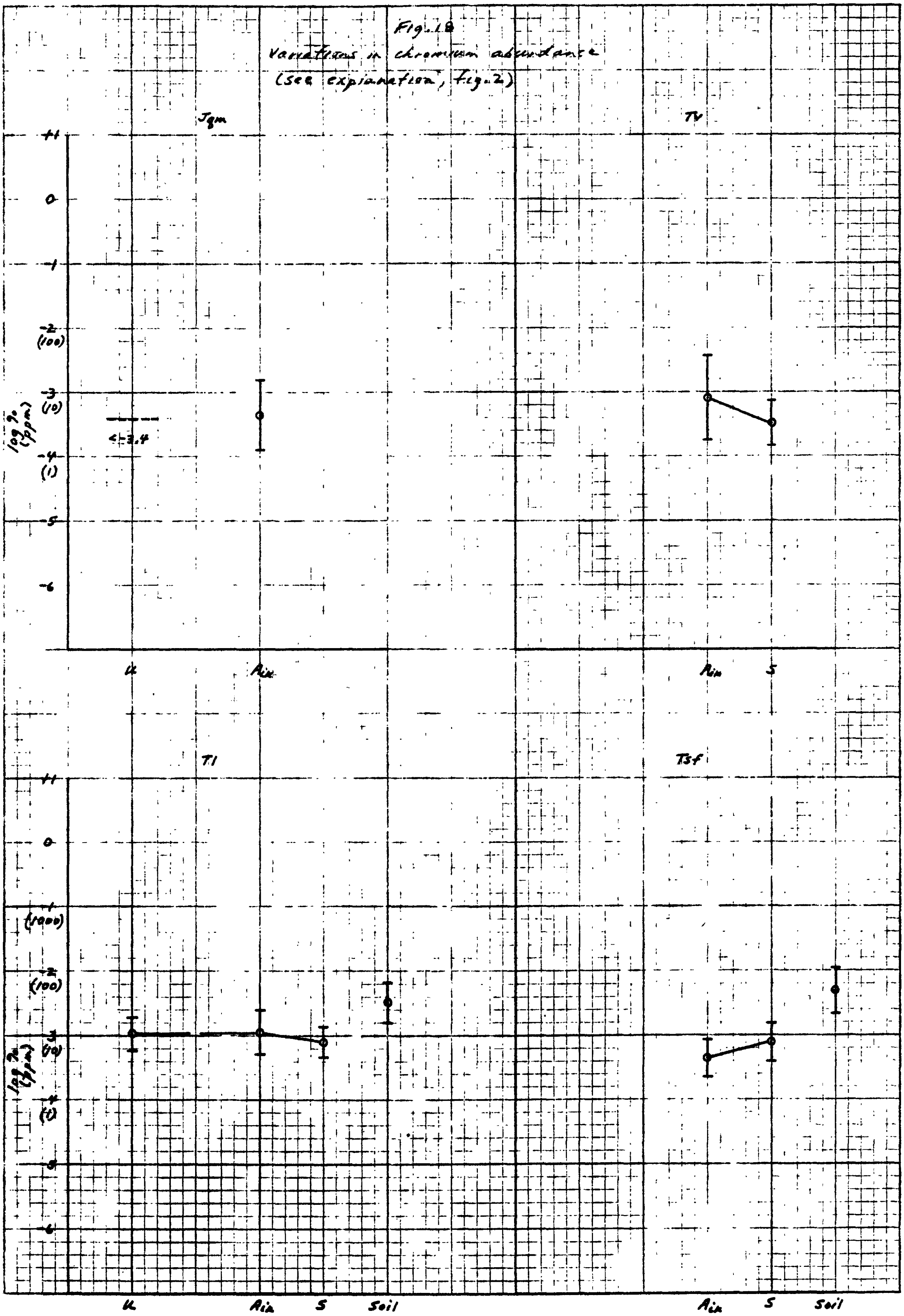
Fig. 18
Variations in chromium abundance
(see explanation, fig. 2)
Jqm
Tv
+1
0
-1
-2
(100)
-3
(10)
-4
(1)
-5
-6
log %
(ppm)
<-3.4
U
Air
Air
S
Tl
Tsf
+1
0
-1
(1000)
-2
(100)
-3
(10)
-4
(1)
-5
-6
log %
(ppm)
U
Air
S
Soil
Air
S
Soil

Figure 18--Continued

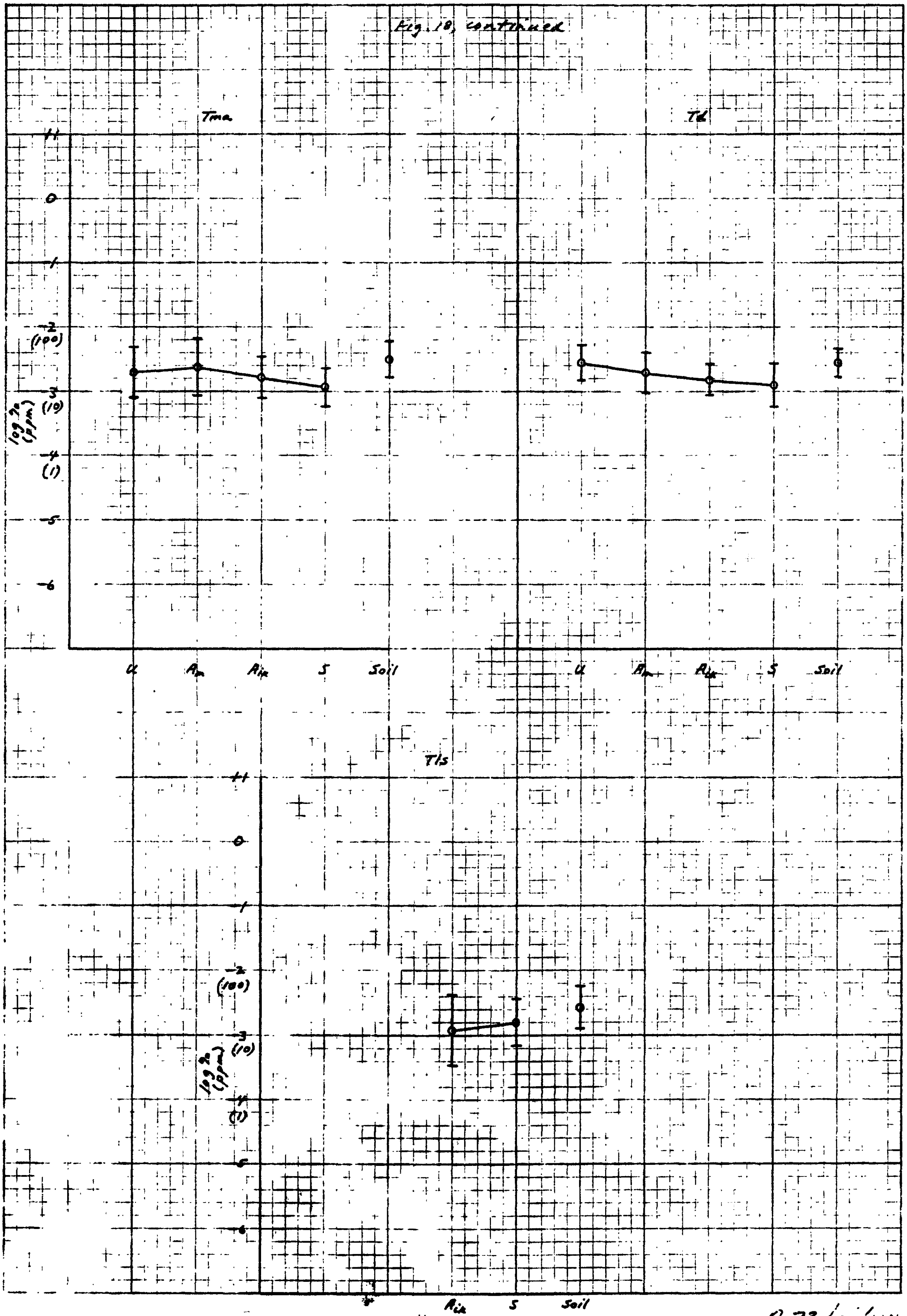

P. 73 fe

Figure 19

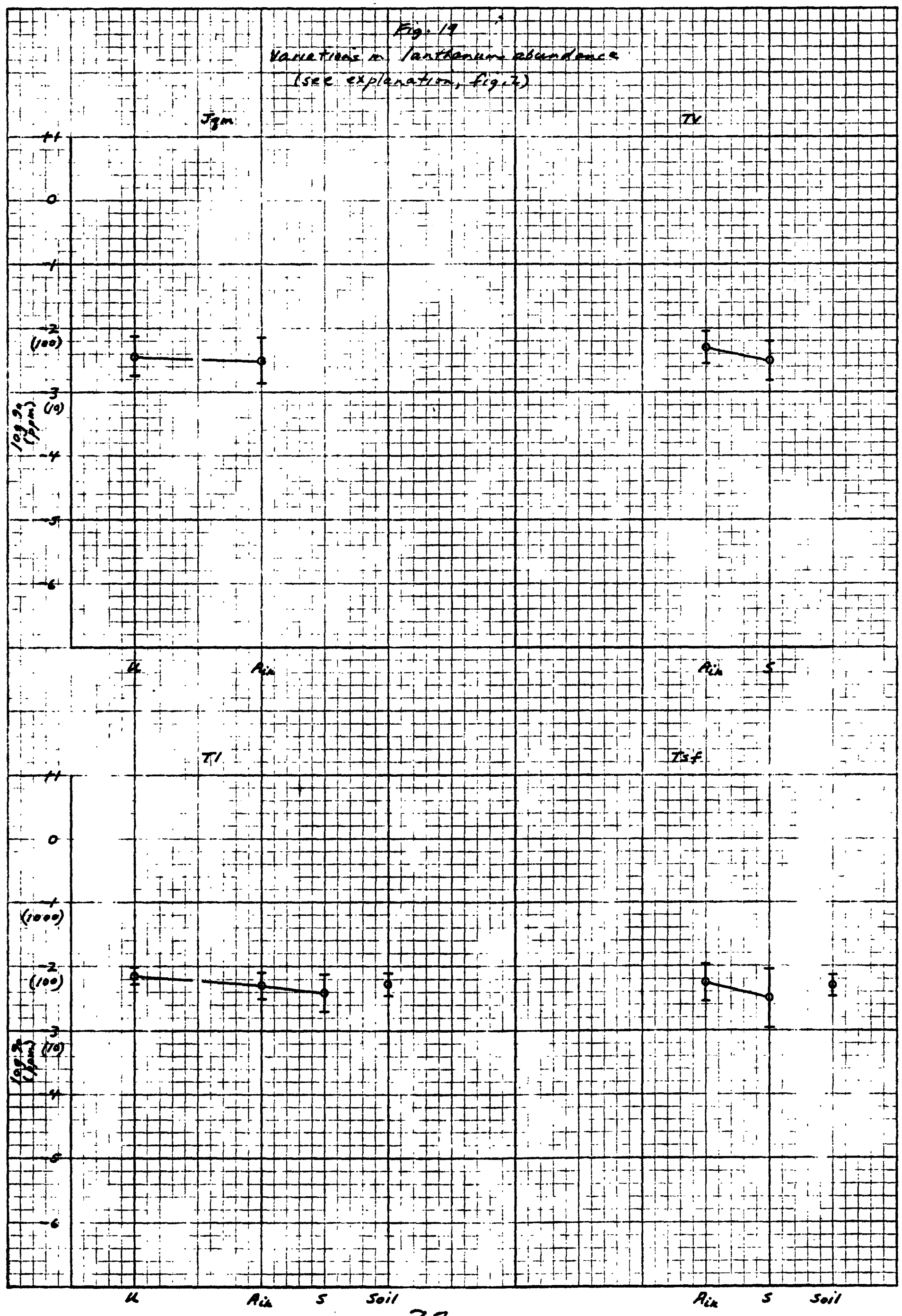
Fig. 19
Variations in lanthanum abundance
(see explanation, fig. 2)
Jgm
TV
+1
0
-1
-2
(100)
-3
(10)
log La (ppm)
-4
-5
-6
U
Ain
Ain
S
Tl
Tsf
+1
0
-1
(1000)
-2
(100)
-3
(10)
log La (ppm)
-4
-5
-6
U
Ain
S
Soil
Ain
S
Soil

Figure 20

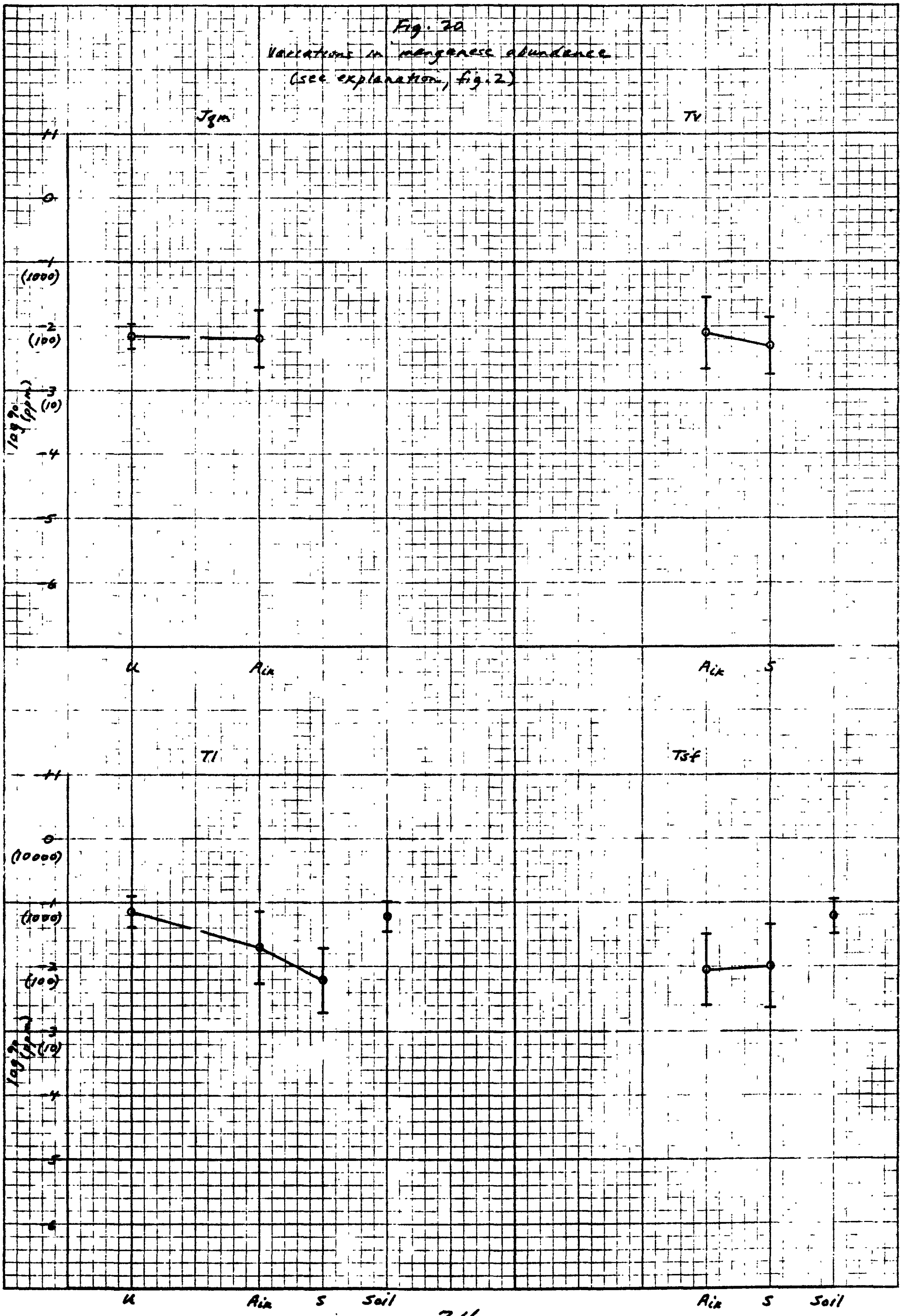

Fig. 20
Variations in manganese abundance
(see explanation, fig. 2)

Figure 21

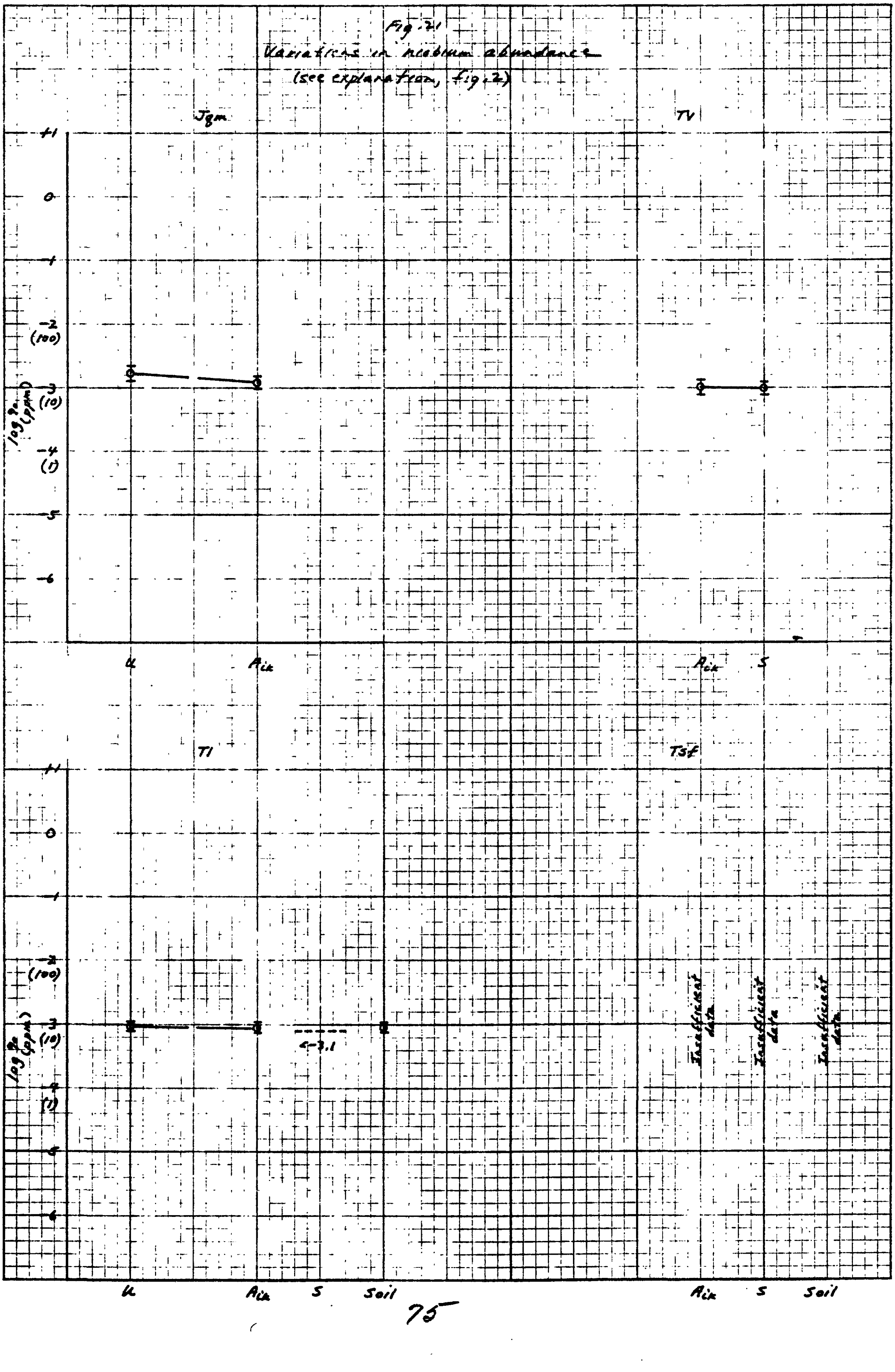
Fig. 21
Variations in niobium abundance
(see explanation, fig. 2)
Jgm
TV
+1
0
-1
-2
(100)
-3
(10)
-4
(1)
-5
-6
log Nb (ppm)
U
Air
Air
S
Tl
Tsf
<-3.1
Insufficient data
Insufficient data
Insufficient data
U
Air
S
Soil
Air
S
Soil

Figure 21--Continued

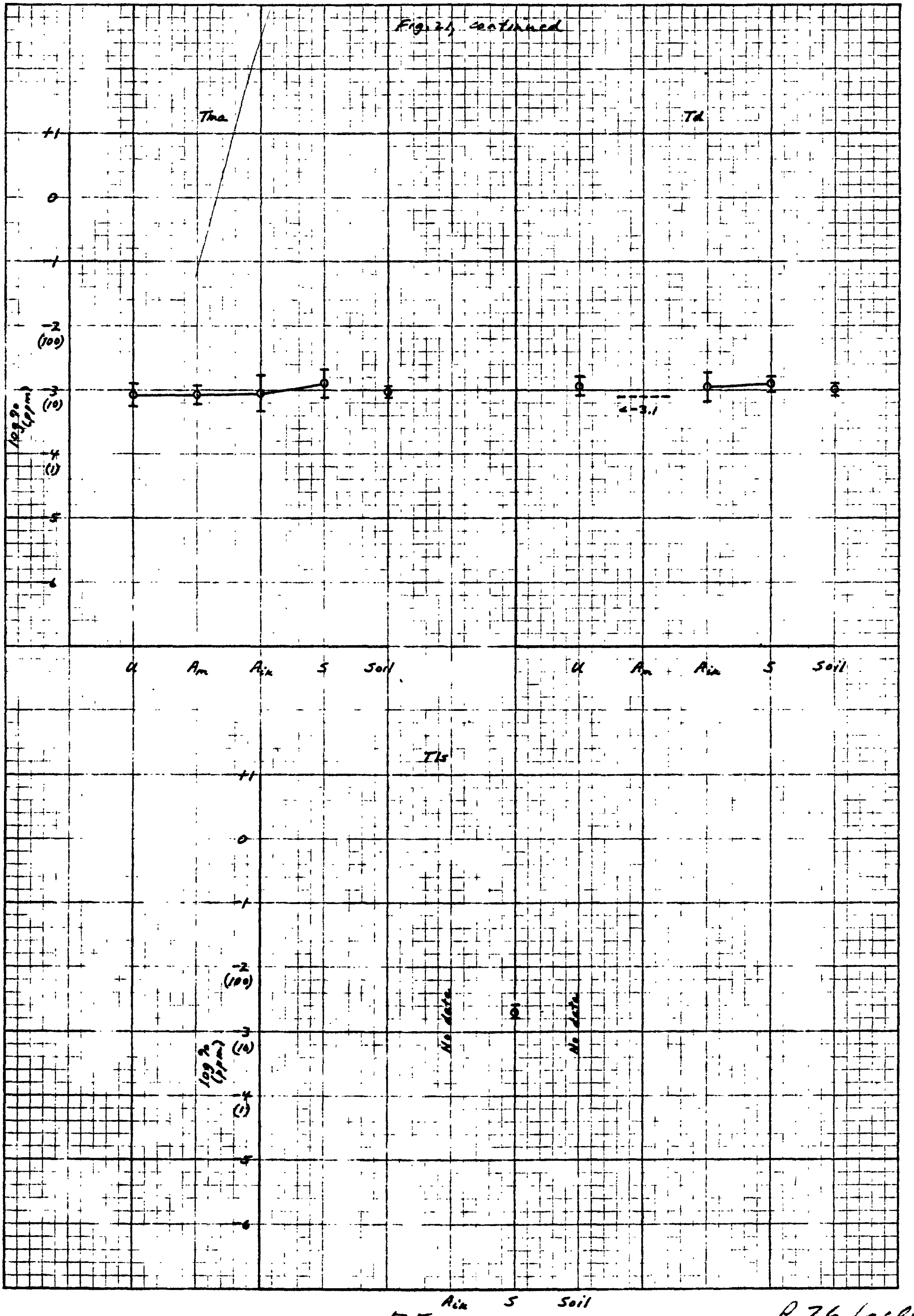

P. 76 follows

Figure 22

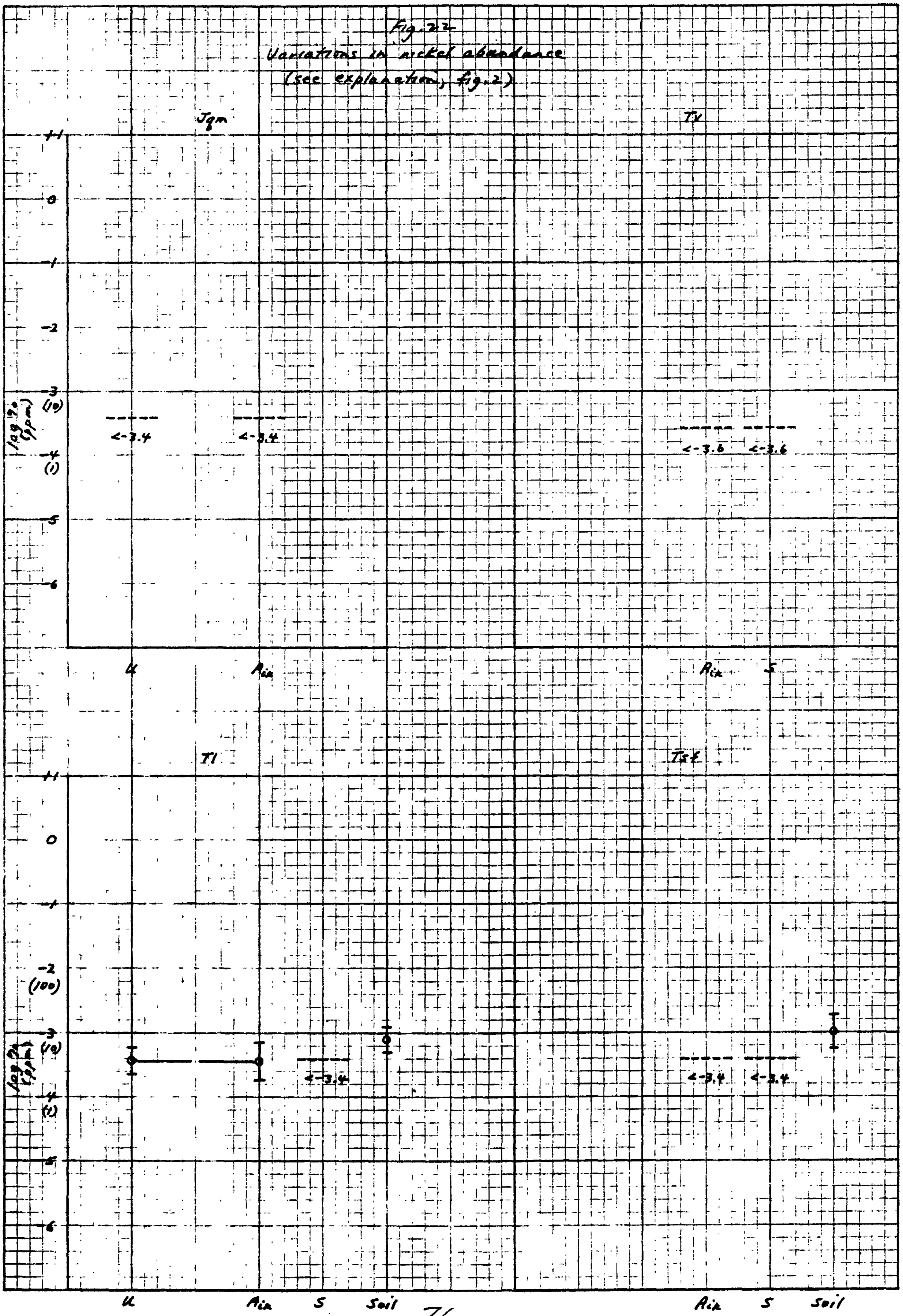
Fig. 22
Variations in nickel abundance
(see explanation, fig. 2)
Jqm
Ty
+1
0
-1
-2
-3 (10)
-4 (1)
-5
-6
log Ni (ppm)
<-3.4
<-3.4
<-3.6
<-3.6
U
Air
Air
S
Tl
Tsf
+1
0
-1
-2 (100)
-3 (10)
-4 (1)
-5
-6
log Ni (ppm)
<-3.4
<-3.4
<-3.4
U
Air
S
Soil
Air
S
Soil

Figure 22--Continued

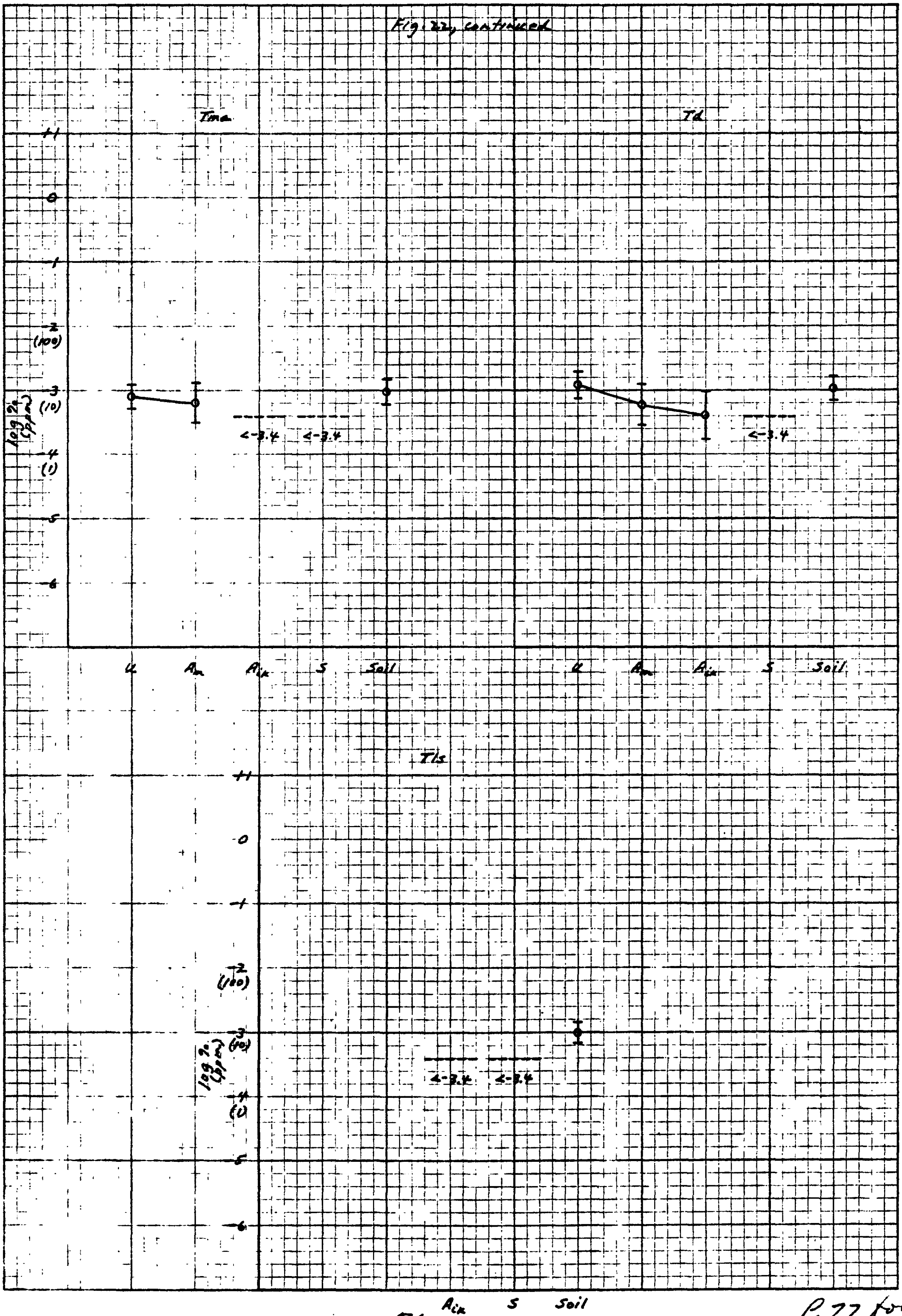

Figure 23

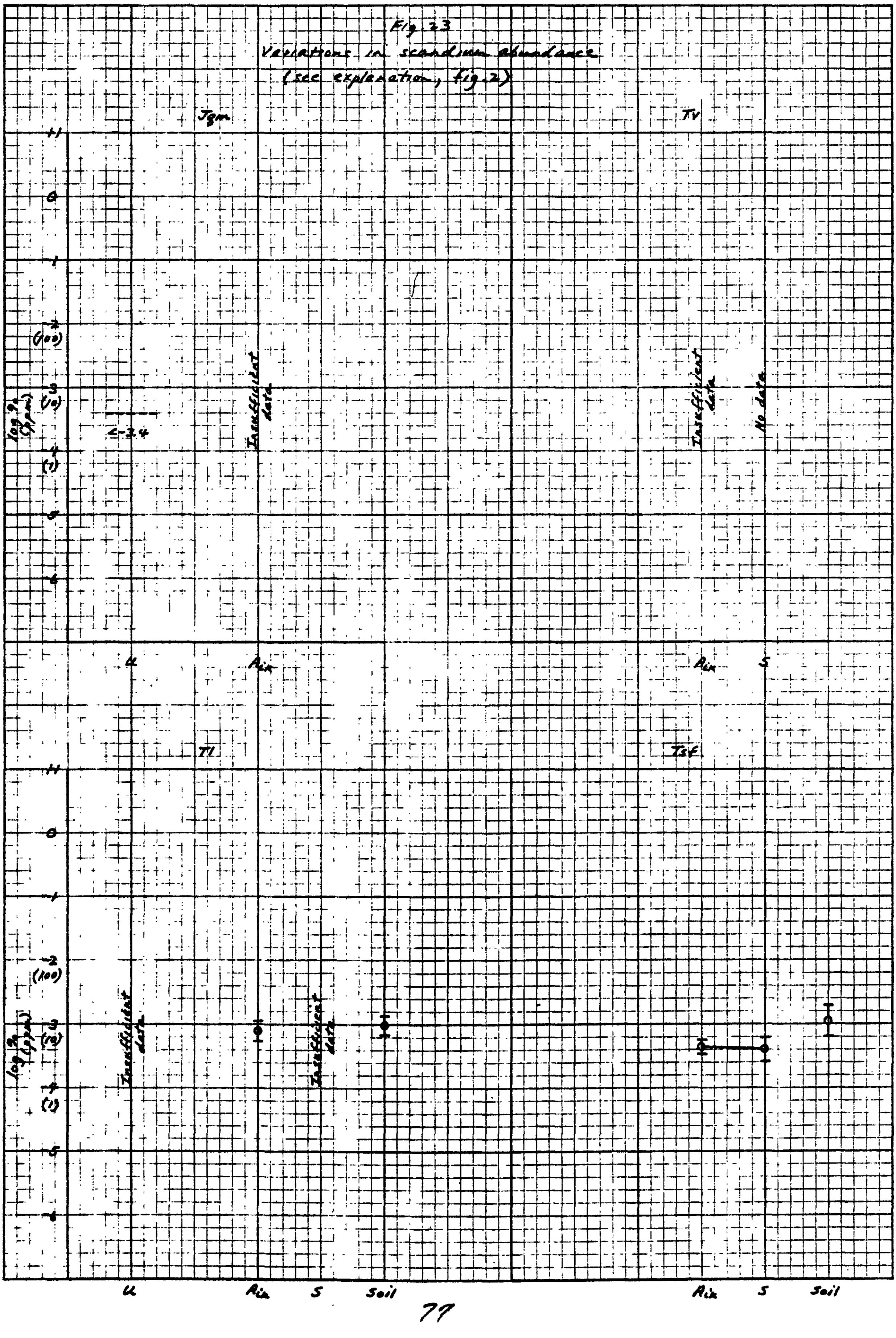
Fig. 23
Variations in scandium abundance
(see explanation, fig. 2)
Jgm
Tv
+1
0
-1
-2
(100)
-3
(10)
-4
(1)
-5
-6
log Sc (ppm)
<-3.4
Insufficient data
Insufficient data
No data
U
Air
Air
S
Tl
Tsf
+1
0
-1
-2
(100)
-3
(10)
-4
(1)
-5
-6
log Sc (ppm)
Insufficient data
Insufficient data
U
Air
S
Soil
Air
S
Soil

Figure 23--Continued

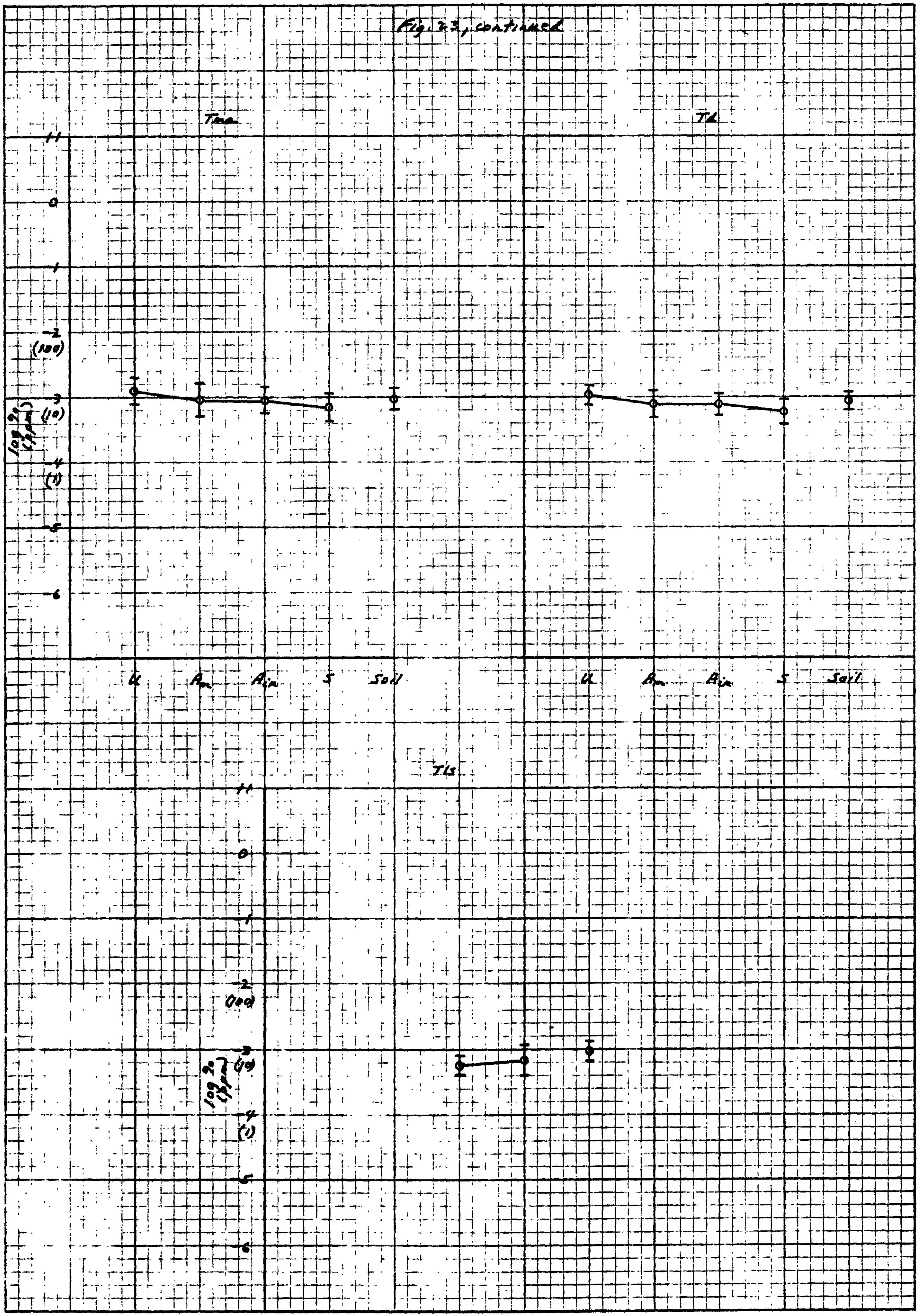

p. 78 fa

Figure 24

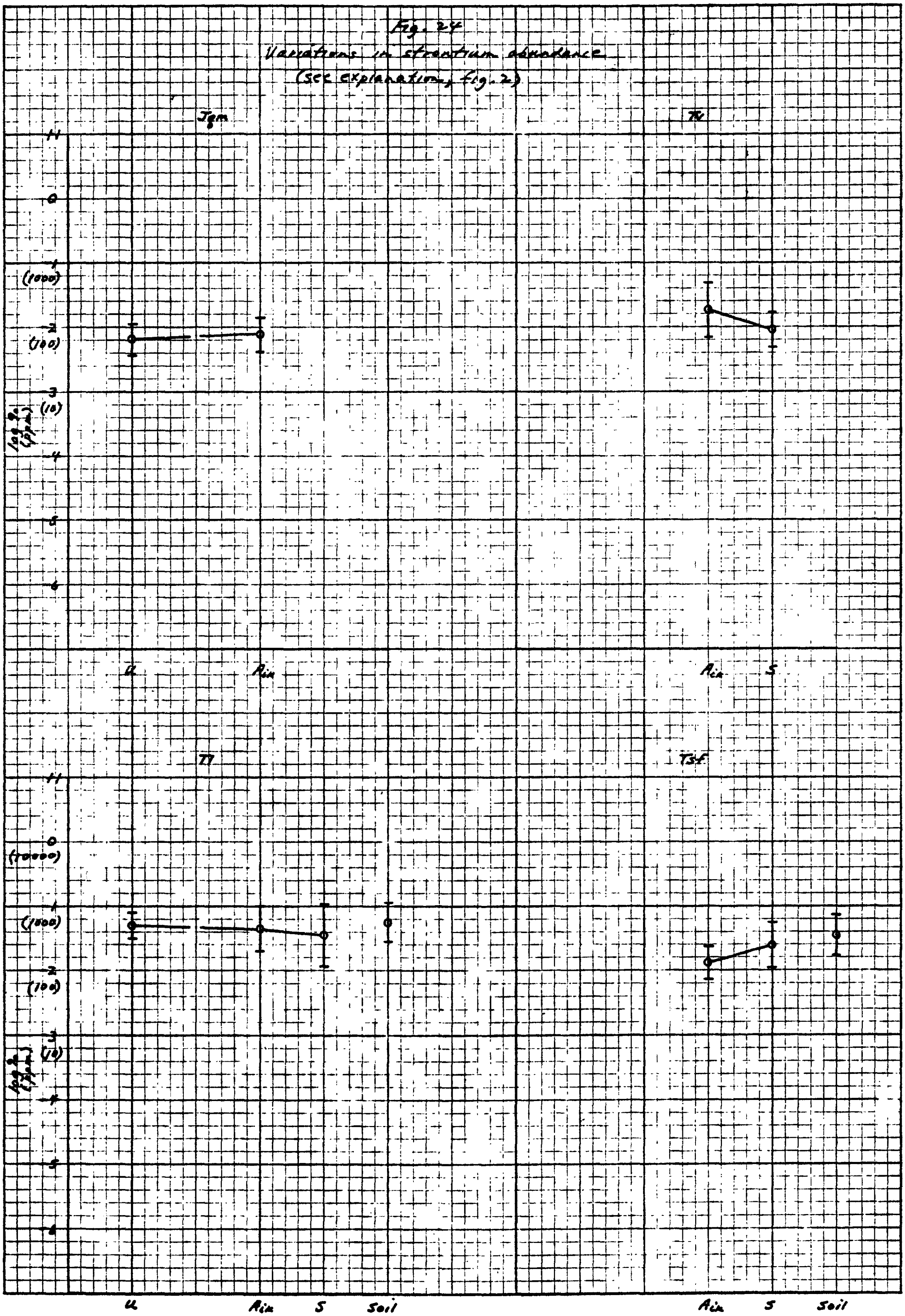

Fig. 24
Variations in strontium abundance
(see explanation, fig. 2)

Figure 24--Continued

P. 79 follows

Figure 25

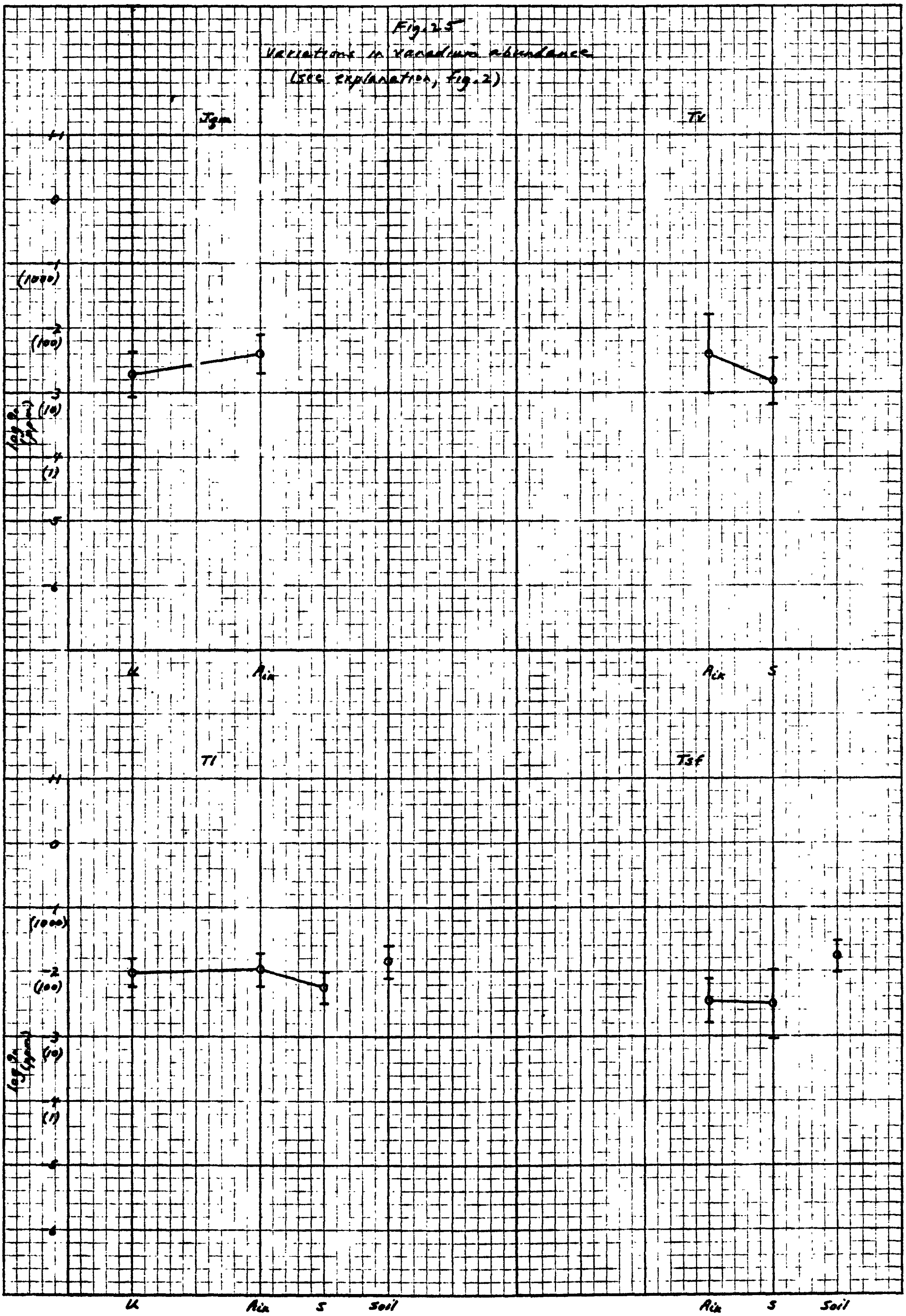
Fig. 25
Variations in vanadium abundance
(see explanation, Fig. 2)
Jgm
Tv
Tl
Tsf
+1
0
1 (1000)
2 (100)
3 (10)
4 (1)
5
6
log Cn (ppm)
U
Air
S
Soil

Figure 25--Continued

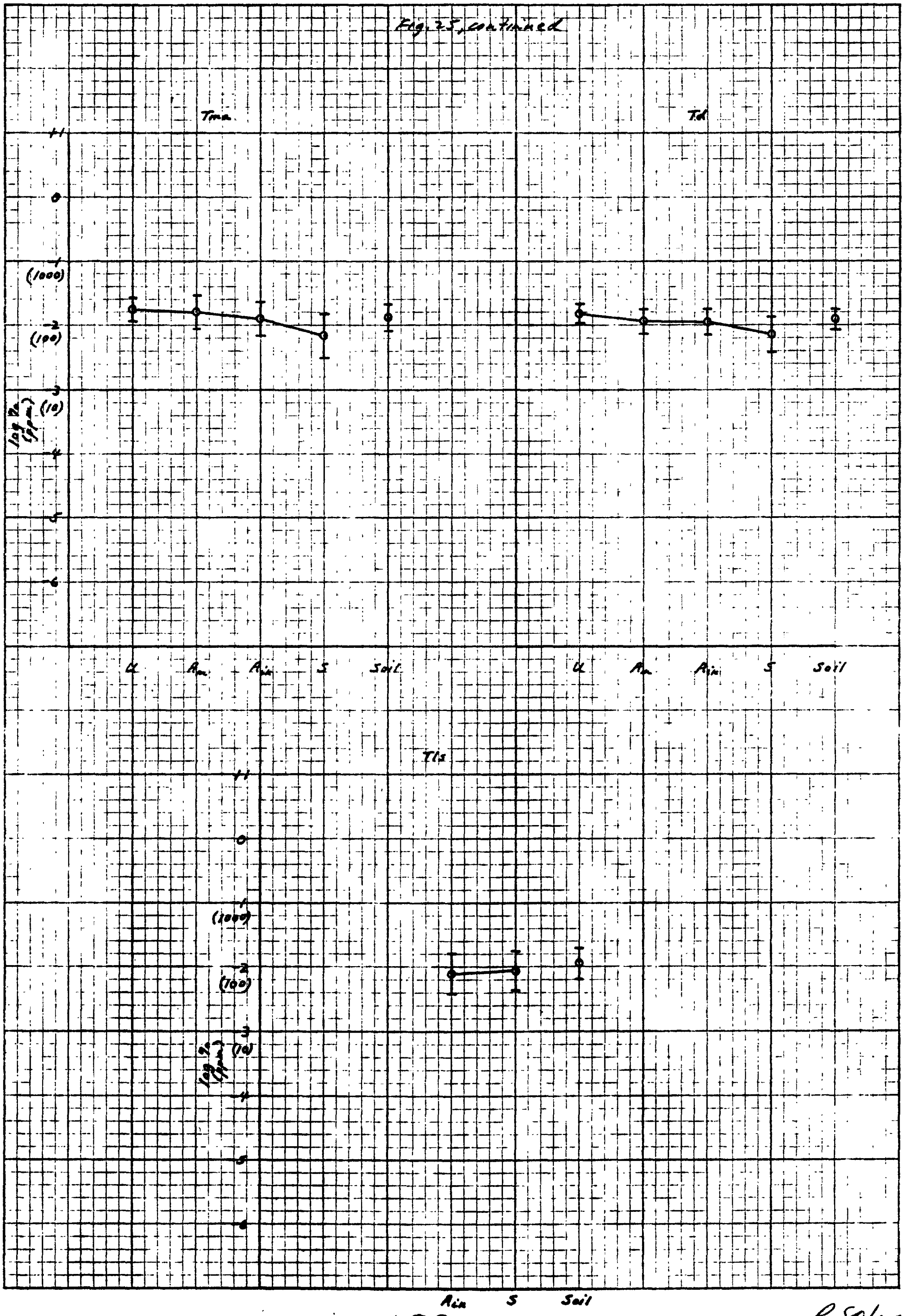

Figure 26

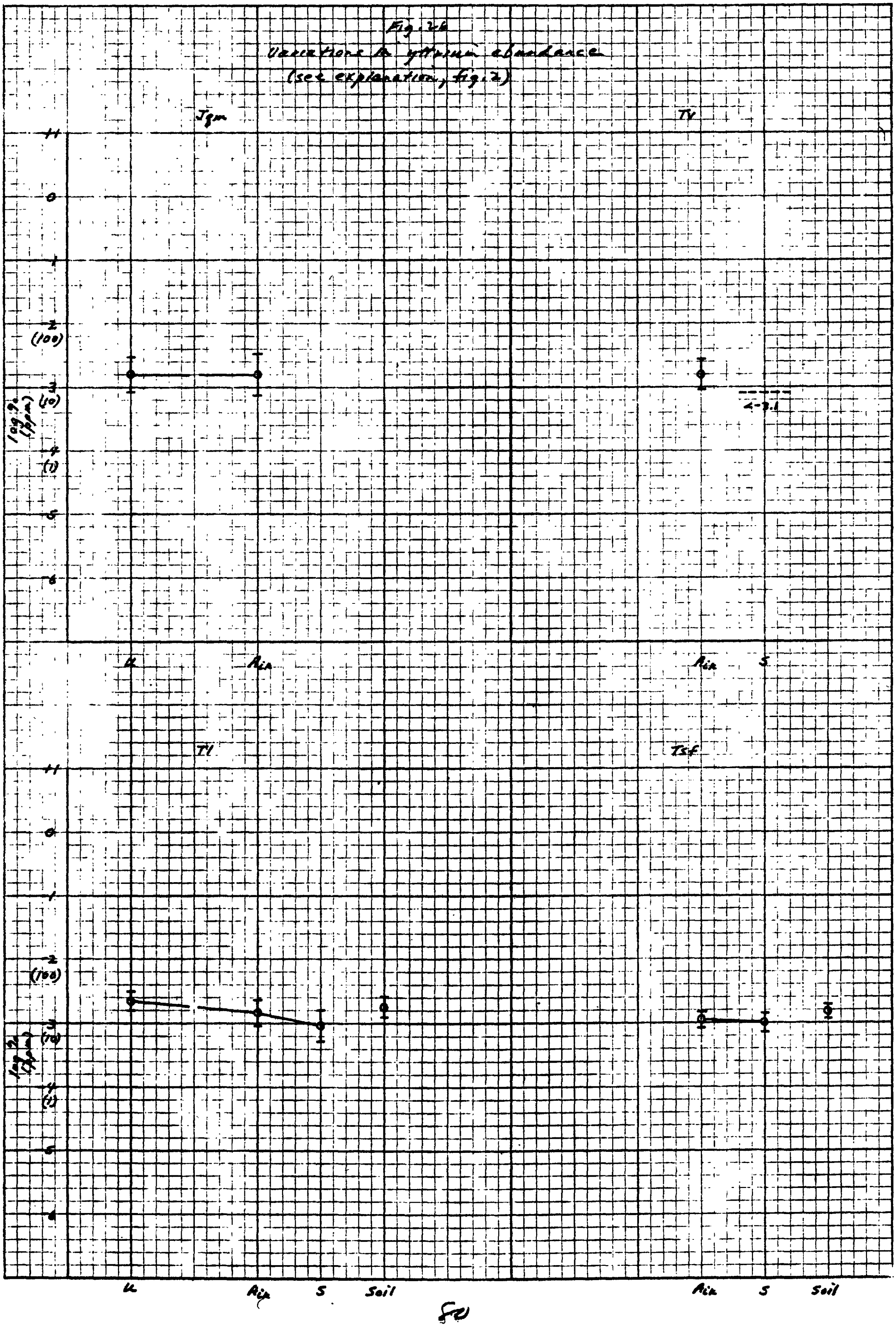

Fig. 26
Variations in yttrium abundance
(see explanation, fig. 2)

Figure 26--Continued

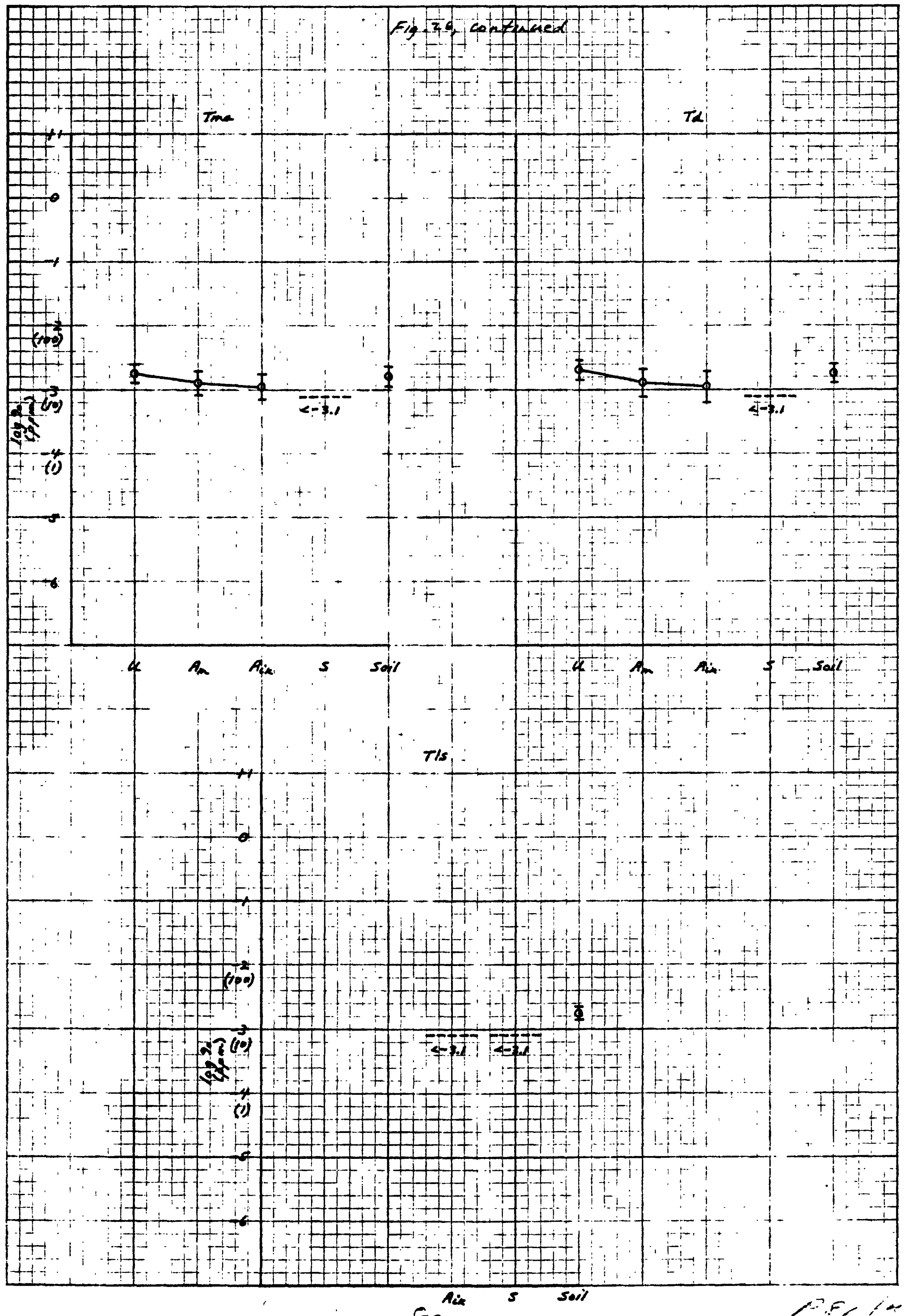

Figure 27

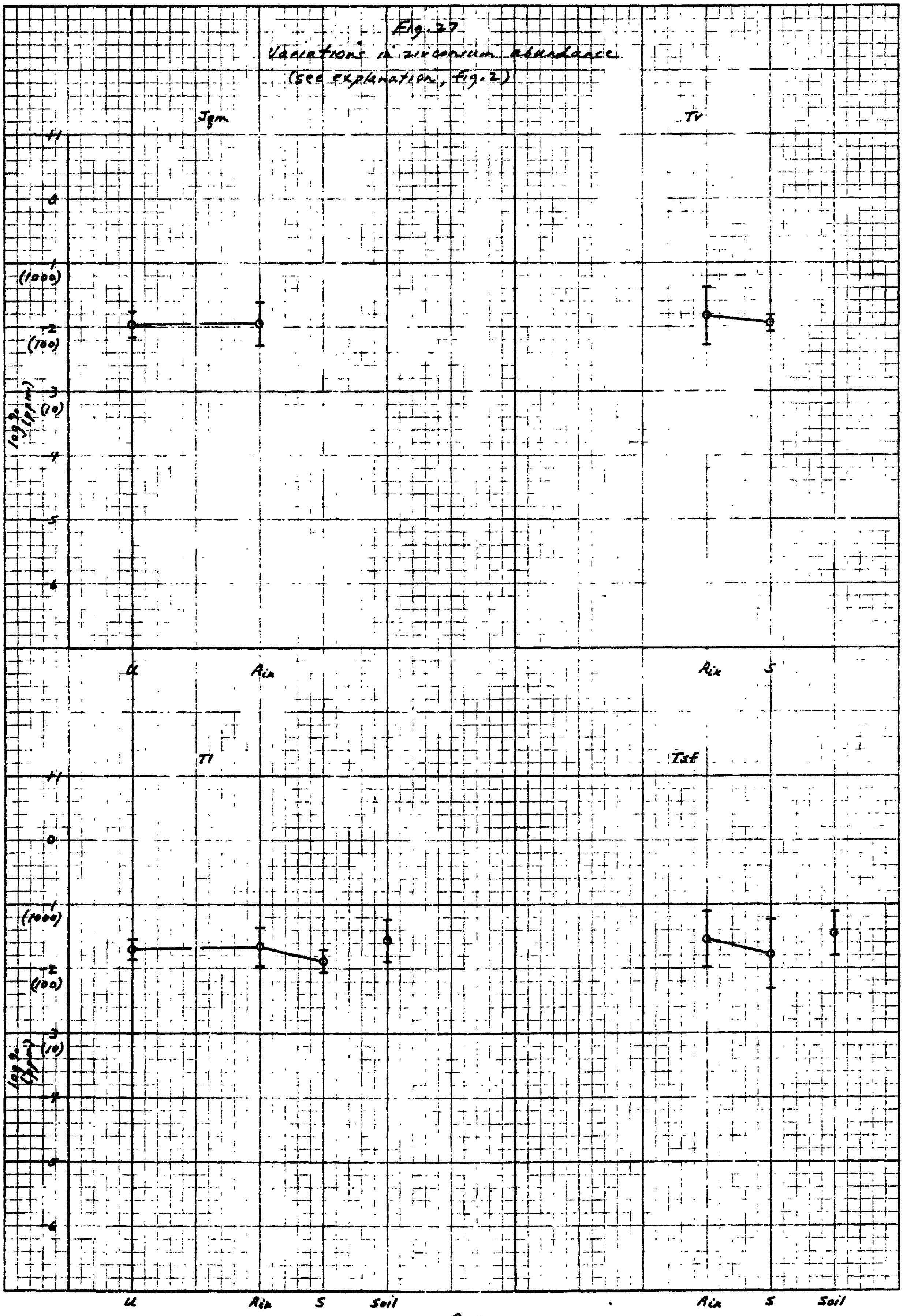

Fig. 27
Variations in zirconium abundance
(see explanation, fig. 2)

Figure 27--Continued

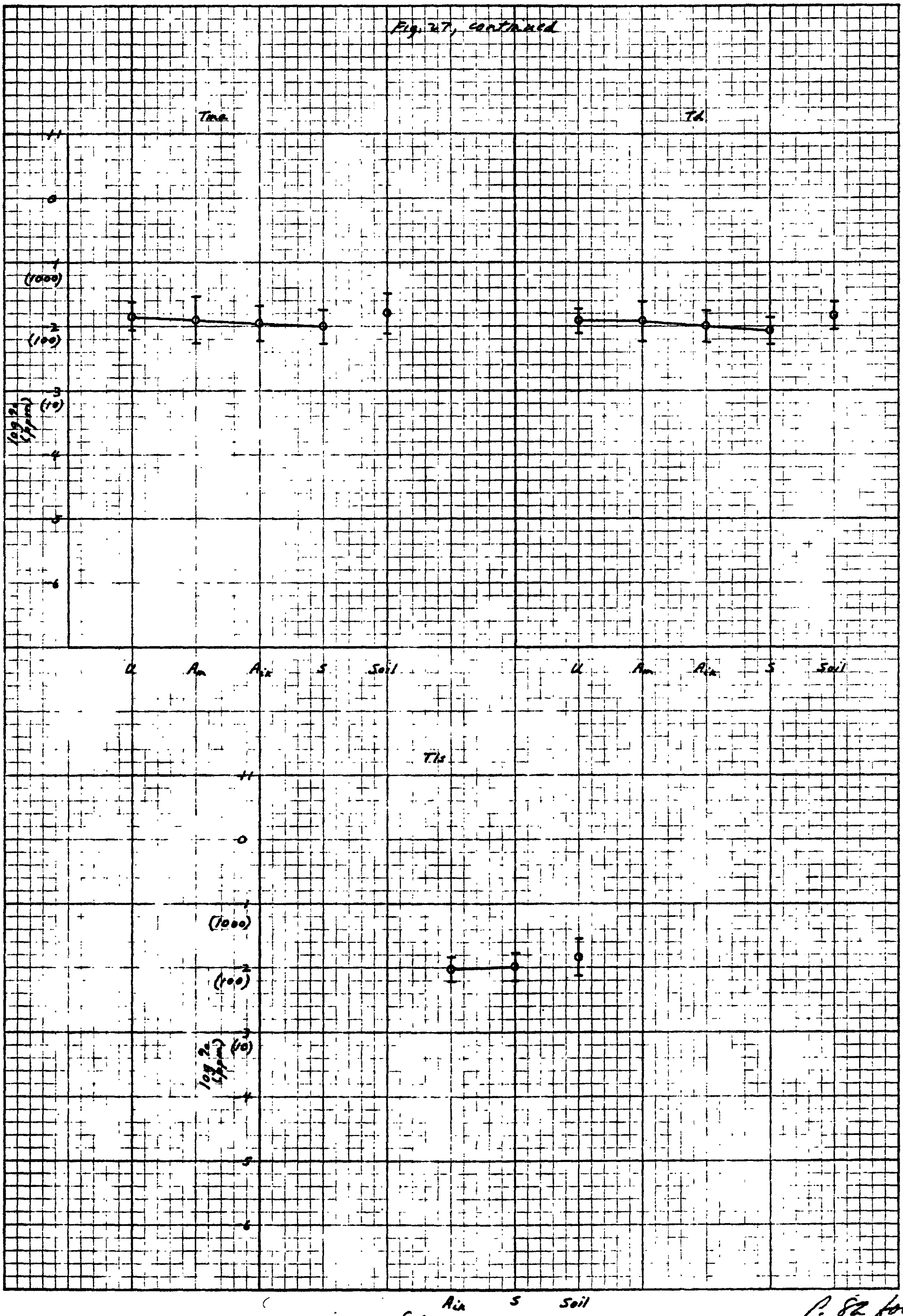

P. 82 follo

silicified Sandstorm Rhyolite, magnesium is, and gold, silver, lead, mercury, and copper are enriched. Gold, silver, and mercury, in fact, are more abundant in silicified rocks from the Sandstorm Rhyolite than in silicified rocks from any other unit. Additional work on the mineralogy of illite-kaolinite rocks and silicified rocks from this unit would be necessary before one could attempt an explanation. In the following discussion, more weight will be placed on results from the remaining four units (Vindicator Rhyolite, latite, Milltown Andesite, and dacite) than on results from the quartz monzonite, Sandstorm Rhyolite, and andesite-dacite breccia.

Boron is most abundant in argillized rocks. It probably resides in the clay minerals, which are capable of adsorbing borate anions (Grim, 1968, p. 227). All of the four unaltered rock data sets contain less than 10 ppm boron, so boron was probably added to the argillized rocks either by the hydrothermal fluids that accomplished the argillization itself, or later by supergene waters. The boron in silicified rocks is probably associated with the small to moderate amounts of kaolinite often found in these rocks. Differences between similarly altered rocks from various formations are small.

In four of the seven units barium decreases slightly in abundance with increasing intensity of alteration. Similar amounts of barium occur in all the volcanic units (1,200-2,000 ppm in unaltered rocks), whereas the unaltered quartz monzonite has notably less barium (330 ppm) than the volcanic rocks do. Barium contents of the volcanic units are large relative to most intermediate volcanic rocks having similar major-element composition, that is, calc-alkalic (Taylor, 1969, p. 48, 60).

The behavior of strontium is similar to that of barium, although the decrease with increasing degree of alteration is not as pronounced; only three units show a significant decrease, and in the case of dacite the overall change from unaltered to silicified rocks is small. As is the case with barium, strontium contents of the unaltered volcanic rocks (520-890 ppm) are larger than those usually found in intermediate calc-alkalic rocks, but not as unusually large as the amounts of barium. As a result, Ba/Sr ratios are unusually high.

In most data subsets the majority of data for beryllium falls below the 1 ppm detection threshold. The available data are inadequate to appraise its geochemical behavior.

Cobalt, chromium, nickel, and vanadium all show a tendency to decrease in abundance with increasing hydrothermal alteration. Scandium shows small decreases in Milltown Andesite and dacite. All these elements are typically associated with mafic minerals and magnetite in unaltered volcanic rocks. Cobalt and nickel are associated with iron in pyrite, and might therefore be expected to show behavior similar to that of iron. The changes in cobalt and nickel, however, are generally more pronounced than associated changes in iron, so some cobalt and nickel must not have been incorporated in pyrite in the early stages of hydrothermal alteration, and were lost as alteration progressed. Chromium and vanadium show similar behavior within each unit, but slightly different behavior between units. With destruction of mafic minerals and magnetite, one would expect much chromium and vanadium to be lost in the early stages of alteration, but such is not the case. They must be retained in one or more of the alteration mineral phases.

Lanthanum and yttrium decrease slightly or in some cases show no change with increasing degree of hydrothermal alteration. They are probably lost as alteration destroys the accessory minerals that contain these elements, particularly apatite. Apatite, however, is destroyed during weak argillization, which should produce a sharp drop from unaltered to argillized rocks, whereas the data show small decreases or no significant change at all. Much lanthanum and yttrium released from the original magmatic minerals must also be retained in some of the alteration minerals.

Our earlier study showed that manganese behaved much as magnesium and calcium did during hydrothermal alteration; more and more manganese was removed as hydrothermal alteration progressed (Ashley and Albers, 1973). Here four of the units do not show manganese depletion, but latite, Milltown Andesite, and dacite do. The units that do are those for which we have the most complete data for the progressive alteration sequence. For Milltown Andesite, amounts of manganese in illite-kaolinite rocks and silicified rocks are not significantly different.

In most data subsets amounts of niobium are below the detection threshold of 10 ppm. Niobium was not determined for all the samples, so fewer determinations are available than the prevailing number for many of the data subsets. Even in the few cases where the majority of samples had detectable amounts of niobium, very few reported values exceed 10 ppm, probably due to poor analytical discrimination near the detection threshold. Thus, even the data subsets yielding average values for niobium may not contain significantly more niobium than the subsets for which calculations are not possible.

In all the rocks under investigation zirconium resides mainly in accessory zircon. Zircon persists through all observed mineralogic changes produced by hydrothermal alteration. Changes in zirconium should therefore be small or nil, and they are. Small but statistically significant differences between geometric means for zirconium are seen in latite, Milltown Andesite, and dacite. The Vindicator Rhyolite data subsets have significantly different geometric deviations. The decreases shown by many of the other minor elements, however, particularly in the latite, Milltown Andesite, and dacite, are not much larger than the decreases shown by zirconium. This serves to emphasize the fact that changes for many of the elements discussed in this section are surprisingly small, considering the rather profound changes in mineralogy that accompanied progressing hydrothermal alteration in the Goldfield area. To find out why these elements remain in the altered rocks, they should first be sought both in clay minerals and in limonite; both hypogene and supergene processes may be involved. Some of the argillized rocks contain opal or allophane, which is not detectable by X-ray analysis and consequently may be more common than we presently realize. If amorphous material, particularly allophane, is common in argillized rocks, its minor element content should be investigated, because it is capable of both cation and anion fixation (Birrell, 1961).

RESULTS AND DISCUSSION--SOIL SAMPLES

At many grid-intersection sampling localities, lack of outcrop forced us to collect soil samples (pl. 1). The sampling procedure used at such localities was given in a previous section. Residual soils encountered at many localities are actually poorly exposed soft clay-bearing altered rocks. As described earlier, these samples are included in the appropriate argillized-rock data subsets, mainly the montmorillonite-bearing rock subsets. The samples considered in this section we have designated colluvial soils, because they are unsorted and generally contain fragments of resistant rock, either fresh or silicified, or both, that crop out upslope. Actually, both mass movement downslope and sheetflood during heavy rainstorms probably play a part in transporting the materials in these soils. The matrix between the resistant fragments is composed of clay minerals, sand-size fresh and silicified rock fragments, and quartz and feldspar crystals from disintegrated fresh and argillized rocks. Organic material is ubiquitous, but is usually a minor constituent. Locally gypsum or limonite are important. The proportions of these constituents vary from place to place depending on the character of the underlying rocks, rocks cropping out upslope, and various geomorphic factors.

Clay minerals are probably always an important matrix constituent of the colluvial soils; they are derived mainly from nearby argillized rocks. The soil samples were prepared for chemical analysis by screening and rejecting everything larger than 80 mesh (Tyler screen, 0.175 mm opening). The portion that passed 80 mesh was mixed, split, and analyzed, so the material actually analyzed contained more clay than the original soil. Average amounts of the various elements for soils taken over a given stratigraphic unit, then, should fall closest to averages determined for one of the argillized rock data sets for that unit. Comparing the geometric means for soil sample data subsets (given in the last column of each diagram in figs. 2-27) with data for rock sample subsets, this is generally the case. In some cases, amounts of an element in soils are the same as amounts in unaltered rocks. The relationships between element abundances in soil and rock samples are particularly well documented for the latite, Milltown Andesite, and dacite, where data is available for the complete alteration series. With the Sandstorm Rhyolite and andesite-dacite breccia, where data is available only for illite-kaolinite and silicified rocks, the ore-related elements are less abundant in soils in several cases, whereas the major elements and other minor elements are more abundant in soils in many cases. If we had data for unaltered and montmorillonite-bearing rocks from these units, we would probably find the amounts of many elements in such subsets similar to the amounts in the soils. Comparisons between soils and rocks are difficult or impossible for gold, silver, bismuth, arsenic, molybdenum, beryllium, and niobium, because large amounts of data are below detection thresholds in all or many of the data subsets.

CONCLUSIONS

The data examined in this report confirm earlier work showing that magnesium and calcium underwent strong leaching during hydrothermal alteration at Goldfield, whereas titanium and iron did not. Unexpectedly, iron shows little indication of supergene leaching in silicified rocks, but our samples may be atypically rich in limonite, and therefore biased toward high iron contents.

Gold, silver, lead, bismuth, mercury, arsenic, and molybdenum probably all generally increase with increasing intensity of hydrothermal alteration, although available data are good only for lead and mercury.

Copper is generally unchanged. We expected some depletion of copper, molybdenum, and possibly arsenic in silicified rocks due to supergene leaching; if supergene processes have concentrated these elements in limonite, the sampling bias possibly responsible for the unexpectedly high iron contents of these rocks may also be responsible for the unexpectedly high values seen in these elements. Supergene processes have definitely affected the distribution of copper in surface samples. The importance of supergene processes for arsenic and molybdenum is not clear, due to large amounts of data below the detection thresholds and the possibility of sampling bias. The increases shown by gold, silver, lead, bismuth, and mercury are the result of hypogene processes, and supergene effects are not large enough to obscure these increases.

We have determined threshold values for distinguishing anomalous amounts of all eight ore-related elements. For all the silicified rocks we sampled, grouped together, threshold values are 0.45 ppm for gold, 3 ppm for silver, 500 ppm for lead, 20 ppm for bismuth, 1.6 ppm for mercury, 160 ppm for arsenic, 300 ppm for copper, and 50 ppm for molybdenum. Threshold values are tabulated also for individual stratigraphic units (mostly representing different rock types), since different units show significantly different amounts of these elements in many cases.

Other minor elements not related to ore metallization were generally more or less strongly depleted with increasingly intense hydrothermal alteration, but decreases are often not as large as one would predict from the mineralogic changes that took place with progressing alteration.

Soil samples taken over each stratigraphic unit generally have element abundances similar to those in argillized rocks from the same stratigraphic unit.

Table 14.--Statistical data for 13 unaltered Jqm samples

Element	Detection limit(s), ppm	% samples outside detection limit	Geometric mean, log %	Geometric standard deviation, log %	Cohen's mean, $\bar{\mu}$, log %	Cohen's standard deviation, $\bar{\sigma}$, log %	Antilog of mean, ppm (% for Fe, Mg, Ca, Ti)
Au	-5.699	100	—	—	—	—	—
Ag	-5.000 -4.417	92	—	—	—	—	—
Pb	-3.083	38	-2.73	0.24	-2.97	0.37	11
Bi	-3.083	92	—	—	—	—	—
Hg	—	0	-4.99	0.22	—	—	0.10
As	-3.000	69	—	—	—	—	—
Cu	—	0	-2.83	0.39	—	—	15
Mo	-3.750	100	—	—	—	—	—
B	-3.083	57 1/	—	—	—	—	—
Ba	-0.250	7.7 (6)	-1.60	0.51	-1.48	0.65	330
Be	-4.083	15	-3.87	0.15	-3.92	0.18	1.2
Co	-3.417	92	—	—	—	—	—
Cr	-3.183 -2.417	54	—	—	—	—	—
La	-4.083 -2.750	15	-2.35	0.26	-2.44	0.32	37
Mn	—	0	-2.16	0.20	—	—	69
Nb	-3.083	0 2/	-2.77	0.12	—	—	17
Ni	-3.417	62	—	—	—	—	—
Sc	-3.583 -3.417	57 1/	—	—	—	—	—
Sr	—	0	-2.19	0.23	—	—	64
V	-3.083	15	-2.62	0.29	-2.72	0.36	19
Y	-3.083	15	-2.72	0.22	-2.80	0.28	16
Zr	—	0	-1.97	0.20	—	—	110
Fe	—	0	0.08	0.34	—	—	1.2
Mg	—	0	-0.71	0.38	—	—	0.20
Ca	—	0	-0.54	0.41	—	—	0.29
Ti	—	0	-0.89	0.25	—	—	0.13

1/ Data for 7 samples.

2/ Data for 6 samples.

Table 15.--Statistical data for 13 illite kaolinite-bearing argillized Jqm samples

Element	Detection limit(s), ppm	% samples outside detection limit	Geometric mean, x̄, log %	Geometric standard deviation, s, log %	Cohen's mean, x̄c, log %	Cohen's standard deviation, sc, log %	Antilog of mean, ppm, % for Fe, Mg, Ca, Ti
Au	-5.699 -5.000	100	—	—	—	—	—
Ag	-4.417	92	—	—	—	—	—
Pb	-3.083	54	—	—	—	—	—
Bi	-3.083	85	—	—	—	—	—
Hg	—	0 1/	-4.97	0.53	—	—	0.11
As	-5.000	50 1/	-2.82	0.21	-3.03	0.28	9.3
Cu	—	0	-2.73	0.60	—	—	19
Mo	-3.750	92	—	—	—	—	—
B	-3.083	25 2/	—	—	—	—	—
Ba	—	0	-1.71	0.49	—	—	190
Be	-4.083	69	—	—	—	—	—
Co	-3.417 -3.583	92	—	—	—	—	—
Cr	-3.417	15	-3.34	0.57	-3.36	0.57	4.3
La	-2.750	31	-2.29	0.20	-2.50	0.37	32
Mn	—	0	-2.19	0.45	—	—	65
Nb	—	0 3/	-2.92	0.09	—	—	12
Ni	-3.417 -3.583	85	—	—	—	—	—
Sc	-3.417	0 2/	—	—	—	—	—
Sr	—	0	-2.11	0.26	—	—	78
V	—	0	-2.40	0.29	—	—	40
Y	-3.083	23	-2.67	0.22	-2.80	0.32	16
Zr	—	0	-1.94	0.33	—	—	110
Fe	—	0	0.09	0.41	—	—	1.2
Mg	—	0	-0.74	0.68	—	—	0.18
Ca	—	0	-0.47	0.74	—	—	0.34
Ti	—	0	-0.94	0.36	—	—	0.11

1/ Data for 12 samples.
2/ Data for 4 samples.
3/ Data for 9 samples.

Table 16.--Statistical data for 16 illite kaolinite-bearing argillized Tv samples

Element	Detection limit(s), ppm	% samples outside the detection limits	Geometric mean, $\bar{x}$, log %	Geometric standard deviation, s, log %	Cohen's mean, $\bar{x}$, log %	Cohen's standard deviation, $\bar{\sigma}$, log %	Antilog of mean, ppm, % for Fe, Mg, Ca, Ti
Au	-5.000	100	—	—	—	—	—
Ag	-5.699 -4.417	94	—	—	—	—	—
Pb	-3.083	25	-2.64	0.31	-2.81	0.42	15
Bi	-3.083	100	—	—	—	—	—
Hg	—	0	-4.90	0.40	—	—	0.13
As	-3.000	81	—	—	—	—	—
Cu	—	0	-2.85	0.37	—	—	14
Mo	-3.750	69	—	—	—	—	—
B	—	0 1/	—	—	—	—	—
Ba	-0.250	19 (6)	-1.12	0.32	-0.90	0.53	1200
Be	-4.083	75	—	—	—	—	—
Co	-3.583 -3.417	69	—	—	—	—	—
Cr	—	0	-3.09	0.67	—	—	8.2
La	-2.750	13	-2.22	0.15	-2.30	0.25	50
Mn	—	0	-2.11	0.55	—	—	77
Nb	-3.083	15 2/	-2.96	0.10	-2.99	0.12	10
Ni	-3.583	56	—	—	—	—	—
Sc	—	0 1/	—	—	—	—	—
Sr	—	0	-1.73	0.43	—	—	190
V	-3.083	13	-2.26	0.50	-2.41	0.61	39
Y	-3.083	19	-2.71	0.14	-2.80	0.23	16
Zr	—	0	-1.82	0.45	—	—	150
Fe	—	0	0.17	0.43	—	—	1.5
Mg	—	0	-0.15	0.62	—	—	0.71
Ca	—	0	0.21	0.84	—	—	1.6
Ti	—	0	-0.83	0.48	—	—	0.15

1/ Data for 3 samples.

2/ Data for 13 samples.

Table 17.--Statistical data for 13 silicified Tv samples

Element	Detection limit(s), log %	% samples outside the detection limit	Geometric mean, $\bar{x}$, log %	Geometric standard deviation, s, log %	Cohen's mean, $\hat{\mu}$, log %	Cohen's standard deviation, $(\hat{\sigma})$, log %	Antilog of mean, ppm, % for Fe, Mg, Ca, Ti
Au	-5.000	92	—	—	—	—	—
Ag	-4.083	85	—	—	—	—	—
Pb	—	0	-2.38	0.34	—	—	42
Bi	-3.083	100	—	—	—	—	—
Hg	—	0	-4.78	0.32	—	—	0.17
As	-3.000	23	-2.34	0.49	-2.58	0.63	26
Cu	—	0	-2.59	0.47	—	—	26
Mo	-3.750	77	—	—	—	—	—
B	—	— [1]	—	—	—	—	—
Ba	—	0	-1.27	0.30	—	—	530
Be	-4.083	100	—	—	—	—	—
Co	-3.583	92	—	—	—	—	—
Cr	—	0	-3.48	0.33	—	—	3.3
La	-2.750	31	-2.34	0.15	-2.52	0.31	30
Mn	—	0	-2.32	0.45	—	—	48
Nb	-3.083	23	-2.96	0.07	-3.01	0.10	9.9
Ni	-3.583	92	—	—	—	—	—
Sc	—	— [1]	—	—	—	—	—
Sr	—	0	-2.05	0.27	—	—	89
V	-3.083	15	-2.74	0.32	-2.82	0.36	15
Y	-3.083	69	—	—	—	—	—
Zr	—	0	-1.96	0.13	—	—	110
Fe	—	0	-0.02	0.35	—	—	0.95
Mg	—	0	-1.63	0.40	—	—	0.024
Ca	—	0	-0.86	0.42	—	—	0.14
Ti	—	0	-1.15	0.32	—	—	0.070

[1] No data.

Table 18.--Statistical data for 33 unaltered T1 samples

Element	Detection limit(s), ppm	% samples outside detection limit	Geometric mean, log %	Geometric standard deviation, s, log %	Cohen's mean, $\hat{\mu}$, log %	Cohen's standard deviation, $\hat{\sigma}$, log %	Antilog of mean, ppm, % for Fe, Mg, Ca, Ti
Au	-5.000	100	—	—	—	—	—
Ag	-5.699 -4.417	100	—	—	—	—	—
Pb	-3.083	9.1	-2.80	0.14	-2.83	0.17	15
Bi	-3.083	100	—	—	—	—	—
Hg	-6.000	6.3 1/	-5.19	0.36	-5.25	0.42	0.056
As	-3.000	91	—	—	—	—	—
Cu	-3.750	6.1	-3.07	0.25	-3.12	0.31	7.7
Mo	-3.750	97	—	—	—	—	—
B	-3.083	50 2/	—	—	—	—	—
Ba	-0.250	3,0(6)	-0.72	0.13	-0.71	0.15	2000
Be	-4.083	73	—	—	—	—	—
Co	-3.417 (-3.583)	9.1	-3.07	0.20	-3.11	0.23	7.7
Cr	—	0	-2.98	0.23	—	—	10
La	—	0	-2.14	0.13	—	—	72
Mn	—	0	-1.14	0.24	—	—	730
Nb	-3.083	28 3/	-3.00	0.0 4/	-3.03	0.05	9.3
Ni	-3.583 (-3.417)	18	-3.40	0.20	-3.43	0.21	3.7
Sc	—	0 2/	—	—	—	—	—
Sr	—	0	-1.29	0.21	—	—	520
V	—	0	-2.02	0.22	—	—	96
Y	—	0	-2.65	0.15	—	—	23
Zr	—	0	-1.70	0.17	—	—	200
Fe	—	0	0.49	0.21	—	—	3.1
Mg	—	0	0.07	0.22	—	—	1.2
Ca	—	0	0.22	0.33	—	—	1.7
Ti	—	0	-0.54	0.24	—	—	0.29

1/ Data for 32 samples.
2/ Data for 4 samples.
3/ Data for 29 samples.

4/ All values -3.00 log % (10 ppm).

Table 19.--Statistical data for 47 illite kaolinite-bearing argillized Tl samples

Element	Detection limit(s) log %	% samples outside detection limit	Geometric mean (x̄) log %	Geometric standard deviation, s, log %	Cohen's mean $\hat{\mu}$, log %	Cohen's standard deviation $\hat{\sigma}$, log %	Antilog of mean, ppm, % for Fe, Mg, Ca, Ti
Au	-5.699	96	—	—	—	—	—
Ag	-5.000 -4.417 -4.083	98	—	—	—	—	—
Pb	-3.083	2.1	-2.64	0.34	-2.65	0.35	22
Bi	-3.083	98	—	—	—	—	—
Hg	—	0 1/	-5.06	0.37	—	—	0.088
As	-3.000	60 1/	—	—	—	—	—
Cu	-3.750	11	-2.79	0.42	-2.91	0.55	12
Mo	-3.750	79	—	—	—	—	—
B	-3.083	17 2/	-2.50	0.30	-2.63	0.41	23
Ba	-0.250	4.3 (6)	-0.73	0.25	-0.70	0.28	2000
Be	-4.083	62	—	—	—	—	—
Co	-3.417 -3.583	57	—	—	—	—	—
Cr	—	0	-2.86	0.34	—	—	14
La	-2.750	4.3	-2.28	0.18	-2.30	0.21	50
Mn	—	0 3/	-1.70	0.55	—	—	200
Nb	-3.083	32	-2.99	0.04	-3.04	0.07	9.2
Ni	-3.417 -3.583	49	-3.23	0.22	-3.44	0.30	3.6
Sc	—	0 2/	-3.09	0.17	—	—	8.2
Sr	—	0	-1.36	0.36	—	—	440
V	—	0	-1.98	0.25	—	—	110
Y	-3.083	13	-2.78	0.16	-2.83	0.20	15
Zr	-0.917	4.3 (6)	-1.71	0.25	-1.67	0.31	210
Fe	—	0	0.46	0.34	—	—	2.9
Mg	—	0	-0.18	0.52	—	—	0.66
Ca	—	0	-0.06	0.65	—	—	0.86
Ti	0.083	2.1 (6)	-0.58	0.22	-0.57	0.24	0.27

1/ Data for 45 samples.
2/ Data for 18 samples.
3/ Data for 31 samples.

Table 20.--Statistical data for 33 silicified Tl samples

Element	Detection limit(s), log %	% samples outside the detection limit	Geometric mean, $\bar{x}$, log %	Geometric standard deviation, s, log %	Cohen's mean, $\bar{x}$, log %	Cohen's standard deviation, s, log %	Antilog of mean, ppm, % for Fe, Mg, Ca, Ti
Au	-5.000 -5.699	94	—	—	—	—	—
Ag	-4.417	97	—	—	—	—	—
Pb	-3.083	6.1	-2.15	0.51	-2.22	0.57	61
Bi	-3.083	88	—	—	—	—	—
Hg	—	0 1/	-5.01	0.29	—	—	0.098
As	-3.000	30	-2.67	0.37	-2.89	0.45	13
Cu	—	0	-2.50	0.52	—	—	32
Mo	-3.750	45	-3.23	0.27	-3.65	0.54	2.3
B	-3.083	100 2/	—	—	—	—	—
Ba	—	0	-1.08	0.32	—	—	840
Be	-4.083	94	—	—	—	—	—
Co	-3.417 -3.583	82	—	—	—	—	—
Cr	—	0	-3.09	0.23	—	—	8.2
La	-2.750	18	-2.30	0.19	-2.41	0.29	39
Mn	—	0	-2.21	0.50	—	—	62
Nb	-3.083	61 3/	—	—	—	—	—
Ni	-3.417 -3.583	79	—	—	—	—	—
Sc	—	0 4/	—	—	—	—	—
Sr	—	0	-1.45	0.48	—	—	360
V	—	0	-2.25	0.24	—	—	56
Y	-3.083	39	-2.88	0.17	-3.03	0.24	9.3
Zr	—	0	-1.88	0.17	—	—	130
Fe	—	0	0.52	0.40	—	—	3.3
Mg	—	0	-1.24	0.66	—	—	0.058
Ca	—	0	-0.69	0.44	—	—	0.21
Ti	—	0	-0.73	0.28	—	—	0.19

1/ Data for 32 samples.
2/ Data for 2 samples.
3/ Data for 31 samples.
4/ Data for 2 samples.

Table 21.--Statistical data for 55 colluvial soil samples taken over T1

Element	Detection limit (S), log %	% samples outside detection limit	Geometric mean, ($\bar{x}$), log %	Geometric standard deviation, S, log %	Cohen's mean, $\hat{\mu}$, log %	Cohen's standard deviation, $\hat{\sigma}$, log %	Antilog of mean, ppm, % for Fe, Mg, Ca, Ti
Au	-5.000 -5.699	96	—	—	—	—	—
Ag	-4.417	93	—	—	—	—	—
Pb	-3.083	1.8	-2.66	0.19	-2.67	0.20	22
Bi	-3.083	100	—	—	—	—	—
Hg	—	0 1/	-5.07	0.30	—	—	0.085
As	-3.000	65 1/	—	—	—	—	—
Cu	-3.750	1.8	-2.65	0.38	-2.67	0.41	21
Mo	-3.750	60	—	—	—	—	—
B	—	0 2/	-2.54	0.30	—	—	.29
Ba	-0.250	16(6)	-0.85	0.27	-0.72	0.38	1900
Be	-4.083	20	-3.95	0.09	-3.99	0.11	1.0
Co	-3.417 (-3.583)	25	-3.19	0.16	-3.28	0.21	5.2
Cr	—	0	-2.48	0.31	—	—	33
La	-2.750	3.6	-2.26	0.15	-2.28	0.18	53
Mn	—	0	-1.22	0.23	—	—	610
Nb	-3.083	37 3/	-3.00	0 4/	-3.04	0.06	9.0
Ni	—	0	-3.09	0.20	—	—	8.1
Sc	—	0 2/	-3.01	0.17	—	—	9.7
Sr	-0.250	1.8(6)	-1.28	0.28	-1.26	0.32	550
V	—	0	-1.85	0.25	—	—	140
Y	-3.083	5.5	-2.72	0.13	-2.75	0.16	18
Zr	-0.917	3.6(6)	-1.59	0.31	-1.57	0.34	270
Fe	—	0	0.62	0.21	—	—	4.2
Mg	—	0	0.18	0.23	—	—	1.5
Ca	—	0	0.41	0.40	—	—	2.6
Ti	0.083	1.8(6)	-0.45	0.26	-0.43	0.27	0.37

1/ Data for 54 samples.
2/ Data for 36 samples.
3/ Data for 19 samples.
4/ All values 10ppm (-3.00 log %).

Table 22.--Statistical data for 13 illite kaolinite-bearing argillized Tsf samples

Element	Detection limit(s), log %	% samples outside the detection limit	Geometric mean, x, log %	Geometric standard deviation, s, log %	Cohen's mean, μ, log %	Cohen's standard deviation, σ, log %	Antilog of mean, ppm, % for Fe, Mg, Ca, Ti
Au	-5.699	92	—	—	—	—	—
Ag	-5.000 -4.417	92	—	—	—	—	—
Pb	-3.083	7.7	-2.68	0.10	-2.71	0.16	19
Bi	-3.083	100	—	—	—	—	—
Hg	—	0 1/	-4.81	0.37	—	—	0.15
As	-3.000	25 1/	-2.59	0.46	-2.79	0.54	16
Cu	—	0	-2.76	0.31	—	—	17
Mo	-3.750	77	—	—	—	—	—
B	-3.083	22 3/	-2.74	0.29	-2.86	0.35	14
Ba	-0.250	15 (6)	-0.90	0.41	-0.75	0.51	1800
Be	-4.083	38	-3.98	0.06	-4.05	0.10	0.90
Co	-3.417	92	—	—	—	—	—
Cr	-3.583 -3.417 (-4.083)	38	-3.19	0.23	-3.37	0.30	4.3
La	-2.750	7.7	-2.21	0.22	-2.26	0.28	55
Mn	-3.083	7.7	-1.94	0.43	-2.05	0.55	89
Nb	-3.083	50 3/	—	—	—	—	—
Ni	-3.417	85	—	—	—	—	—
Sc	-3.583 -3.417	33 2/	-3.28	0.06	-3.35	0.12	4.5
Sr	—	0	-1.88	0.26	—	—	130
V	—	0	-2.46	0.34	—	—	34
Y	-3.083	15	-2.92	0.11	-2.96	0.13	11
Zr	—	0	-1.54	0.44	—	—	290
Fe	—	0	0.27	0.29	—	—	1.9
Mg	—	0	-0.35	0.49	—	—	0.44
Ca	—	0	-0.27	0.54	—	—	0.53
Ti	—	0	-0.84	0.25	—	—	0.15

1/ Data for 12 samples.
2/ Data for 9 samples.
3/ Data for 4 samples.

Table 23.--Statistical data for 16 silicified Tsf samples

Element	Detection limit (L) log %	% samples outside detection limit	Geometric mean (X̄) log %	Geometric standard deviation (S) log %	Cohen's mean (x̄) log %	Cohen's standard deviation (σ) log %	Antilog of mean, ppm, % for Fe, Mg, Ca, Ti
Au	-5.699 (-5.000)	38	-4.40	0.65	-5.18	1.20	0.065
Ag	-4.417	50	-3.50	0.48	-4.35	1.01	0.45
Pb	-3.083	6.3	-2.33	0.52	-2.39	0.57	41
Bi	-3.083	100	—	—	—	—	—
Hg	—	0	-4.44	0.52	—	—	0.37
As	-3.000	6.3	-2.52	0.44	-2.57	0.47	27
Cu	—	0	-2.48	0.42	—	—	33
Mo	-3.750	63	—	—	—	—	—
B	-3.083	62 1/	—	—	—	—	—
Ba	-0.250	6.3 (6)	-1.04	0.37	-0.98	0.43	1000
Be	-4.083	50	-3.91	0.25	-4.13	0.31	0.74
Co	-3.417	81	—	—	—	—	—
Cr	-3.583 -3.417	13	-3.01	0.25	-3.08	0.30	8.4
La	-2.750	31	-2.29	0.19	-2.50	0.37	31
Mn	—	0	-2.00	0.64	—	—	100
Nb	-3.083	100 2/	—	—	—	—	—
Ni	-3.417	75	—	—	—	—	—
Sc	-3.583 -3.417	46 1/	-3.26	0.11	-3.40	0.19	4.0
Sr	—	0	-1.61	0.37	—	—	250
V	-3.083	19	-2.32	0.35	-2.51	0.52	31
Y	-3.083	31	-2.92	0.09	-3.00	0.15	10
Zr	—	0	-1.78	0.53	—	—	170
Fe	—	0	0.23	0.47	—	—	1.7
Mg	—	0	-1.09	0.65	—	—	0.080
Ca	—	0	-0.26	0.59	—	—	0.55
Ti	—	0	-1.06	0.38	—	—	0.087

1/ Data for 13 samples.
2/ Data for 3 samples.

Table 24.--Statistical data for 39 colluvial soil samples taken over Tsf

Element	Detection limit (S), log %	% samples outside detection limits	Geometric mean, $\bar{X}$, log %	Geometric standard deviation, S, log %	Cohen's mean, $\hat{\mu}$, log %	Cohen's standard deviation, $\hat{\sigma}$, log %	Antilog of mean, ppm, % for Fe, Mg, Ca, Ti
Au	-5.699 -5.000	54	—	—	—	—	—
Ag	-4.417	72	—	—	—	—	—
Pb	—	0	-2.49	0.31	—	—	33
Bi	-3.083	97	—	—	—	—	—
Hg	—	0	-5.00	0.25	—	—	0.10
As	-3.000	45 1/	-2.71	0.33	-3.00	0.44	10
Cu	—	0	-2.41	0.29	—	—	39
Mo	-3.750	54	—	—	—	—	—
B	—	0 2/	-2.42	0.27	—	—	38
Ba	-0.250	5.1 (6)	-0.73	0.28	-0.70	0.31	2000
Be	-4.083	7.7	-3.92	0.11	-3.94	0.12	1.2
Co	-3.417 (-3.583)	21	-3.24	0.25	-3.31	0.27	4.9
Cr	—	0	-2.31	0.34	—	—	50
La	—	0	-2.30	0.17	—	—	50
Mn	—	0	-1.22	0.27	—	—	600
Nb	-3.083	20 3/	—	—	—	—	—
Ni	—	0	-2.99	0.27	—	—	10
Sc	-3.417	2.9 2/	-2.93	0.24	-2.95	0.25	11
Sr	-0.250	5.1 (6)	-1.32	0.20	-1.26	0.32	550
V	—	0	-1.78	0.24	—	—	160
Y	—	0	-2.82	0.11	—	—	15
Zr	-0.917	5.1 (6)	-1.48	0.32	-1.45	0.35	360
Fe	—	0	0.72	0.16	—	—	5.3
Mg	—	0	0.23	0.17	—	—	1.7
Ca	—	0	0.44	0.29	—	—	2.8
Ti	0.083	2.6 (6)	-0.27	0.25	-0.26	0.26	0.55

1/ Data for 38 samples.
2/ Data for 34 samples.
3/ Data for 5 samples.

Table 25.--Statistical data for 82 unaltered Tma samples

Element	Detection limit(s), log %	% samples outside detection limit	Geometric mean, $\bar{x}$, log %	Geometric standard deviation, s, log %	Cohen's mean, $\hat{\mu}$, log %	Cohen's standard deviation, $\hat{\sigma}$, log %	Antilog of mean, ppm, % for Fe, Mg, Ca, Ti
Au	-5.699	98	—	—	—	—	—
Ag	-5.000 -4.417	99	—	—	—	—	—
Pb	-4.083 -3.083	11	-2.83	0.18	-2.87	0.21	13
Bi	-3.083	100	—	—	—	—	—
Hg	—	0 [1]	-4.89	0.34	—	—	0.13
As	-3.000	89	—	—	—	—	—
Cu	-3.750	4.9	-2.92	0.41	-2.97	0.45	11
Mo	-3.750	67	—	—	—	—	—
B	-3.083	58 [2]	—	—	—	—	—
Ba	-0.250	3.7 (6)	-0.80	0.29	-0.77	0.31	1700
Be	-4.083	57	—	—	—	—	—
Co	-3.417	1.2	-3.00	0.21	-3.01	0.21	9.9
Cr	—	0	-2.70	0.39	—	—	20
La	-2.750	3.7	-2.32	0.15	-2.34	0.17	46
Mn	—	0	-1.11	0.33	—	—	770
Nb	-3.083	44 [3]	-2.95	0.12	-3.07	0.18	8.6
Ni	-3.417	2.4	-3.07	0.18	-3.08	0.19	8.4
Sc	—	0 [2]	-2.91	0.20	—	—	12
Sr	-0.250	1.2 (6)	-1.07	0.24	-1.06	0.26	880
V	—	0	-1.77	0.19	—	—	170
Y	—	0	-2.74	0.14	—	—	18
Zr	—	0	-1.84	0.22	—	—	140
Fe	—	0	0.75	0.20	—	—	5.6
Mg	—	0	0.21	0.21	—	—	1.6
Ca	—	0	0.39	0.31	—	—	2.5
Ti	0.083	4.9 (6)	-0.38	0.20	-0.35	0.23	0.45

[1] Data for 81 samples.

[2] Data for 50 samples.

[3] Data for 39 samples.

Table 26.--Statistical data for 85 montmorillonite-bearing argillized Tma samples

Element	Detection limit (L), log %	% samples outside detection limit	Geometric mean, M, log %	Geometric standard deviation, S, log %	Cohen's mean, μ̂, log %	Cohen's standard deviation, σ̂, log %	Antilog of mean, ppm, % for Fe, Mg, Ca, Ti
Au	-5.699 -5.000	96	—	—	—	—	—
Ag	-4.417 -4.083	95	—	—	—	—	—
Pb	-3.083	12	-2.84	0.20	-2.88	0.23	13
Bi	-3.083	100	—	—	—	—	—
Hg	—	0 1/	-4.88	0.46	—	—	0.13
As	-3.000	57 2/	—	—	—	—	—
Cu	-3.750	5.8	-2.86	0.47	-2.93	0.53	12
Mo	-3.750	62	—	—	—	—	—
B	-3.083	11 3/	-2.46	0.37	-2.55	0.44	28
Ba	-0.250	11 (G)	-0.94	0.39	-0.84	0.47	1400
Be	-4.083	44	-3.97	0.10	-4.06	0.14	0.86
Co	-3.417 (-3.583)	42	-3.04	0.31	-3.35	0.46	4.5
Cr	-3.417	3.5	-2.59	0.40	-2.62	0.43	24
La	-2.750	11	-2.42	0.20	-2.47	0.24	34
Mn	-3.083	1.2	-1.59	0.66	-1.61	0.68	250
Nb	-3.083	48 4/	-2.97	0.09	-3.08	0.14	8.4
Ni	-3.417 (-3.583)	21	-3.08	0.24	-3.19	0.31	6.4
Sc	-3.417	4.5 3/	-3.00	0.23	-3.03	0.25	9.4
Sr	-0.250	2.4 (G)	-1.20	0.29	-1.18	0.33	670
V	—	0	-1.80	0.27	—	—	160
Y	-3.083	16	-2.84	0.15	-2.90	0.19	13
Zr	—	0	-1.90	0.37	—	—	130
Fe	—	0	0.64	0.35	—	—	4.4
Mg	—	0	0.01	0.36	—	—	1.0
Ca	—	0	0.31	0.55	—	—	2.1
Ti	0.083	3.5 (G)	-0.44	0.29	-0.42	0.31	0.38

1/ Data for 84 samples.

2/ Data for 83 samples.

3/ Data for 66 samples.

4/ Data for 21 samples.

Table 27

Statistical data for 124 illite kaolinite-bearing argillized Tina samples

Element	Detection limit(s), log %	% samples outside detection limit	Geometric mean, $\bar{x}$, log %	Geometric standard deviation, s, log %	Cohen's mean, $\bar{x}$, log %	Cohen's standard deviation, $\bar{\sigma}$, log %	Antilog of mean, ppm; % for Fe, Mg, Ca, Ti
Au	-5.699	90	—	—	—	—	—
Ag	-5.000 -4.417	98	—	—	—	—	—
Pb	-4.083 -3.083	14.5	-2.72	0.27	-2.80	0.32	16
Bi	-3.083	100	—	—	—	—	—
Hg	—	0 1/	-4.83	0.41	—	—	0.15
As	-3.000	38 2/	-2.68	0.32	-2.92	0.42	12
Cu	-3.750	10	-2.90	0.44	-3.01	0.54	9.7
Mo	-3.750	46	-3.38	0.31	-3.72	0.47	1.9
B	-3.083	10 3/	-2.66	0.28	-2.72	0.32	19
Ba	-0.250	3.2 (6)	-1.09	0.33	-1.06	0.37	870
Be	-4.083	68	—	—	—	—	—
Co	-3.417	81	—	—	—	—	—
Cr	-3.583 -3.417	0.8	-2.79	0.32	-2.79	0.33	16
La	-2.750	24	-2.43	0.21	-2.55	0.28	28
Mn	-3.083	1.6	-2.26	0.56	-2.27	0.58	53
Nb	-3.083	46 4/	-2.85	0.17	-3.05	0.28	8.8
Ni	-3.417	56	—	—	—	—	—
Sc	-3.583 -3.417	2.1 3/	-3.04	0.19	-3.05	0.20	9.0
Sr	-0.250	1.6 (6)	-1.24	0.36	-1.22	0.39	600
V	—	0	-1.91	0.26	—	—	120
Y	-3.083	30	-2.87	0.14	-2.97	0.20	11
Zr	—	0	-1.96	0.28	—	—	110
Fe	—	0	0.53	0.45	—	—	3.4
Mg	-1.750	0.8	-0.55	0.49	-0.57	0.51	0.27
Ca	-1.417	1.6	-0.38	0.52	-0.40	0.54	0.40
Ti	0.083	0.8 (6)	-0.49	0.27	-0.49	0.27	0.33

1/ Data for 117 samples.
2/ Data for 122 samples.
3/ Data for 97 samples.
4/ Data for 37 samples.

Table 28

Statistical data for 139 silicified Tma samples

	Detection limit(s), log %	% samples outside detection limit	Geometric mean, X̄, log %	Geometric standard deviation, s, log %	Cohen's mean, μ̂, log %	Cohen's standard deviation, σ̂, log %	Antilog of mean, ppm; % for Fe, Mg, Ca, Ti
Au	-5.699 -5.000	78	—	—	—	—	—
Ag	-4.417 -4.083	82	—	—	—	—	—
Pb	-3.083	28	-2.50	0.39	-2.76	0.55	17
Bi	-3.083	97	—	—	—	—	—
Hg	-6.000	0.8 1/	-4.65	0.43	-4.66	0.45	0.22
As	-3.000	31 2/	-2.55	0.37	-2.81	0.50	16
Cu	-3.750	14	-2.91	0.54	-3.08	0.66	8.3
Mo	-3.750	41	-3.16	0.42	-3.60	0.66	2.5
B	-3.083	35 3/	-2.77	0.30	-2.97	0.39	11
Ba	-0.250	2.9(6)	-1.12	0.41	-1.09	0.44	820
Be	-4.083	96	—	—	—	—	—
Co	-3.417 -3.583	93 4/	—	—	—	—	—
Cr	-3.417	3.6	-2.94	0.29	-2.96	0.31	11
La	-2.750	50	-2.50	0.21	-2.75	0.32	18
Mn	-3.083	1.4	-2.13	0.45	-2.15	0.47	71
Nb	-3.083	33 5/	-2.82	0.16	-2.91	0.22	12
Ni	-3.417 -3.583	70	—	—	—	—	—
Sc	-3.417	9.7 6/	-3.14	0.18	-3.17	0.21	6.7
Sr	-0.250	0.7 (6)	-1.35	0.50	-1.34	0.51	450
V	—	0	-2.17	0.35	—	—	68
Y	-3.083	64	—	—	—	—	—
Zr	-0.917	0.7(6)	-2.00	0.26	-2.00	0.27	100
Fe	—	0	0.57	0.45	—	—	3.7
Mg	-1.750	5.8	-1.09	0.47	-1.14	0.51	0.073
Ca	-1.417	3.6	-0.59	0.45	-0.63	0.48	0.24
Ti	0.083	2.2(6)	-0.51	0.26	-0.50	0.28	0.32

1/ Data for 127 samples.
2/ Data for 136 samples.
3/ Data for 124 samples.
4/ Data for 138 samples.
5/ Data for 31 samples.
6/ Data for 124 samples.

Table 29

Statistical data for 431 colluvial soil samples taken over Tma

Element	Detection limit(s), log %	% samples outside detection limit	Geometric mean ($\bar{x}$), log %	Geometric standard deviation (s), log %	Cohen's mean ($\hat{\mu}$), log %	Cohen's standard deviation ($\hat{\sigma}$), log %	Antilog of mean, ppm, Mg, % for Fe, Ca, Ti
Au	-5.000 -5.699	98	—	—	—	—	—
Ag	-4.417	95	—	—	—	—	—
Pb	-3.083	2.1	-2.71	0.18	-2.72	0.19	19
Bi	-3.083	99.8	—	—	—	—	—
Hg	—	0 1/	-4.98	0.29	—	—	0.10
As	-3.000	35 2/	-2.85	0.20	-2.96	0.24	11
Cu	—	0	-2.87	0.36	—	—	13
Mo	-3.750	62	—	—	—	—	—
B	-3.083	0.5 3/	-2.53	0.24	-2.53	0.24	29
Ba	-0.250	3.0(G)	-1.05	0.31	-1.02	0.34	950
Be	-4.083	9.0	-3.98	0.07	-3.99	0.08	1.0
Co	-3.417	15	-3.12	0.21	-3.18	0.25	6.6
Cr	-3.417	0.5	-2.49	0.28	-2.50	0.28	32
La	-2.750	3.7	-2.37	0.17	-2.39	0.19	41
Mn	—	0	-1.35	0.31	—	—	450
Nb	-3.083	24 4/	-2.98	0.05	-3.02	0.08	9.6
Ni	-3.417	2.6	-3.00	0.18	-3.02	0.20	9.6
Sc	-3.417	0.5 3/	-3.02	0.17	-3.02	0.17	9.5
Sr	—	0	-1.25	0.22	—	—	570
V	—	0	-1.88	0.21	—	—	130
Y	-3.083	3.7	-2.78	0.14	-2.79	0.16	16
Zr	-0.917	0.2(G)	-1.80	0.31	-1.80	0.31	160
Fe	—	0	0.65	0.21	—	—	4.5
Mg	—	0	0.06	0.19	—	—	1.1
Ca	—	0	0.22	0.39	—	—	1.6
Ti	0.083	2.3(G)	-0.46	0.23	-0.44	0.24	0.36

1/ Data for 427 samples.
2/ Data for 426 samples.
3/ Data for 396 samples.
4/ Data for 38 samples.

Table 30

Statistical data for 65 unaltered Td samples

Element	Detection limit (L), log %	% samples outside detection limit	Geometric mean, $\bar{x}$, log %	Geometric standard deviation, s, log %	Cohen's mean, $\hat{\mu}$, log %	Cohen's standard deviation, $\hat{\sigma}$, log %	Antilog of mean, ppm; % for Fe, Mg, Ca, Ti
Au	-5.699 -5.000	89	—	—	—	—	—
Ag	-4.417	100	—	—	—	—	—
Pb	-3.083	1.5	-2.81	0.13	-2.82	0.14	15
Bi	-3.083	100	—	—	—	—	—
Hg	-6.000	3.2 1/	-5.11	0.40	-5.15	0.44	0.071
As	-3.000	98	—	—	—	—	—
Cu	-3.750	9.2	-2.98	0.47	-3.08	0.55	8.4
Mo	-3.750	75	—	—	—	—	—
B	-3.083	45 2/	-2.89	0.22	-3.08	0.29	8.3
Ba	—	0	-0.91	0.19	—	—	1200
Be	-4.083	48	-3.99	0.04	-4.07	0.10	0.85
Co	-3.417	3.1	-2.93	0.23	-2.95	0.25	11
Cr	—	0	-2.54	0.28	—	—	29
La	—	0	-2.23	0.15	—	—	58
Mn	—	0	-1.19	0.31	—	—	640
Nb	—	0 3/	-2.93	0.15	—	—	12
Ni	-3.417	1.5	-2.91	0.20	-2.92	0.22	12
Sc	—	0 2/	-2.98	0.16	—	—	10
Sr	—	0	-1.05	0.17	—	—	890
V	—	0	-1.82	0.16	—	—	150
Y	-3.083	1.5	-2.67	0.14	-2.68	0.15	21
Zr	—	0	-1.91	0.19	—	—	120
Fe	—	0	0.67	0.19	—	—	4.7
Mg	—	0	0.19	0.27	—	—	1.5
Ca	—	0	0.38	0.26	—	—	2.4
Ti	—	0	-0.37	0.19	—	—	0.43

1/ Data for 63 samples.
2/ Data for 42 samples.
3/ Data for 28 samples.

Table 31

Statistical data for 51 montmorillonite-bearing argillized Td samples

Element	Detection limit (L), log %	% samples with detection limit	Geometric mean, x̄, log %	Geometric standard deviation, s, log %	Cohen's mean, $\hat{\mu}$, log %	Cohen's standard deviation, $\hat{\sigma}$, log %	Antilog of mean, ppm, or % for Fe, Mg, Ca, Ti
Au	-5.699 -5.000	86	—	—	—	—	—
Ag	-4.417	94	—	—	—	—	—
Pb	-3.083	9.8	-2.75	0.21	-2.79	0.24	16
Bi	-3.083	100	—	—	—	—	—
Hg	—	0 1/	-5.01	0.31	—	—	0.099
As	-3.000	74 2/	—	—	—	—	—
Cu	-3.750	7.8	-2.86	0.41	-2.95	0.49	11
Mo	-3.750	69	—	—	—	—	—
B	-3.083	9.1 3/	-2.65	0.29	-2.70	0.33	20
Ba	-0.250	2.0 (6)	-1.00	0.36	-0.98	0.38	1000
Be	-4.083	39	-3.96	0.09	-4.04	0.14	0.91
Co	-3.417 (-3.583)	46 4/	-3.08	0.30	-3.40	0.45	4.0
Cr	-3.417	2.0	-2.70	0.31	-2.71	0.32	19
La	-2.750	7.8	-2.36	0.22	-2.40	0.26	40
Mn	—	0	-1.86	0.51	—	—	140
Nb	-3.083	53 5/	—	—	—	—	—
Ni	-3.417 (-3.583)	25	-3.08	0.24	-3.22	0.32	6.0
Sc	-3.417	3.0 3/	-3.09	0.18	-3.10	0.20	7.9
Sr	—	0	-1.25	0.25	—	—	560
V	—	0	-1.94	0.19	—	—	120
Y	-3.083	18	-2.82	0.17	-2.89	0.21	13
Zr	—	0	-1.92	0.31	—	—	120
Fe	—	0	0.61	0.21	—	—	4.0
Mg	—	0	-0.03	0.26	—	—	0.94
Ca	—	0	0.16	0.54	—	—	1.4
Ti	—	0	-0.50	0.22	—	—	0.32

1/ Data for 45 samples.
2/ Data for 46 samples.
3/ Data for 33 samples.
4/ Data for 50 samples.
5/ Data for 19 samples.

Table 32
Statistical data for 82 illite kaolinite-bearing Td samples

Element	Detection limit(s), log %	Pct. samples outside detection limit	Geometric mean (X), log %	Geometric standard deviation (s), log %	Cohen's mean ($\hat{\mu}$), log %	Cohen's standard deviation ($\hat{\sigma}$), log %	Antilog of mean, ppm, % for Fe, Mg, Ca, Ti
Au	-5.699	85	—	—	—	—	—
Ag	-5.000 -4.417	98	—	—	—	—	—
Pb	-3.083	2.4	-2.72	0.26	-2.73	0.27	19
Bi	-3.083	100	—	—	—	—	—
Hg	-6.000	2.6 1/	-4.91	0.41	-4.94	0.45	0.12
As	-3.000	52 2/	—	—	—	—	—
Cu	-3.750	21	-2.94	0.48	-3.19	0.65	6.5
Mo	-3.750	41	-3.47	0.22	-3.69	0.33	2.1
B	-3.083	16 3/	-2.72	0.27	-2.81	0.32	16
Ba	—	0	-1.08	0.31	—	—	820
Be	-4.083	57	—	—	—	—	—
Co	-3.417 -3.583	57	—	—	—	—	—
Cr	—	0	-2.82	0.24	—	—	15
La	-2.750	9.8	-2.45	0.21	-2.49	0.23	32
Mn	-3.083	2.4	-2.13	0.58	-2.16	0.60	70
Nb	-3.083	8 4/	-2.94	0.12	-2.96	0.13	11
Ni	-3.417 (-3.583)	44	-3.14	0.27	-3.39	0.38	4.1
Sc	-3.417	4.8 3/	-3.10	0.15	-3.12	0.17	7.8
Sr	—	0	-1.24	0.28	—	—	570
V	—	0	-1.95	0.20	—	—	110
Y	-3.083	28	-2.84	0.18	-2.95	0.24	11
Zr	—	0	-2.00	0.23	—	—	100
Fe	—	0	0.51	0.35	—	—	3.2
Mg	-1.750	3.7	-0.47	0.56	-0.52	0.62	0.30
Ca	-1.417	3.7	-0.40	0.54	-0.44	0.58	0.36
Ti	0.083	1.2 (6)	-0.53	0.21	-0.52	0.23	0.30

1/ Data for 77 samples.

2/ Data for 79 samples.

3/ Data for 63 samples.

4/ Data for 25 samples.

Table 33

Statistical data for 88 silicified Td samples

Element	Detection limit(s), log %	% samples outside detection limit	Geometric mean, log %	Geometric standard deviation, log %	Cohen's mean $\hat{\mu}$, log %	Cohen's standard deviation $\hat{\sigma}$, log %	Antilog of mean, ppm, % (Fe, Mg, Ca, Ti)
Au	-5.699	82	—	—	—	—	—
Ag	-5.000 -4.417 -4.083	83	—	—	—	—	—
Pb	-3.083	7.8	-2.25	0.51	-2.34	0.57	46
Bi	-3.083	95	—	—	—	—	—
Hg	-6.000	1.2 1/	-4.74	0.43	-4.76	0.45	0.18
As	-3.000	27	-2.58	0.36	-2.78	0.46	17
Cu	-3.750	18	-2.94	0.50	-3.15	0.64	7.0
Mo	-3.750	33	-3.24	0.42	-3.54	0.57	2.9
B	-3.083	33 2/	-2.89	0.16	-3.00	0.22	10
Ba	-0.250	1.1 (6)	-1.19	0.31	-1.18	0.33	660
Be	-4.083	91	—	—	—	—	—
Co	-3.417 -3.583	90	—	—	—	—	—
Cr	-3.417	3.4	-2.89	0.32	-2.91	0.34	12
La	-2.750	26	-2.49	0.22	-2.60	0.28	25
Mn	-3.083	3.4	-2.20	0.48	-2.24	0.51	58
Nb	—	0 3/	-2.91	0.12	—	—	12
Ni	-3.417 -3.583	70	—	—	—	—	—
Sc	-3.417	13 4/	-3.18	0.16	-3.22	0.19	6.0
Sr	-0.250	1.1 (6)	-1.17	0.37	-1.16	0.39	690
V	—	0	-2.14	0.27	—	—	73
Y	-3.083	68	—	—	—	—	—
Zr	—	0	-2.07	0.21	—	—	86
Fe	—	0	0.55	0.37	—	—	3.5
Mg	-1.750	5.7	-1.16	0.43	-1.20	0.46	0.063
Ca	-1.417	6.8	-0.63	0.45	-0.70	0.50	0.20
Ti	—	0	-0.61	0.22	—	—	0.24

1/ Data for 82 samples.
2/ Data for 79 samples.
3/ Data for 17 samples.
4/ Data for 79 samples.

Table 34

Statistical data for 170 colluvial soil samples taken over Td

Element	Detection limit(s), log %	% samples outside detection limit	Geometric mean, $\bar{X}$, log %	Geometric standard deviation, s, log %	Cohen's mean, $\hat{\mu}$, log %	Cohen's stand. deviation, $\hat{\sigma}$, log %	Antilog of mean, ppm, % for Fe, Mg, Ca, Ti
Au	-5.000 -5.699	93	—	—	—	—	—
Ag	-4.447	96	—	—	—	—	—
Pb	-3.083	0.6	-2.70	0.17	-2.70	0.17	20
Bi	-3.083	98	—	—	—	—	—
Hg	-6.000	0.6	-4.97	0.34	-4.98	0.35	0.11
As	-3.000	43	-2.84	0.18	-2.99	0.23	10
Cu	-3.750	0.6	-2.80	0.37	-2.81	0.38	16
Mo	-3.750	62	—	—	—	—	—
B	-3.083	0.9 [1]	-2.56	0.22	-2.56	0.22	27
Ba	-0.250	0.6 (9)	-1.06	0.29	-1.05	0.30	880
Be	-4.083	18	-3.98	0.09	-4.01	0.11	0.98
Co	-3.417 (-3.583)	8.8	-3.04	0.24	-3.09	0.28	8.2
Cr	—	0	-2.56	0.22	—	—	27
La	-2.750	1.2	-2.32	0.17	-2.32	0.17	48
Mn	—	0	-1.38	0.34	—	—	410
Nb	-3.083	15 [2]	-2.98	0.06	-3.00	0.08	10
Ni	-3.417 (-3.583)	2.4	-2.97	0.17	-2.98	0.19	10
Sc	—	0 [1]	-3.06	0.14	—	—	8.7
Sr	—	0	-1.23	0.22	—	—	590
V	—	0	-1.92	0.16	—	—	120
Y	-3.083	1.8	-2.73	0.14	-2.74	0.15	18
Zr	—	0	-1.83	0.22	—	—	150
Fe	—	0	0.61	0.20	—	—	4.1
Mg	—	0	0.03	0.20	—	—	1.1
Ca	—	0	0.12	0.35	—	—	1.3
Ti	—	0	-0.49	0.[illegible]7	—	—	0.32

[1] Data for 111 samples.
[2] Data for 60 samples.

Table 35

Statistical data for 16 illite kaolinite-bearing argillized Tls samples

Element	Detection limit(s), ppm	% samples outside detection limit		Geometric mean, $\bar{X}$, log %	Geometric standard deviation, s, log %	Cohen's mean, $\bar{X}$, log %	Cohen's standard deviation, σ, log %	Antilog of mean, ppm, % for Fe, Mg, Ca, Ti
Au	-5.699	88		—	—	—	—	—
Ag	-4.417	100		—	—	—	—	—
Pb	-3.083	13		-2.64	0.38	-2.73	0.43	19
Bi	-3.083	100		—	—	—	—	—
Hg	—	0	1/	-4.71	0.37	—	—	0.19
As	-3.000	13	1/	-2.62	0.30	-2.70	0.34	20
Cu	-3.750	50		-3.02	0.47	-3.72	0.86	1.9
Mo	-3.750	56		—	—	—	—	—
B	-3.083	50		-2.87	0.30	-3.14	0.38	7.3
Ba	—	0		-1.12	0.33	—	—	760
Be	-4.083	81		—	—	—	—	—
Co	-3.417	88		—	—	—	—	—
Cr	-3.417	19		-2.75	0.41	-2.93	0.53	12
La	-2.750	6.3		-2.40	0.21	-2.42	0.23	38
Mn	-3.083	6.3		-2.46	0.43	-2.51	0.46	31
Nb	—	—	2/	—	—	—	—	—
Ni	-3.417	88		—	—	—	—	—
Sc	-3.417	6.3		-3.21	0.14	-3.23	0.15	5.9
Sr	—	0		-1.16	0.31	—	—	700
V	—	0		-2.10	0.31	—	—	79
Y	-3.083	63		—	—	—	—	—
Zr	—	0		-2.02	0.19	—	—	96
Fe	—	0		0.42	0.43	—	—	2.6
Mg	-1.750	19		-1.14	0.44	-1.31	0.55	0.048
Ca	—	0		-0.58	0.57	—	—	0.26
Ti	—	0		-0.53	0.27	—	—	0.29

1/ Data for 15 samples.

2/ No data.

Table 36

Statistical data for 21 silicified Tls samples

Element	Detection limit, X(s), log %	% samples outside detection limit	Geometric mean (X), log %	Geometric standard deviation (S), log %	Cohen's mean ($\hat{x}$), log %	Cohen's standard deviation ($\hat{\sigma}$), log %	Antilog of mean, ppm, % for Fe, Mg, Ca, Ti
Au	-5.699	86	—	—	—	—	—
Ag	-4.417	100	—	—	—	—	—
Pb	-3.083	4.8	-2.68	0.24	-2.70	0.26	20
Bi	-3.083	95	—	—	—	—	—
Hg	—	0 1/	-4.65	0.52	—	—	0.23
As	-3.000	24	-2.63	0.19	-2.76	0.29	18
Cu	-3.750	29	-3.16	0.31	-3.41	0.50	3.9
Mo	-3.750	33	-3.26	0.34	-3.53	0.50	2.9
B	-3.083	33	-2.90	0.20	-3.11	0.28	7.8
Ba	—	0	-1.09	0.26	—	—	810
Be	-4.083	86	—	—	—	—	—
Co	-3.417	100	—	—	—	—	—
Cr	-3.417	9.5	-2.72	0.29	-2.80	0.37	16
La	-2.750	24	-2.38	0.19	-2.50	0.29	31
Mn	—	0	-2.20	0.34	—	—	64
Nb	—	0 2/	-2.69	0.10	—	—	20
Ni	-3.417	57	—	—	—	—	—
Sc	-3.417	9.5	-3.12	0.20	-3.16	0.23	6.9
Sr	—	0	-1.10	0.32	—	—	790
V	—	0	-2.07	0.31	—	—	85
Y	-3.083	71	—	—	—	—	—
Zr	—	0	-1.99	0.21	—	—	100
Fe	—	0	0.57	0.38	—	—	3.7
Mg	-1.750	4.8	-1.32	0.30	-1.35	0.32	0.045
Ca	-1.417	4.8	-0.45	0.50	-0.51	0.55	0.31
Ti	—	0	-0.55	0.16	—	—	0.28

1/ Data for 20 samples.

2/ Data for 6 samples.

Table 37

Statistical data for 16 colluvial soil samples taken over T1s

Element	Detection limit(s), log %	No. samples outside detection limit	Geometric mean, $\bar{x}$, log %	Geometric standard deviation, s, log %	Cohen's mean, $\hat{\mu}$, log %	Cohen's standard deviation, $\hat{\sigma}$, log %	Antilog of mean, ppm, % for Fe, Mg, Ca, Ti
Au	-5.000 -5.699	100	—	—	—	—	—
Ag	-4.417	100	—	—	—	—	—
Pb	-3.083	6.3	-2.72	0.05	-2.75	0.11	18
Bi	-3.083	100	—	—	—	—	—
Hg	—	0	-4.87	0.42	—	—	0.13
As	-3.000	81	—	—	—	—	—
Cu	—	0	-3.03	0.26	—	—	9.3
Mo	-3.750	75	—	—	—	—	—
B	—	0	-2.52	0.27	—	—	30
Ba	—	0	-1.16	0.24	—	—	690
Be	—	0	-3.95	0.18	—	—	1.1
Co	—	0	-2.97	0.35	—	—	11
Cr	—	0	-2.58	0.32	—	—	27
La	-2.750	6.3	-2.40	0.15	-2.42	0.18	38
Mn	—	0	-1.28	0.30	—	—	530
Nb	—	— 1/	—	—	—	—	—
Ni	—	0	-3.00	0.17	—	—	10
Sc	—	0	-3.02	0.16	—	—	9.6
Sr	-0.250	6.3 (G)	-1.27	0.17	-1.20	0.31	630
V	—	0	-1.95	0.25	—	—	110
Y	—	0	-2.75	0.11	—	—	18
Zr	—	0	-1.83	0.29	—	—	150
Fe	—	0	0.55	0.16	—	—	3.5
Mg	—	0	0.13	0.12	—	—	1.4
Ca	—	0	0.21	0.28	—	—	1.6
Ti	—	0	-0.47	0.17	—	—	0.34

1/ No data.

Table 38

Statistical data for 323 silicified rock samples

Element	Detection limit, (t), log %	% samples outside detection limit	Geometric mean, X̄, log %	Geometric standard deviation, S, log %	Cohen's mean, μ̂, log %	Cohen's standard deviation, σ̂, log %	Antilog of mean, ppm, % for Fe, Mg, Ca, Ti
Au	-5.699	80	—	—	—	—	—
Ag	-5,000 -4.417 -4.083	84	—	—	—	—	—
Pb	-3.083	16	-2.35	0.49	-2,52	0.61	30
Bi	-3.083	94	—	—	—	—	—
Hg	-6.000	0.7 1/	-4.71	0.44	-4.72	0.45	0.19
As	-3.000	28 2/	-2.57	0.37	-2.77	0.48	17
Cu	-3.750	13	-2,82	0.55	-2.99	0.68	10
Mo	-3.750	41	-3.20	0.40	-3.61	0.62	2.5
B	-3.083	36 3/	-2.81	0.29	-3.00	0.36	9.9
Ba	-0.250	1.9 (6)	-1.15	0.37	-1.13	0.39	740
Be	-4.083	91	—	—	—	—	—
Co	-3.417 -3.583	90 4/	—	—	—	—	—
Cr	-3.417	3.7	-2.96	0.32	-2.98	0.34	10
La	-2.750	37	-2.44	0.22	-2.64	0.33	23
Mn	-3.083	1.6	-2.17	0.47	-2.19	0.48	65
Nb	-3.083	31 5/	-2.88	0.14	-2.98	0.20	10
Ni	-3.417 -3.583	71	—	—	—	—	—
Sc	-3.417	13	-3.16	0.18	-3.21	0.21	6.2
Sr	-0.250	0.6 (6)	-1.35	0.49	-1.35	0.50	450
V	-3.083	1.5	-2.19	0.34	-2.21	0.36	62
Y	-3.083	62	—	—	—	—	—
Zr	-0.917	0.3 (6)	-2.01	0.27	-2.00	0.28	99
Fe	—	0	0.51	0.44	—	—	3.2
Mg	-1.750	5.0	-1.17	0.49	-1.21	0.52	0.062
Ca	-1.417	4.0	-0.61	0.47	-0.65	0.50	0.23
Ti	0.083	0.9 (6)	-0.64	0.33	-0.64	0.34	0.23

1/ Data for 303 samples.
2/ Data for 320 samples.
3/ Data for 242 samples.
4/ Data for 321 samples.
5/ Data for 111 samples.
6/ Data for 242 samples.

References cited

Albers, J. P., and Cornwall, H. R., 1968, Revised interpretation of the stratigraphy and structure of the Goldfield district, Esmeralda and Nye Counties, Nevada [abs.]: Geol. Soc. America Spec. Paper 101, p. 285.

Anderson, R. L., and Bancroft, T. A., 1952, Statistical theory in research: New York, McGraw-Hill Book Co., Inc., 399 p.

Andrews-Jones, D. A., 1968, The application of geochemical techniques to mineral exploration: Colorado School Mines Mineral Industries Bull., v. 11, no. 6, 31 p.

Ashley, R. P., 1971, Preliminary geologic map of the Goldfield mining district, Nevada: U.S. Geol. Survey open-file map.

Ashley, R. P., and Albers, J. P., 1969, Elements associated with gold in the oxidized zone at Goldfield, Nevada [abs.]: Geol. Soc. America Spec. Paper 121, p. 480.

______1973, Distribution of gold and other ore-related elements near ore bodies in the oxidized zone at Goldfield, Nevada: U.S. Geol. Survey open-file report.

Birrell, K. S., 1961, Ion fixation by allophane: New Zealand Jour. Sci., v. 4, p. 393-414.

Cohen, A. C. Jr., 1959, Simplified estimators for the normal distribution when samples are singly censored or truncated: Technometrics, v. 1, no. 3, p. 217-237.

______1961, Tables for maximum likelihood estimates; singly truncated and singly censored samples: Technometrics, v. 3, no. 4, p. 535-541.

Flanagan, F. J., 1957, Semiquantitative spectrographic analysis and rank correlation in geochemistry: Geochim. et Cosmochim. Acta, v. 12, p. 315-322.

Garrels, R. M., and Christ, C. L., 1965, Solutions, minerals, and equilibria: New York, Harper and Row Publishers, 450 p.

Grim. R. E., 1968, Clay mineralogy, 2d ed.: New York, McGraw-Hill Book Co., Inc., 596 p.

Grimes, D. J., and Marranzino, A. P., 1968, Direct-current arc and alternating-current spark emission spectrographic field methods for the semiquantitative analysis of geologic materials: U.S. Geol. Survey Circ. 591, 6 p.

Hansuld, J. A., 1966, Eh and pH in geochemical prospecting, in Proceedings, Symposium on geochemical prospecting, Ottawa, April 1966: Canada Geol. Survey Paper 66-54, p. 172-187.

Harvey, R. D., and Vitaliano, C. J., 1964, Wall-rock alteration in the Goldfield district, Nevada: Jour. Geology, v. 72, p. 564-579.

Hawkes, H. E., and Webb, J. S., 1962, Geochemistry in mineral exploration: New York, Harper and Row Publishers, 415 p.

Huffman, Claude, Jr., Mensik, J. D., and Riley, L. B., 1967, Determination of gold in geologic materials by solvent extraction and atomic-absorption spectrometry: U.S. Geol. Survey Circ. 544, 6 p.

Keroher, G. C., and others, 1966, Lexicon of geologic names of the United States for 1936-1960: U.S. Geol. Survey Bull. 1200, 4341 p.

Krumbein, W. C., and Graybill, F. A., 1965, An introduction to statistical models in geology: New York, McGraw-Hill Book Co., Inc., 475 p.

Searls, Fred, Jr., 1948, A contribution to the published information on the geology and ore deposits of Goldfield, Nevada: Nevada Univ. Bull., v. 42, no. 5, Geology and Mining ser. 48, 24 p.

Lepeltier, Claude, 1969, A simplified statistical treatment of geochemical data by graphical representation: Econ. Geology, v. 64, p. 538-550.

Lovering, T. G., 1963, Use of nonparametric statistical tests in the interpretation of geological data: Soc. Mining Engineers Trans., v. 226, no. 2, p. 137-140.

Miesch, A. T., 1967, Methods of computation for estimating geochemical abundance: U.S. Geol. Survey Prof. Paper 574-B, 15 p.

Moroney, M. J., 1956 [repr. 1969], Facts from figures, 3d ed.: Baltimore, Md., Penguin Books, 472 p.

Ransome, F. L., 1909, Geology and ore deposits of Goldfield, Nevada: U.S. Geol. Survey Prof. Paper 66, 258 p.

Siegel, Sidney, 1956, Nonparametric statistics for the behavioral sciences: New York, McGraw-Hill Book Co., 312 p.

Silberman, M. L., and Ashley, R. P., 1970, Age of ore deposition at Goldfield, Nevada, from potassium-argon dating of alunite: Econ. Geology, v. 65, p. 352-354.

Snedecor, G. W., 1956, Statistical methods: Ames, Iowa State Univ. Press, 534 p.

Taylor, S. R., 1969, Trace element chemistry of andesites and associated calc-alkaline rocks, in McBirney, A. R., ed., Proceedings of the andesite conference: Oregon Dept. Geology and Mineral Industries Bull. 65, p. 43-63.

Thompson, C. E., Nakagawa, H. M., and VanSickle, G. H., 1968, Rapid analysis for gold in geologic materials, in Geological Survey Research 1968: U.S. Geol. Survey Prof. Paper 600-B, p. B130-B132.

Vaughn, W. W., 1967, A simple mercury vapor detector for geochemical prospecting: U.S. Geol. Survey Circ. 540, 8 p.

Vaughn, W. W., and McCarthy, J. H., Jr., 1964, An instrumental technique for the determination of submicrogram concentrations of mercury in soils, rocks, and gas, in Geological Survey Research 1964: U.S. Geol. Survey Prof. Paper 501-D, p. D123-D127.

Ward, F. N., Lakin, H. W., Canney, F. C., and others, 1963, Analytical methods used in geochemical exploration by the U.S. Geological Survey: U.S. Geol. Survey Bull. 1152, 100 p.

Wedow, Helmuth, Jr., and Ericksen, G. E., 1971, Log-probability graphs of geochemical data and their use in exploration [abs.]: Econ. Geology, v. 66, p. 1270.